Eur. Phys. J. Plus (2024) 139:527
https://doi.org/10.1140/epjp/s13360-024-05327-4

THE EUROPEAN PHYSICAL JOURNAL PLUS

Regular Article

Assessing the influence of public behavior and governmental action on disease dynamics: a PRCC analysis and optimal control approach

Protyusha Dutta[1,a], **Sangeeta Saha**[2,b], **Guruprasad Samanta**[1,c]

[1] Department of Mathematics, Indian Institute of Engineering Science and Technology, Shibpur, Howrah 711103, India
[2] MS2Discovery Interdisciplinary Research Institute, Wilfrid Laurier University, Waterloo, Canada

Received: 18 April 2024 / Accepted: 30 May 2024

Abstract A compartmental SIRIS epidemiological system containing two separate susceptible compartments (depending on immunity power) has been assessed in the present work involving governmental action, public reaction and social behavioral dynamics. In addition, the impact of environmental perturbations as well as time-dependent control techniques have been investigated. Present study analyzes that a few previously infectious individuals become susceptible to infection again after they have recovered, some infected persons build immunity after infection and some previously diseased populations become contaminated again after having recovered. More particularly, this study demonstrates the significance of social and governmental interventions on disease dynamics, along with the relevance of nonlinear dynamical modeling of epidemiological systems. As indicated by numerical simulation, the activities of government, social behavior act an essential role in preventing a pandemic scenario and if government takes action at incipient phases during an outbreak, the system becomes infection-free much sooner. Sensitivity analysis is used to assess how changes in different parameters of a model affect the spread of a disease. In this case, Latin hypercube sampling is used to perform both uncertainty and sensitivity analyses on input parameters. This sampling method helps to observe how these parameters impact the reproduction number of the disease. After that, Kendall's tau and Spearman's rank correlation coefficients are calculated to delve deeper into how these uncertainties affect the dynamics of the disease. Moreover, it is remarkable that random variations might inhibit the propagation of ailment, that can contribute in emergence of beneficial control strategies to govern the dynamics of disease. In this model, the policies implemented by government and pharmaceutical therapy are regarded as most adequate control pair, and it is determined that simultaneous execution of control mechanisms considerably diminishes the ailment burden.

1 Introduction

Viral infections have significant repercussions for communities or societies, while also having enough potential to exert a substantial influence on overall societal well-being, economy and health and other facets of daily activities. According to the World Health Organization (WHO), infectious diseases are accountable for one-third of all mortalities that occur on a worldwide scale. Contagious infections were involved in four out of the top ten crucial reasons of mortality on a global scale in 2008; in low-income countries, infectious agents were involved in five out of the top ten major causes of death. During twentieth century, people have seen various pandemic scenarios driven by influenza virus, as well as the appearance of new disorders including Hepatitis C, Hepatitis E, Lyme disease, Legionnaire's disease, Hantavirus and Toxic-Shock Syndrome. Since 1981, Human Immunodeficiency Virus (HIV), which is the important pathogen that caused the emergence of Acquired Immunodeficiency Syndrome (AIDS), has been primarily responsible for more than 3 million fatalities throughout the world every year. As a consequence of evolving social and traveling patterns, new infectious disease threats are arising which must be addressed. One such example is the fact that West Nile virus has been transported to North America. The threat of biological terrorism, in which diseases such as smallpox or plague has been recognized as potential hazard.

During recent decades, there has been a substantial improvement achieved in medical centers. However, identification, treatment, and prevention of disease propagation tend to be great challenges for authorities across worldwide as a result of rising morbidity rate, fatality rate together with the intricacies of infections. Whenever an infectious virus becomes widespread in a certain region, ailment control agencies attempt to prevent the spread of disease. The prediction of characteristics of bacterial infection and the suggestion of effective regulatory measures could possibly be accomplished by various approaches and strategies. Mathematical models have emerged as a great resource for investigating contagious disease transmission. Even though mathematical models in

[a] e-mail: protyusha1996@gmail.com (corresponding author)
[b] e-mail: sangeetasaha629@gmail.com
[c] e-mails: g_p_samanta@yahoo.co.uk; gpsamanta@math.iiests.ac.in

Published online: 15 June 2024

epidemiological studies have a deep knowledge reaching back to previous systems presented by Bernoulli in 18th century [1], the majority of modern study focused on compartmental systems depends on the framework founded by Kermack and McKendrick in 1930s [2]. Researchers have examined a wide variety of pharmaceutical and non-pharmaceutical remedies, including confinement, immunization, quarantine, vaccination, and treatment, etc. [3, 4].

Deterministic approaches have been employed in several notable classical studies of contagious diseases [5–7]. On the other hand, the formation and transmission of epidemics are inherently uncertain due to random interactions that individuals have with one another as well as the notion that populations are subject to a constant spectrum of disturbances. It is important to integrate this ambiguity in the relevant models due to accurately anticipate the development of communicable ailments, as the amount of affected in initial stages of a pandemic will be extremely low, and random fluctuation itself might enable this crisis to die out [8]. There is a variety of situations in which stochastic systems might be more suitable for representing infectious disease propagation. Moreover, it has been demonstrated that stochastic epidemic models, in contrast to their deterministic versions, may convey an additional sensation of authenticity. Random variations can indeed be implemented into a system in a wide range of ways, from both biological and mathematical points of view. The stochastic differential equation (SDE) SIRIS system which is proffered in this manuscript makes use of the method that has been introduced by Mao et al. [9]. The concept depends on the hypothesis that the relevant system parameters differ around some average values because of continuous perturbation in ecosystem. Thereafter, an extended stochastic SIRIS system has been investigated, in which it is assumed that environmental variations have some influence on natural death rate d.

One of the most important issues for government is to make investment in public healthcare system. Taking precautions to stave against potentially expensive health problems early in life may result in saving money in the long term. Besides voluntary managements and amenities, the responsibilities associated with public health system include other entities such as quarantine, mandatory vaccination regulation, and surveillance authority. Moreover, owing to the precarious state of regional healthcare infrastructure, it is conceivable that the resources for detecting, segregating, as well as treating people who are infected with ailment, in addition to tracing and quarantining will be extremely inadequate. In this context, public welfare along with social initiatives should be assessed against unforeseen dangers to the community, such as financial difficulties, exposure to fundamental facilities, social safety nets, and undernutrition. Additionally, they are required to be realistic and harness the advantages provided by regional structures and processes, especially through social mobilization with active participation from society. This interim guideline explains how to execute significant public health and social activities to reduce the chances of a severe disease outbreak. As a consequence, two critical aspects may be integrated to the conventional SIRS model, namely the effect of governmental intervention and public response. We demonstrate that these behavioral reactions exhibit social dynamical factors and they are incredibly essential to the accuracy of predictions.

Uncertainty analysis (UA) is performed to investigate the variability in a model's outcomes resulting from uncertainties in input parameters. Following UA, sensitivity analysis (SA) is conducted to ascertain how alterations in model outputs can be attributed to various input sources, either qualitatively or statistically [10]. This study delves into SA methodologies within deterministic dynamical models in the realm of biology. In a deterministic model, outputs are solely determined by input parameters and the model's structure. Consequently, repeating the model simulation will consistently yield the same results for a given input, with any output uncertainty stemming from variations in the input-a type of uncertainty known as epistemic [11]. Epistemic uncertainty arises from incomplete knowledge about parameter values, inputs, or quantities presumed to remain constant during model evaluation. In contrast, stochastic models exhibit output variability due to the inherent unpredictability of the system's behavior, termed aleatory uncertainty [11]. This differentiation remains a focal point in engineering and risk assessment research. SA facilitates model simplification by identifying and removing parameters with minimal impact on outcomes. This analysis helps elucidate the directional impact of input variable changes, shedding light on the factors influencing model behavior. It is crucial for pinpointing parameters significantly contributing to output uncertainty, often with asymmetric consequences [12].

As indicated previously, epidemiological research has a glorious background, following the footsteps of Kermack and McKendrick's, initial study [2]. There is a variety of information accessible in [13, 14] that illustrates the methodology of epidemiological data. The compartmental framework, of which SIS and SIR are examples of fundamental models, may be used to provide a brief summary of the propagation of infection. SIS model explains the circumstances in which all recovered persons do not get immunity and cannot prevent themselves from becoming susceptible once again. In contrast to SIS model, SIR theory specifies the scenario in which all individuals who have been cured achieved lifetime immunity. Those who have been exposed to infections like COVID-19 [15], influenza [16] typically develop antibodies to the virus; however, these antibodies only remain effective for a limited time after illness. Reinfection modeling is significant tool for describing the situation in which a portion of individuals acquires only partial immunity. Several unforeseen behaviors will emerge as a result of the virus's reinfection. In [17], researchers have discovered a bistable phenomenon in a SIRI (susceptible-infected-recovered-infected) system, which represents the condition in which it is difficult for someone to become susceptible to an ailment again after having infected for first time. This has been occurred when the rate of reinfection is high. Parameter regions for various dynamic events have been determined in [18], which generalize the observations of [17] to network study. The previous references about SIRI model suggest that once an individual has been exposed to an virus, they will never again be susceptible to that disease anymore. This notion does not consider the possibility that certain persons could become susceptible to an epidemic and then get afflicted once more. Even though there are a few referrals concern-

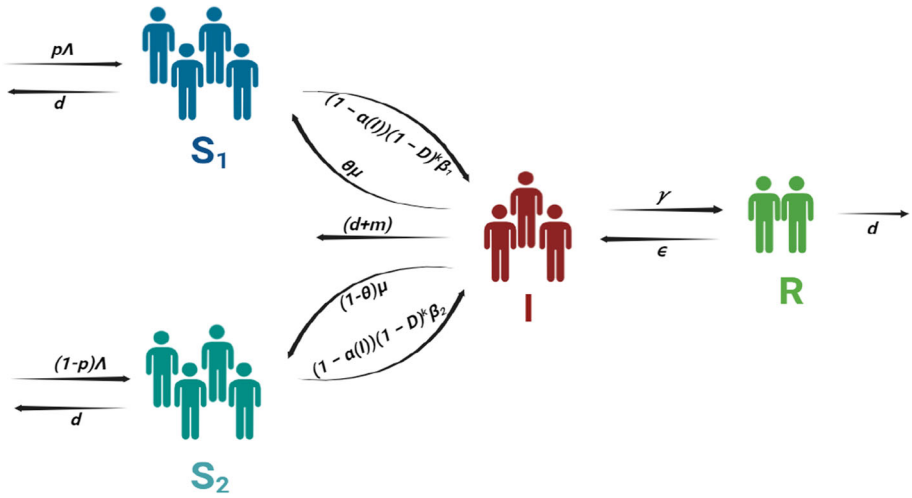

Fig. 1 Schematic diagram of system (2.1)

ing heterogeneous susceptibility [19, 20], to the best of our knowledge, there is currently no analysis investigating the affect of heterogeneous susceptibility including partial immunity, government action, social interaction, and public response.

In this manuscript, an SIRIS epidemiological system with heterogeneous susceptibility has been explored by assessing the influence of governmental interventions, social behavioral dynamics, and public reaction on the evolution of disease. To achieve a broader degree of comprehension, we require to take into consideration the environmental fluctuation. As natural fatality rates of every compartment are key factors that are affected by its ecosystem, it is reasonable to expect that these parameters will oscillate as a result of environmental variations [21]. Despite its irregular nature, Gaussian white-noise provides an effective model for rapidly fluctuating phenomena. Additionally, the system is converted into an optimal control problem by assuming governmental policies (a) as well as pharmaceutical treatment (γ) as time-dependent controls. In Sect. 2, an SIRIS epidemiological model has been established in which the spread of ailment is governed by several biological and sociological factors. In Sect. 3, a few basic preliminaries associated with proposed stochastic framework (2.2) are presented. Positivity, boundedness along with geometrically ergodic property have been investigated in Sect. 4 to emphasize that the system is biologically exist. Section 5 studies whether or not a coexistence steady state arise in accordance with basic reproduction number. The significance of some model parameters on disease propagation is going to be addressed in the following Sect. 6. In Sect. 7, dynamic characteristics of steady states of the model (2.1) as well as that stochastic version of it have been described. The alteration of stability of infection-free steady state of the system through transcritical bifurcation is analyzed in Sect. 8. Section 9 employs PRCC analysis as a method for conducting a global sensitivity analysis. This analysis aims to comprehensively grasp the collective influence of parameters that induce changes in the dynamics of the system. In order to illustrate all of the theoretical assertions in numerical scenario, MATLAB simulation is carried out in Sect. 10. Next, in Sect. 11, an equivalent optimal control problem is constructed excluding environmental fluctuation with the purpose of reducing the disease burden. The consequences of optimal control measures on the behavior of model system are depicted using numerical figures within Sect. 12. In the concluding stage of this work, a precise report has been embellished, together with some possible prospects for future (see Sect. 13).

2 Model formulation

The article is dealt with a compartmental SIRIS model, where two different susceptible states are considered based on the immunity power. The total population $N(t)$ is divided into four sub-classes, named as, susceptible population with lower immunity ($S_1(t)$), susceptible population with higher immunity ($S_2(t)$), infected population ($I(t)$) and recovered population ($R(t)$), and the way of disease propagation is depicted in Fig. 1. The mode of transmission follows mass action law in this model. Now, when people recover from a disease, either they achieve permanent recovery, or the recovery is temporary leaving a chance of reinfection and so moving to susceptible class due to the waning effect of medicines or vaccines. The immunity power is not same for all people. Some get infected very soon due to lower immunity power, whereas for others the virus take some time to affect the immune system. Here, we have presumed that rate of propagation of infection for S_1 class (β_1) is higher than S_2 class (β_2). It means the people in S_2 class have the higher resistance power against a disease, and people in S_1 class can easily become infected while coming in contact with an infected person ($\beta_2 < \beta_1$). We have considered that the infection here do not confer any long-lasting immunity. So, the disease do not give permanent immunity upon recovery from infection, and individuals become infected again. In fact, people become infected further if they neglect the necessary medication and precautionary measures, and move to I class direct from recovered class with rate ϵ. So, it is considered that this reinfection rate will not be as high as the disease transmission rate among people with weak immune system ($\epsilon < \beta_1$). During an epidemic, there are different social platforms that disseminate

important information about disease symptoms, appropriate precautions, and medications via various media, such as TV and radio or even via educational campaigns. People are encouraged to keep adequate protection for safety and the government imposes various limitations based on the severity. Therefore, successfully executed governmental regulations and social behavior of individuals are crucial in preventing the spread of infection. The societal component α here indicates the effectiveness of governmental intervention, meanwhile D and k stand for, respectively, the effectiveness of social behavioral dynamics and public reaction. It is considered that $0 \leq \alpha < 1,\ 0 \leq D < 1$. As the governmental restrictions imposed depending on the infection level, so instead of a constant value, it would be logical to choose α as a function of infected people ($\alpha(I)$) with $0 \leq \alpha(I) < 1$. In this manuscript, we have chosen $\alpha(I(t)) = \frac{aI(t)}{b+I(t)}$ (see, Fig. 2), where a is the rate of restrictions and b^{-1} is the effectiveness of the imposed limitations. So, people from both susceptible classes move to infected class after coming in contact with an infected person with the disease transmission rate $(1-\alpha(I))(1-D)^k(\beta_1 S_1(t)+\beta_2 S_2(t))I(t)$. The recruitment rate is parameterized by Λ, and p portion of the recruitment goes in S_1 class. The natural death rate, denoted by d, is considered in each compartment, whereas m is the disease-related mortality rate, considered in the diseased class only. Moreover, the infectious people, move to susceptible class with rate μ, if they stop taking medicines midway. The probabilities of this progression to susceptible class with lower and higher immunity are θ and $(1-\theta)$, respectively. After taking into account all the details, the following model has been suggested:

$$\begin{aligned}
\frac{\mathrm{d}S_1(t)}{\mathrm{d}t} &= p\Lambda - (1-\alpha(I(t)))(1-D)^k\beta_1 S_1(t)I(t) + \theta\mu I(t) - \mathrm{d}S_1(t),\ S_1(0) > 0\\
\frac{\mathrm{d}S_2(t)}{\mathrm{d}t} &= (1-p)\Lambda - (1-\alpha(I(t)))(1-D)^k\beta_2 S_2(t)I(t) + (1-\theta)\mu I(t) - \mathrm{d}S_2(t),\ S_2(0) > 0\\
\frac{\mathrm{d}I(t)}{\mathrm{d}t} &= (1-\alpha(I(t)))(1-D)^k(\beta_1 S_1(t)+\beta_2 S_2(t))I(t) - (d+m)I(t) - \gamma I(t) - \mu I(t) + \epsilon I(t)R(t),\ I(0) \geq 0\\
\frac{\mathrm{d}R(t)}{\mathrm{d}t} &= \gamma I(t) - \epsilon I(t)R(t) - \mathrm{d}R(t),\ R(0) \geq 0.
\end{aligned} \tag{2.1}$$

Now, a continuous SIRIS system has been assumed incorporating random fluctuation. In the situation of propagation of infection, natural death rate d serves as one of the most crucial parameters. In reality, the natural death rate d will continuously oscillate around some average value owing to the continuous evolution that occurs in environment. Consequently, d might be regarded as a random variable $\tilde{d}$. Consistent with the natural phenomena, it is assumed that in $[t,\ t+\mathrm{d}t)$:

$$-\tilde{d}\mathrm{d}t = -d\mathrm{d}t + \nu_j(x_j)\mathrm{d}W_j(t), \quad j = 1,\ 2,\ 3,\ 4$$

here $(x_1(t),\ x_2(t),\ x_3(t),\ x_4(t)) = (S_1(t),\ S_2(t),\ I(t),\ R(t))$, and $\mathrm{d}W_j(t) = W_j(t+\mathrm{d}t) - W_j(t)$ expresses the increment of usual Brownian motion. In the sake of keeping simple, let us suppose that $\nu_j,\ j = 1,\ 2,\ 3,\ 4$ are real constants and the intensity of noises for $S_1,\ S_2,\ I$ and R are indicated in terms of $\nu_j^2,\ j = 1,\ 2,\ 3,\ 4$, respectively. Hence, we replace $-d\mathrm{d}t$ in model (2.1) with $-\tilde{d}\mathrm{d}t = -d\mathrm{d}t + \nu_j\mathrm{d}W_j(t),\ j = 1,\ 2,\ 3,\ 4$. Integrating stochastic perturbation in the growth equations of susceptibles (higher and lower immunity), infected, and recovered communities, it is plausible to develop an stochastic epidemiological model associated with deterministic system of equation (2.1). The corresponding model is provided as follows:

$$\begin{aligned}
\frac{\mathrm{d}S_1(t)}{\mathrm{d}t} &= \left\{p\Lambda - (1-\alpha(I(t)))(1-D)^k\beta_1 S_1(t)I(t) + \theta\mu I(t) - \mathrm{d}S_1(t)\right\} + \nu_1 S_1(t)\frac{\mathrm{d}W_1(t)}{\mathrm{d}t},\\
\frac{\mathrm{d}S_2(t)}{\mathrm{d}t} &= \left\{(1-p)\Lambda - (1-\alpha(I(t)))(1-D)^k\beta_2 S_2(t)I(t) + (1-\theta)\mu I(t) - \mathrm{d}S_2(t)\right\} + \nu_2 S_2(t)\frac{\mathrm{d}W_2(t)}{\mathrm{d}t},\\
\frac{\mathrm{d}I(t)}{\mathrm{d}t} &= \left\{(1-\alpha(I(t)))(1-D)^k(\beta_1 S_1(t)+\beta_2 S_2(t))I(t) - (\gamma+\mu+d+m)I(t) + \epsilon I(t)R(t)\right\} + \nu_3 I(t)\frac{\mathrm{d}W_3(t)}{\mathrm{d}t},\\
\frac{\mathrm{d}R(t)}{\mathrm{d}t} &= \left\{\gamma I(t) - \epsilon I(t)R(t) - d\mathrm{R}(t)\right\} + \nu_4 R(t)\frac{\mathrm{d}W_4(t)}{\mathrm{d}t}.
\end{aligned} \tag{2.2}$$

The models (2.1) and (2.2) are associated with positive initial conditions $S_1(0) > 0$, $S_2(0) > 0$, $I(0) \geq 0$ and $R(0) \geq 0$. In this scenario, it is noted that $\eta_j(t) = \frac{\mathrm{d}}{\mathrm{d}t}(W_j(t))$ are independent standard zero mean Gaussian white-noises [22] and with the following properties:

$$\langle \eta_j(t) \rangle = 0 \text{ and } \langle \eta_j(t_1)\eta_j(t_2) \rangle = \delta_j(t_1 - t_2), \quad \text{for } j = 1,\ 2,\ 3,\ 4$$

in which δ_j is the Dirac delta function specified by

$$\begin{cases}
\delta_j(x) = 0, & \text{for } x \neq 0\\
\displaystyle\int_{-\infty}^{\infty} \delta_j(x)\mathrm{d}x = \lim_{\varepsilon \to 0^+} \int_{-\varepsilon}^{\varepsilon} \delta_j(x)\mathrm{d}x = 1
\end{cases}$$

and $\langle \cdot \rangle$ denotes ensemble average of considered stochastic process.

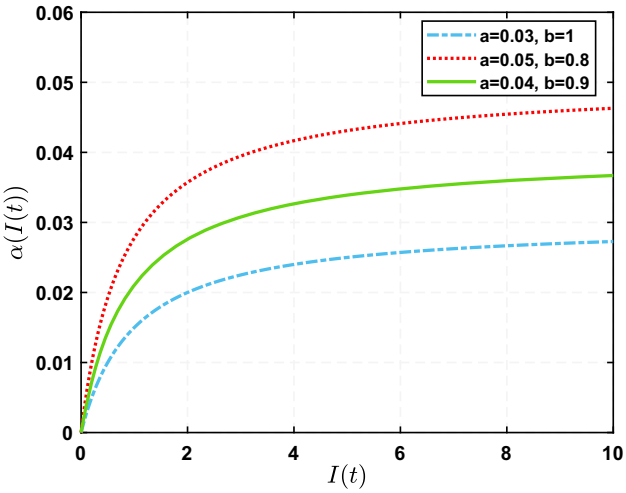

Fig. 2 The function $\alpha(I(t)) = \frac{aI(t)}{b+I(t)}$ is caused to differ substantially due to growing size of infective class. The behavior of this functions is illustrated in the diagram with increasing density of infected population, for various values of a and b as described in the inset

3 Basic properties

Suppose $(\Omega, \mathcal{F}, \{\mathcal{F}_t\}_{t\geq 0}, \mathbb{P})$ be a complete probability space with a filtration $\{\mathcal{F}_t\}_{t\geq 0}$ complying the usual conditions (i.e., it is increasing and right continuous while $\mathcal{F}_0$ contains all $\mathbb{P}$-null sets), $W_j(t)$ $(j = 1, 2, 3, ..., r)$ are defined on this complete probability space. Meanwhile, we define $\mathbb{R}^n_+ = \{X \in \mathbb{R}^n : x_j > 0,\ 1 \leq j \leq n\}$. Specifically, the n-dimensional SDE system is assumed as follows:

$$\mathrm{d}X(t) = \hat{f}(X(t), t)\mathrm{d}t + \hat{h}(X(t), t)\mathrm{d}\hat{W}(t) \tag{3.1}$$

with initial value $X(0) = X_0 \in \mathbb{R}^n$, where $\hat{f}(X(t), t)$ is a function defined on $\mathbb{R}^n \times [t_0, +\infty)$, $\hat{h}(X(t), t)$ is an $n \times r$ matrix; $\hat{f}$, $\hat{h}$ are locally Lipschitz continuous functions, $\hat{W}(t)$ indicates an r-dimensional usual Brownian motion defined on complete probability space $(\Omega, \mathcal{F}, \{\mathcal{F}_t\}_{t\geq 0}, \mathbb{P})$, i.e.,

$$\begin{aligned} X(t) &= \left[x_1(t), x_2(t), ..., x_n(t)\right]^T \\ \hat{f}(X(t), t) &= \left[f_1(X(t), t), f_2(X(t), t), ..., f_n(X(t), t)\right]^T \\ \hat{W}(t) &= \left[W_1(t), W_2(t), ..., W_r(t)\right]^T \\ \hat{h}(X(t), t) &= \left[h_{ji}(X(t), t)\right]_{n\times r}. \end{aligned}$$

The differential operator L is defined as follows:

$$L \equiv \frac{\partial}{\partial t} + \sum_{j=1}^{n} f_j(t)\frac{\partial}{\partial x_j} + \frac{1}{2}\sum_{j,i=1}^{n}\left[\hat{h}^T(t, X)\hat{h}(t, X)\right]_{ji}\frac{\partial^2}{\partial x_j \partial x_i}. \tag{3.2}$$

If L operates on a function $V \in C^{2,1}(\mathbb{R}^n \times [t_0, +\infty); \mathbb{R}_+)$, then

$$LV(X,t) = V_t(X,t) + V_X(X,t)\hat{f}(X,t) + \frac{1}{2}trace\left[\hat{h}^T(X,t)V_{XX}\hat{h}(X,t)\right] \tag{3.3}$$

where $V_t = \frac{\partial V}{\partial t}$, $V_X = \left(\frac{\partial V}{\partial x_1}, \frac{\partial V}{\partial x_2}, ..., \frac{\partial V}{\partial x_n}\right)$, $V_{XX} = \left(\frac{\partial^2 V}{\partial x_j \partial x_i}\right)_{n\times n}$; $C^{2,1}(\mathbb{R}^n \times [t_0, +\infty); \mathbb{R}_+)$ indicate the family of all non-negative functions defined on $\mathbb{R}^n \times [t_0, +\infty)$ and twice differentiable in X and once in t. If $X(t) \in \mathbb{R}^n$, using $It\hat{o}'s$ formula, we have

$$\begin{aligned} \mathrm{d}V(X,t) &= LV(X,t)\mathrm{d}t + V_X(X,t)\hat{h}(X,t)\mathrm{d}\hat{W}(t) \\ &= \left(\frac{\partial V}{\partial t} + \sum_{j=1}^{n} f_j\frac{\partial V}{\partial x_j} + \frac{1}{2}\sum_{j=1}^{n}\sum_{i=1}^{n}\sum_{l=1}^{r}\frac{\partial^2 V}{\partial x_j \partial x_i}h_{jl}h_{il}\right)\mathrm{d}t + \sum_{j=1}^{n}\sum_{i=1}^{r}\frac{\partial V}{\partial x_j}h_{ji}\mathrm{d}W_i(t). \end{aligned} \tag{3.4}$$

It is preferable to represent the system (2.2) in terms of (3.1), as well as $X(t) = (x_1(t), x_2(t), x_3(t), x_4(t)) = (S_1(t), S_2(t), I(t), R(t))$ and

$$\hat{f}(X) = \begin{pmatrix} p\Lambda - (1-\alpha(I))(1-D)^k\beta_1 S_1 I + \theta\mu I - \mathrm{d}S_1 \\ (1-p)\Lambda - (1-\alpha(I))(1-D)^k\beta_2 S_2 I + (1-\theta)\mu I - \mathrm{d}S_2 \\ (1-\alpha(I))(1-D)^k(\beta_1 S_1 + \beta_2 S_2)I - (\gamma+\mu+d+m)I + \epsilon I R \\ \gamma I - \epsilon I R - \mathrm{d}R \end{pmatrix}$$

$$\hat{h}(X) = \begin{pmatrix} \nu_1 S_1 & 0 & 0 & 0 \\ 0 & \nu_2 S_2 & 0 & 0 \\ 0 & 0 & \nu_3 I & 0 \\ 0 & 0 & 0 & \nu_4 R \end{pmatrix}, \ \hat{W} = \begin{pmatrix} W_1 \\ W_2 \\ W_3 \\ W_4 \end{pmatrix}.$$

Here, $\hat{J}(X) = \hat{h}^T \hat{h} = \text{diag}(\nu_1^2 S_1^2,\ \nu_2^2 S_2^2,\ \nu_3^2 I^2,\ \nu_4^2 R^2)$ signifies the diffusion matrix. Moreover, denote $P_t(X_0,\ A) = \mathbb{P}[X(t) \in A | X(0) = X_0],\ \forall\, t \in \mathbb{R}_+,\ \forall\, X_0 \in \mathbb{R}_+^4,\ \forall\, A \in \mathcal{F}$.

4 Preliminary findings

The suggested deterministic system (2.1) is biologically relevant since the system variables are positive and bounded, and this is shown in the following two theorems.

Theorem 4.1 *All solutions of model (2.1) in $\mathbb{R}_+^4$ are positive for all $t > 0$.*

Proof The RHS functions of model (2.1) are continuous and locally Lipschitzian. So, the system has a unique solution on $[0,\ \eta)$, for $0 < \eta \leq +\infty$ [23]. Let, $\phi(S_1,\ S_2,\ I,\ R) = (1 - \alpha(I))(1 - D)^k(\beta_1 S_1 + \beta_2 S_2) - (d + m + \gamma + \mu) + \epsilon R$. From the third equation of (2.1) we have,

$$I(t) = I(0) \exp\left[\int_0^t \phi(S_1(u),\ S_2(u),\ I(u),\ R(u))\, \mathrm{d}u\right] \geq 0, \ \text{ as } I(0) \geq 0.$$

Now, we want to show, $S_1(t) > 0,\ \ S_2(t) > 0\, \forall\, t \in [0,\ \eta)$. If the assumptions are not true, then $\exists\, t_1,\ \ t_2 \in (0,\ \eta)$ so that $S_1(t_1) = 0$, $\dot{S}_1(t_1) \leq 0,\ \ S_1(t) > 0,\ \ \forall\, t \in [0,\ t_1)$ and $S_2(t_2) = 0,\ \ \dot{S}_2(t_2) \leq 0,\ \ S_2(t) > 0,\ \ \forall\, t \in [0,\ t_2)$. From the first equation we get

$$\left.\frac{\mathrm{d}S_1}{\mathrm{d}t}\right|_{t=t_1} = p\Lambda + \theta\mu I(t_1) > 0$$

which is a contradiction to $\dot{S}_1(t_1) \leq 0$. And, the second equation gives

$$\left.\frac{\mathrm{d}S_2}{\mathrm{d}t}\right|_{t=t_2} = (1 - p)\Lambda + (1 - \theta)\mu I(t_2) > 0$$

which contradicts $\dot{S}_2(t_2) \leq 0$. So we get, $S_1(t) > 0$ and $S_2(t) > 0,\ \ \forall\, t \in [0,\ \eta)$, where $0 < \eta \leq +\infty$. Next, we claim is $R(t) \geq 0$, $\forall\, t \in [0,\ \eta)$. If it does not hold, then $\exists\, t_3 \in (0,\ \eta)$ such that $R(t_3) = 0,\ \ \dot{R}(t_3) < 0$ and $R(t) > 0,\ \ \forall\, t \in [0,\ t_3)$. From the last equation, we get

$$\left.\frac{\mathrm{d}R}{\mathrm{d}t}\right|_{t=t_3} = \gamma I(t_3) - (d + \epsilon I(t_3))R(t_3) = \gamma I(t_3) \geq 0$$

which contradicts the assumption $\dot{R}(t_3) < 0$. So, $R(t) \geq 0,\ \ \forall\, t \in [0,\ \eta)$ for $0 < \eta \leq +\infty$. □

Theorem 4.2 *All solutions of model (2.1), starting from $\mathbb{R}_+^4$, are bounded for all $t > 0$.*

Proof Let us consider the total population as $N(t) = S_1(t) + S_2(t) + I(t) + R(t)$. Then we have

$$\frac{\mathrm{d}N}{\mathrm{d}t} = \Lambda - \mathrm{d}S_1 - \mathrm{d}S_2 - (d + m)I - \mathrm{d}R \leq \Lambda - dN$$

$$\Rightarrow 0 < N(t) \leq \frac{\Lambda}{d} + \left(N(0) - \frac{\Lambda}{d}\right)e^{-\mathrm{d}t}$$

where $N(0) = S_1(0) + S_2(0) + I(0) + R(0)$. Then, $0 < \lim\limits_{t\to\infty} N(t) \leq \dfrac{\Lambda}{d} + \varepsilon$, for any $\varepsilon > 0$. Hence, the solution of model (2.1) are confined in the region: $\bar{\Omega} = \left\{(S_1,\ S_2,\ I,\ R) \in \mathbb{R}_+^4 : 0 < N(t) \leq \dfrac{\Lambda}{d} + \varepsilon,\ \text{ for any } \varepsilon > 0\right\}$. □

Next, we are going to concentrate on the performance of stochastic version (2.2). The underlying theories establish certain fundamental aspects, including existence, uniqueness, geometric ergodicity, ultimately boundedness, and system permanence of (2.2). With the assist of Lemma 4.3, we shall demonstrate that system (2.2) possesses a unique global positive solution implementing Lyapunov analysis method.

Lemma 4.3 *The inequality, $\hat{y} \leq 2\hat{y} - 1 - \ln \hat{y}$ exists $\forall\ \hat{y} > 0$ and $\hat{y} \in \mathbb{R}_+$.*

Proof We define for $\hat{y} > 0$, $l_1 = \hat{y} - 1 - \ln \hat{y}$, which implies $\dfrac{\mathrm{d}l_1}{\mathrm{d}\hat{y}} = 1 - \dfrac{1}{\hat{y}}$.

- Case 1: $0 < \hat{y} < 1$
  Here, $\frac{dl_1}{d\hat{y}} < 0$ and so l_1 decreases as $\hat{y}$ increases.
  Hence, $l_1 = \hat{y} - 1 - \ln \hat{y} > 1 - 1 - \ln 1 = 0$.
- Case 2: $\hat{y} > 1$
  Here, $\frac{dl_1}{d\hat{y}} > 0$ and so l_1 increases as $\hat{y}$ increases.
  Hence, $l_1 = \hat{y} - 1 - \ln \hat{y} > 1 - 1 - \ln 1 = 0$.

Hence the result. □

Theorem 4.4 *For any initial value* $(S_1(0),\ S_2(0),\ I(0),\ R(0)) \in \mathbb{R}^4_+$ *of system (2.2), the solutions* $X(t) = (S_1(t),\ S_2(t),\ I(t),\ R(t)) \in \mathbb{R}^4_+$ *for all* $t \geq 0$ *almost surely (a.s.).*

Proof For any known initial condition X_0, the stochastic system (2.2) possesses a unique local solution in $[0,\ \hat{\tau}_e)$, where the coefficients of (2.2) are locally Lipschitz continuous. Here, the explosion time is denoted by $\hat{\tau}_e$.

We will now be going to explain that the solution is global, i.e., $\hat{\tau}_e = \infty$ a.s. To this end, let $\hat{\kappa}_0 \geq 1$ be sufficiently large such that $S_1(0) \in \left(\frac{1}{\hat{\kappa}_0},\ \hat{\kappa}_0\right)$, $S_2(0) \in \left(\frac{1}{\hat{\kappa}_0},\ \hat{\kappa}_0\right)$, $I(0) \in \left(\frac{1}{\hat{\kappa}_0},\ \hat{\kappa}_0\right)$ and $R(0) \in \left(\frac{1}{\hat{\kappa}_0},\ \hat{\kappa}_0\right)$. For each integer $\hat{\kappa} \geq \hat{\kappa}_0$, define the stopping time as follows:

$$\hat{\tau}_{\hat{\kappa}} = \inf\left\{t \in [0,\ \hat{\tau}_e)\ :\ S_1(t) \notin \left(\frac{1}{\hat{\kappa}},\ \hat{\kappa}\right) \text{ or } S_2(t) \notin \left(\frac{1}{\hat{\kappa}},\ \hat{\kappa}\right) \text{ or } I(t) \notin \left(\frac{1}{\hat{\kappa}},\ \hat{\kappa}\right) \text{ or } R(t) \notin \left(\frac{1}{\hat{\kappa}},\ \hat{\kappa}\right)\right\}$$

taking ϕ as empty set, we consider $\inf \phi = \infty$. Clearly, $\hat{\tau}_{\hat{\kappa}}$ is increasing as $\hat{\kappa} \to \infty$. Set, $\hat{\tau}_\infty = \lim_{\hat{\kappa}\to\infty} \hat{\tau}_{\hat{\kappa}}$, hence $\hat{\tau}_\infty \leq \hat{\tau}_e$. If it can be proved that $\hat{\tau}_\infty = \infty$ a.s., then $\hat{\tau}_e = \infty$ and $X(t) \in \mathbb{R}^4_+$ with probability one for all $t \geq 0$. If the assertion is incorrect, then there exists a pair of constants $\varepsilon \in (0,\ 1)$ and $T_1 > 0$ s.t. $\mathbb{P}\{\hat{\tau}_\infty \leq T_1\} > \varepsilon$. For any $\hat{\kappa} \geq \hat{\kappa}_0$, assume the $\mathbb{C}^4$-function $\hat{U}_1 : \mathbb{R}^4_+ \to \mathbb{R}_+$ as follows:

$$\hat{U}_1(S_1(t), S_2(t), I(t), R(t)) = 2S_1 - 1 - \ln S_1 + 2S_2 - 1 - \ln S_2 + 2I - 1 - \ln I + 2R - 1 - \ln R. \tag{4.1}$$

For any $(\hat{\tau}_{\hat{\kappa}} \wedge T_1) \geq 0$, using Ito'^s formula, we have

$$d\hat{U}_1 = L\hat{U}_1 dt + \left(2 - \frac{1}{S_1}\right)\nu_1 S_1 dW_1 + \left(2 - \frac{1}{S_2}\right)\nu_2 S_2 dW_2 + \left(2 - \frac{1}{I}\right)\nu_3 I dW_3 + \left(2 - \frac{1}{R}\right)\nu_4 R dW_4 \tag{4.2}$$

where

$$\begin{aligned}
L\hat{U}_1 &= \left(2 - \frac{1}{S_1}\right)\left\{p\Lambda - (1-\alpha(I))(1-D)^k\beta_1 S_1 I + \theta\mu I - dS_1\right\} + \left(2 - \frac{1}{S_2}\right)\left\{(1-p)\Lambda - (1-\alpha(I))(1-D)^k\beta_2 S_2 I\right.\\
&\left. + (1-\theta)\mu I - dS_2\right\} + \left(2 - \frac{1}{I}\right)\left\{(1-\alpha(I))(1-D)^k(\beta_1 S_1 + \beta_2 S_2)I - (\gamma + \mu + d + m)I + \epsilon I R\right\} +\\
&\left(2 - \frac{1}{R}\right)\left\{\gamma I - \epsilon I R - dR\right\} + \frac{\nu_1^2 + \nu_2^2 + \nu_3^2 + \nu_4^2}{2}\\
&\leq \left[2\Lambda + 4d + \gamma + \mu + m + \frac{\nu_1^2 + \nu_2^2 + \nu_3^2 + \nu_4^2}{2}\right] + \left[2\mu + \epsilon + (1-D)^k(\beta_1 + \beta_2)\right]I\\
&= \hat{A}_1 + \hat{A}_2 I \ \text{(say)}.
\end{aligned} \tag{4.3}$$

Here,

$$\begin{aligned}
\hat{A}_1 &= 2\Lambda + 4d + \gamma + \mu + m + \frac{\nu_1^2 + \nu_2^2 + \nu_3^2 + \nu_4^2}{2}\\
\hat{A}_2 &= 2\mu + \epsilon + (1-D)^k(\beta_1 + \beta_2).
\end{aligned}$$

By applying Lemma 4.3, it is obtained that

$$L\hat{U}_1 \leq \hat{A}_1 + \hat{A}_2\hat{U}_1.$$

Furthermore, for $\hat{\kappa} \geq \hat{\kappa}_0$, integrating both sides of (4.2) from 0 to $\hat{\tau}_{\hat{\kappa}} \wedge T_1$, and taking expectation, we have

$$\begin{aligned}
\mathbb{E}\hat{U}_1(X(\hat{\tau}_{\hat{\kappa}} \wedge T_1)) &\leq \hat{U}_1(X_0) + \hat{A}_1\mathbb{E}(\hat{\tau}_{\hat{\kappa}} \wedge T_1) + \hat{A}_2\int_0^{\hat{\tau}_{\hat{\kappa}}\wedge T_1} \mathbb{E}\hat{U}_1(X(t))dt\\
&\leq \hat{U}_1(X_0) + \hat{A}_1 T_1 + \hat{A}_2\int_0^{\hat{\tau}_{\hat{\kappa}}\wedge T_1} \mathbb{E}\hat{U}_1(X(t))dt.
\end{aligned}$$

By the Gronwall inequality [24], it is obtained that

$$\mathbb{E}\hat{U}_1(X(\hat{\tau}_{\hat{\kappa}} \wedge T_1)) \leq \left\{\hat{U}_1(X_0) + \hat{A}_1 T_1\right\} \exp(\hat{A}_2 T_1). \tag{4.4}$$

There is at least one of $S_1(\hat{\tau}_{\hat{\kappa}}, \hat{\omega})$, $S_2(\hat{\tau}_{\hat{\kappa}}, \hat{\omega})$, $I(\hat{\tau}_{\hat{\kappa}}, \hat{\omega})$ or $R(\hat{\tau}_{\hat{\kappa}}, \hat{\omega})$ which is equal to $\hat{\kappa}$ or $\frac{1}{\hat{\kappa}}$, for each $\hat{\omega} \in \Omega_{\hat{\kappa}}$. Therefore, $\hat{U}_1(X(\hat{\tau}_{\hat{\kappa}}, \hat{\omega}))$ is not less than either $2\hat{\kappa} - 1 - \ln\hat{\kappa}$ or $\frac{2}{\hat{\kappa}} - 1 - \ln\frac{1}{\hat{\kappa}} = \frac{2}{\hat{\kappa}} - 1 + \ln\hat{\kappa}$, i.e.

$$\hat{U}_1(X(\hat{\tau}_{\hat{\kappa}}, \hat{\omega})) \geq (2\hat{\kappa} - 1 - \ln\hat{\kappa}) \wedge \left(\frac{2}{\hat{\kappa}} - 1 + \ln\hat{\kappa}\right). \tag{4.5}$$

It follows from (4.4) and (4.5):

$$\begin{aligned}\left\{\hat{U}_1(X_0) + \hat{A}_1 T_1\right\} \exp(\hat{A}_2 T_1) &\geq \mathbb{E}\hat{U}_1(X(\hat{\tau}_{\hat{\kappa}} \wedge T_1)) \\ &\geq \mathbb{E}\left[\mathbb{I}_{\Omega_{\hat{\kappa}}(\hat{\omega})}\hat{U}_1(X(\hat{\tau}_{\hat{\kappa}}, \hat{\omega}))\right] \\ &\geq \varepsilon(2\hat{\kappa} - 1 - \ln\hat{\kappa}) \wedge \left(\frac{2}{\hat{\kappa}} - 1 + \ln\hat{\kappa}\right)\end{aligned}$$

where $\mathbb{I}_{\Omega_{\hat{\kappa}}(\hat{\omega})}$ is the indicator function of $\Omega_{\hat{\kappa}}$. Taking $\hat{\kappa} \to \infty$, it implies

$$\infty > \left\{\hat{U}_1(X_0) + \hat{A}_1 T_1\right\} \exp(\hat{A}_2 T_1) = \infty$$

this is inconsistent. Subsequently, it should be $\hat{\tau}_\infty = \infty$ with probability one.

Therefore, the solution of SDE system (2.2) will not explore at a finite time with probability one. Thus the proof comes to the end. □

Now, the existence of V-geometric ergodic property of Markov process $X(t) = (S_1(t),\ S_2(t)I(t),\ R(t))$ has been investigated for the SDE model (2.2).

Theorem 4.5 *Markov process X(t) of model (2.2) associated to initial condition $X_0 \in \mathbb{R}^4_+$ is V-geometrically ergodic.*

Proof Define

$$\hat{U}_2(S_1(t),\ S_2(t),\ I(t),\ R(t)) = \hat{N}(t) + \frac{1}{\hat{N}(t)}$$

where $(S_1(t),\ S_2(t),\ I(t),\ R(t)) \in \mathbb{R}^4_+$ and $\hat{N}(t) = S_1(t) + S_2(t) + I(t) + R(t)$, which infers the following:

$$\hat{U}_2(S_1(t),\ S_2(t),\ I(t),\ R(t)) = \hat{U}_2(X(t)) \to \infty \text{ as } |X(t)| \to \infty.$$

It can be observed by employing $It\hat{o}'s$ formula that

$$\begin{aligned}L\hat{U}_2(X(t)) &\leq -d\left(\hat{N} + \frac{1}{\hat{N}}\right) + \Lambda - \frac{\Lambda}{\hat{N}^2} + \frac{2d}{\hat{N}} + \frac{mI}{\hat{N}^2} + \frac{1}{\hat{N}^3}\left[\nu_1^2 S_1^2 + \nu_2^2 S_2^2 + \nu_3^2 I^2 + \nu_4^2 R^2\right] \\ &\leq -\mathrm{d}\hat{U}_2 + \Lambda - \frac{\Lambda}{\hat{N}^2} + \frac{2d}{\hat{N}} + \frac{m}{\hat{N}} + \frac{1}{\hat{N}}(\nu_1^2 + \nu_2^2 + \nu_3^2 + \nu_4^2) \\ &= -\mathrm{d}\hat{U}_2 + \Lambda - \frac{\Lambda}{\hat{N}^2} + \frac{1}{\hat{N}}(2d + m + \nu_1^2 + \nu_2^2 + \nu_3^2 + \nu_4^2) \\ &\leq \hat{A}_3 - \mathrm{d}\hat{U}_2(X)\end{aligned} \tag{4.6}$$

where, $\hat{A}_3 = \dfrac{4\Lambda^2 + (2d + m + \nu_1^2 + \nu_2^2 + \nu_3^2 + \nu_4^2)^2}{4\Lambda}$.

Thereafter, the condition (ii) of Lemma A.1 in [25] is fulfilled.

As system (2.2) is uniformly elliptic, so Proposition 11.1 in [26] ensures the existence of the function $p : \mathbb{R}_+ \times \mathbb{R}^4_+ \times \mathbb{R}^4_+ \to (0, \infty)$ s.t. p is jointly continuous, $p_t(X_0,\ X)$ is strictly positive, for all $(t,\ X_0,\ X)$, and measurable set A:

$$P_t(X_0,\ A) = \int_A p_t(X_0,\ X)\mathrm{d}X.$$

It suggests that for any $\hat{\omega} > 0$, $\exists$ a positive constant $\hat{a}_4 = \hat{a}_4(\hat{\omega}, t) > 0$ such that $\inf\{p_t(X_0,\ X) : X_0,\ X \in \mathbb{R}^4_+,\ |X_0|,\ |X| \leq \hat{\omega}\} \geq \hat{a}_4$. As, for any measurable set A:

$$P_t(\chi, A) = \int_A p_t(X_0, X)\mathrm{d}X \geq \hat{a}_4 \mathrm{Leb}(A \cap \mathcal{B}_{\hat{\omega}}(0)) = \hat{a}_4 \mathrm{Leb}(\mathcal{B}_{\hat{\omega}}(0))(\mathrm{Leb}(A \cap \mathcal{B}_{\hat{\omega}}(0))/\mathrm{Leb}(\mathcal{B}_{\hat{\omega}}(0))) \tag{4.7}$$

hence, condition (i) of Lemma A.1 in [25] is fulfilled. Therefore, the conclusion is arrived. □

Theorem 4.6 *The solutions of the stochastic framework (2.2) are ultimately bounded and stochastically permanent associated with the initial value* $X_0 \in \mathbb{R}^4_+$.

Proof From inequality (4.6), we have

$$\hat{U}_2(t)e^{\mathrm{d}t} \leq \hat{U}_2(0) + \frac{\hat{A}_3}{d}(e^{\mathrm{d}t} - 1). \tag{4.8}$$

After considering expectation of both sides of above inequality (4.8), it is derived that

$$\begin{aligned}
&\mathbb{E}(\hat{U}_2(t)e^{\mathrm{d}t}) \leq \mathbb{E}(\hat{U}_2(0)) + \frac{\hat{A}_3}{d}(e^{\mathrm{d}t} - 1)\\
&\Rightarrow \mathbb{E}(\hat{U}_2(t)) \leq e^{-\mathrm{d}t}\mathbb{E}(\hat{U}_2(0)) + \frac{\hat{A}_3}{d}(1 - e^{-\mathrm{d}t})\\
&\qquad\qquad \leq \mathbb{E}(\hat{U}_2(0)) + \frac{\hat{A}_3}{d}\\
&\qquad\qquad = \hat{A}_4 \ \text{(say)}.
\end{aligned} \tag{4.9}$$

Let us assume that $\hat{\zeta}$ sufficiently large s.t. $\frac{\hat{A}_4}{\hat{\zeta}} < 1$. Through implementing Chebyshev's inequality, we obtain

$$\mathbb{P}\left\{\hat{N} + \frac{1}{\hat{N}} > \hat{\zeta}\right\} \leq \frac{1}{\hat{\zeta}}\mathbb{E}\left\{\hat{N} + \frac{1}{\hat{N}}\right\} \leq \frac{\hat{A}_4}{\hat{\zeta}} := \hat{\varepsilon}. \tag{4.10}$$

The above inequality (4.10) provides that

$$1 - \hat{\varepsilon} \leq \mathbb{P}\left\{\hat{N} + \frac{1}{\hat{N}} \leq \hat{\zeta}\right\} \leq \mathbb{P}\left\{\frac{1}{\hat{\zeta}} \leq \hat{N} \leq \hat{\zeta}\right\}.$$

This is a well-established fact that $\hat{N}^2 \leq 4|X|^2 \leq 4\hat{N}^2$, hence we observe

$$\mathbb{P}\left\{\frac{1}{2\hat{\zeta}} \leq \frac{\hat{N}}{2} \leq |X| \leq \hat{N} \leq \hat{\zeta}\right\} \geq 1 - \hat{\varepsilon}. \tag{4.11}$$

Therefore, the SDE model (2.2) is ultimately bounded and stochastically permanent in accordance with Definition (3.2) and (3.6), both of which are addressed in [27]. Thus the proof comes to the end. □

5 Equilibrium point analysis of model (2.1)

System (2.1) possesses a disease-free equilibrium (DFE) point $E_0(S_{10}, S_{20}, 0, 0)$ with $S_{10} = \frac{p\Lambda}{d}$ and $S_{20} = \frac{(1-p)\Lambda}{d}$. Basic reproduction number (R_0) represents the number of newly infected people from a single infected individual in a susceptible environment. The procedure developed by van den Driessche and Watmough is usually used to obtain R_0 [28]. Let, $x \equiv (I, R)$. Then we have: $\frac{\mathrm{d}x}{\mathrm{d}t} = \mathfrak{F}(x) - \nu(x)$, where

$$\mathfrak{F}(x) = \begin{pmatrix} (1-\alpha(I))(1-D)^k(\beta_1 S_1 + \beta_2 S_2)I \\ 0 \end{pmatrix} \text{ and } \nu(x) = \begin{pmatrix} (\gamma + \mu + d + m)I - \epsilon IR \\ -\gamma I + \epsilon IR + \mathrm{d}R \end{pmatrix}.$$

Here, $\mathfrak{F}(x)$ and $\nu(x)$ contain the compartment with new infection term and rest of the terms, respectively. Then at $E_0(S_{10}, S_{20}, 0, 0)$, we have

$$F = (D\mathfrak{F}(x))_{E_0} = \begin{pmatrix} (1-D)^k(\beta_1 S_{10} + \beta_2 S_{20}) & 0 \\ 0 & 0 \end{pmatrix} \text{ and } V = (D\nu(x))_{E_0} = \begin{pmatrix} (\gamma + \mu + d + m) & 0 \\ -\gamma & d \end{pmatrix}.$$

Now, R_0 is the spectral radius of the next generation matrix FV^{-1} and is denoted by:

$$\begin{aligned}
R_0 &= R_{10} + R_{20}\\
&= \frac{(1-D)^k\beta_1 S_{10}}{(\gamma + \mu + d + m)} + \frac{(1-D)^k\beta_2 S_{20}}{(\gamma + \mu + d + m)}.
\end{aligned} \tag{5.1}$$

Endemic equilibrium point: The endemic equilibrium point $E^*(S_1^*, S_2^*, I^*, R^*)$ of system (2.1) can be obtained by solving the following equations:

$$p\Lambda - (1-\alpha(I))(1-D)^k\beta_1 S_1 I - \mathrm{d}S_1 + \theta\mu I = 0$$

$$(1-p)\Lambda-(1-\alpha(I))(1-D)^k\beta_2 S_2 I-\mathrm{d}S_2+(1-\theta)\mu I=0$$
$$(1-\alpha(I))(1-D)^k(\beta_1 S_1+\beta_2 S_2)I-p_1 I+\epsilon I R=0$$
$$\gamma I-\epsilon I R-\mathrm{d}R=0$$

where $p_1 = \gamma+\mu+d+m$. Solving, we get $R^* = \dfrac{\gamma I^*}{\epsilon I^*+d}$, $S_1^* = \dfrac{p\Lambda+\theta\mu I^*}{d+(1-\alpha(I^*))(1-D)^k\beta_1 I^*}$, $S_2^* = \dfrac{(1-p)\Lambda+(1-\theta)\mu I^*}{d+(1-\alpha(I^*))(1-D)^k\beta_2 I^*}$, and I^* is the positive root of the following equation:

$$f(I)\equiv X_1 I^5+X_2 I^4+X_3 I^3+X_4 I^2+X_5 I+X_6=0$$

where $A_1=(1-D)^k$, $A_2=\beta_1+\beta_2$, $A_3=R_0-1$, $A_4=\beta_1(\theta\mu-p_1)+\beta_2\{(1-\theta)\mu-p_1\}$, $A_5=\mu-p_1$, $A_6=1-a$

$$X_1=\epsilon A_1^2A_6^2\beta_1\beta_2(\gamma+\mu-p_1)<0$$
$$X_2=\beta_1\beta_2A_1A_6[A_1A_6[(\Lambda\epsilon+dA_5)+2b\epsilon A_1(\gamma+A_5)]+\mathrm{d}\epsilon A_1A_6(A_4+\gamma A_2)$$
$$X_3=d^2\epsilon p_1(A_3-aR_0)+\beta_1\beta_2A_1^2[2bA_6(\Lambda\epsilon+dA_5)+\Lambda\mathrm{d}A_6^2+b^2\epsilon(\gamma+A_5)]+b\mathrm{d}\epsilon A_1(\gamma A_2+A_4)(1+A_6)$$
$$+d^2(\epsilon\gamma+A_1A_4A_6)$$
$$X_4=d^3p_1(A_3-aR_0)+bd^2\epsilon p_1(2A_3-aR_0)+bd^2A_1A_4(1+A_6)+\Lambda b\beta_1\beta_2A_1^2(b\epsilon+2dA_6)+b^2\mathrm{d}\beta_1\beta_2A_1^2A_5$$
$$+bd^2\epsilon A_1(A_4+\gamma A_2)+2bd^2\epsilon\gamma$$
$$X_5=b^2d^2[\epsilon(\gamma+p_1A_3)+A_1A_4]+bd^3p_1(2A_3-aR_0)+\Lambda b^2dA_1^2\beta_1\beta_2$$
$$X_6=b^2d^3p_1(R_0-1).$$

Now, $f(0)=X_6>0$ when $R_0>1$, and $f(\infty)=-\infty$. So, there will be at least one positive root of the equation for $R_0>1$. It means system (2.1) contains at least one endemic equilibrium point $E^*(S_1^*, S_2^*, I^*, R^*)$ when basic reproduction number exceeds unity.

6 Local sensitivity analysis

The basic reproduction number (R_0) depends on some of the model parameters, and hence, analysis of the implication of system parameters on disease propagation has its own importance. The basic reproduction number for (2.1) is $R_0 = \dfrac{(1-D)^k(\beta_1 S_{10}+\beta_2 S_{20})}{p_1}$, where $p_1=(\gamma+\mu+d+m)$, $S_{10}=\dfrac{p\Lambda}{d}$ and $S_{20}=\dfrac{(1-p)\Lambda}{d}$. Hence we have:

$$\frac{\partial R_0}{\partial\beta_1}=\frac{(1-D)^kS_{10}}{p_1}>0,\quad \frac{\partial R_0}{\partial\beta_2}=\frac{(1-D)^kS_{20}}{p_1}>0,$$
$$\frac{\partial R_0}{\partial D}=-\frac{k(1-D)^{k-1}(\beta_1S_{10}+\beta_2S_{20})}{p_1}<0,\quad \frac{\partial R_0}{\partial\gamma}=-\frac{(1-D)^k(\beta_1S_{10}+\beta_2S_{20})}{p_1^2}<0$$
$$\frac{\partial R_0}{\partial k}=\frac{(1-D)^k(\beta_1S_{10}+\beta_2S_{20})\ln(1-D)}{p_1}<0\ (\text{since } 0<D<1\Rightarrow\ln(1-D)<0).$$

The normalized forward sensitivity indices for the sytem parameters are provided as follows [29]:

$$\Gamma_{\beta_1}=\left[\frac{\frac{\partial R_0}{R_0}}{\frac{\partial\beta_1}{\beta_1}}\right]=\left[\frac{\beta_1}{R_0}\frac{\partial R_0}{\partial\beta_1}\right]=\frac{\beta_1S_{10}}{(\beta_1S_{10}+\beta_2S_{20})},\quad \Gamma_{\beta_2}=\left[\frac{\frac{\partial R_0}{R_0}}{\frac{\partial\beta_2}{\beta_2}}\right]=\left[\frac{\beta_2}{R_0}\frac{\partial R_0}{\partial\beta_2}\right]=\frac{\beta_2S_{20}}{(\beta_1S_{10}+\beta_2S_{20})}$$
$$\Gamma_D=\left[\frac{\frac{\partial R_0}{R_0}}{\frac{\partial D}{D}}\right]=\left[\frac{D}{R_0}\frac{\partial R_0}{\partial D}\right]=-\left(\frac{kD}{1-D}\right),\quad \Gamma_\gamma=\left[\frac{\frac{\partial R_0}{R_0}}{\frac{\partial\gamma}{\gamma}}\right]=\left[\frac{\gamma}{R_0}\frac{\partial R_0}{\partial\gamma}\right]=-\frac{\gamma}{p_1}$$
$$\Gamma_k=\left[\frac{\frac{\partial R_0}{R_0}}{\frac{\partial k}{k}}\right]=\left[\frac{k}{R_0}\frac{\partial R_0}{\partial k}\right]=k\ln(1-D).$$

It is observed that the disease transmission rates (β_1, β_2) maintain a direct proportional relation with R_0. It is relevant as higher contact rate increases the chance of people becoming infected. And this situation ultimately leads to an endemic system with high disease prevalence. On the other hand, if people opt for some changes in their social behavior to save themselves from becoming infected, then the higher propagation will be restrained with time. In a similar manner, increased rate of propagation may be decreased if the individual starts to respond to the necessary precautionary measures during the period of ailment prevalence. Lastly, a higher

recovery rate leads to a system with lesser count of infected people. Recovery of a higher portion of infected population, through natural immunity, or by pharmaceutical therapy, control the infection fatality with time.

7 Stability analysis

7.1 Dynamics of model (2.1)

According to Routh–Hurwitz criterion, a particular steady state point of a system is considered to be locally asymptotically stable (LAS) whether all the eigenvalues of the Variational matrix that corresponds to it contain negative real parts. Let, $p_1 = \gamma + \mu + d + m$. The Jacobian matrix of system (2.1) is:

$$\overline{J} = \begin{pmatrix} a_{11} & 0 & a_{13} & 0 \\ 0 & a_{22} & a_{23} & 0 \\ a_{31} & a_{32} & a_{33} & a_{34} \\ 0 & 0 & a_{43} & a_{44} \end{pmatrix} \tag{7.1}$$

where $a_{11} = -d - (1-\alpha(I))(1-D)^k\beta_1 I$, $a_{13} = -(1-\alpha(I))(1-D)^k\beta_1 S_1 + \frac{abI}{(b+I)^2}(1-D)^k\beta_1 S_1 + \theta\mu$, $a_{22} = -d - (1-\alpha(I))(1-D)^k\beta_2 I$, $a_{23} = -(1-\alpha(I))(1-D)^k\beta_2 S_2 + \frac{abI}{(b+I)^2}(1-D)^k\beta_2 S_2 + (1-\theta)\mu$, $a_{31} = (1-\alpha(I))(1-D)^k\beta_1 I$, $a_{32} = (1-\alpha(I))(1-D)^k\beta_2 I$, $a_{33} = \left[(1-\alpha(I)) - \frac{abI}{(b+I)^2}\right](1-D)^k(\beta_1 S_1 + \beta_2 S_2) - p_1 + \epsilon R$, $a_{34} = \epsilon I$, $a_{43} = \gamma - \epsilon R$, $a_{44} = -(\epsilon I + d)$.

Theorem 7.1 *The disease-free steady state* (E_0) *is LAS if* $R_0 < 1$.

Proof At DFE, $E_0 \equiv (S_{10}, S_{20}, 0, 0)$ with $S_{10} = \frac{p\Lambda}{d}$ and $S_{20} = \frac{(1-p)\Lambda}{d}$, the Jacobian matrix is:

$$\overline{J}|_{E_0} = \begin{pmatrix} -d & 0 & -(1-D)^k\beta_1 S_{10} + \theta\mu & 0 \\ 0 & -d & -(1-D)^k\beta_2 S_{20} + (1-\theta)\mu & 0 \\ 0 & 0 & (1-D)^k(\beta_1 S_{10} + \beta_2 S_{20}) - p_1 & 0 \\ 0 & 0 & \gamma & -d \end{pmatrix}.$$

The eigenvalues of $\overline{J}|_{E_0}$ are $\lambda_1 = \lambda_2 = \lambda_3 = -d$ and $\lambda_4 = p_1(R_0 - 1)$. So, $\lambda_i < 0$, for $i = 1, 2, 3$, and $\lambda_4 < 0$ when $R_0 < 1$. □

Theorem 7.2 *The interior equilibrium* (E^*) *is locally asymptotically stable under the conditions stated in the proof.*

Proof At E^*, the variational matrix is represented as follows:

$$\overline{J}|_{E^*} = \begin{pmatrix} a_{11} & 0 & a_{13} & 0 \\ 0 & a_{22} & a_{23} & 0 \\ a_{31} & a_{32} & a_{33} & a_{34} \\ 0 & 0 & a_{43} & a_{44} \end{pmatrix}$$

where $a_{11} = -d - (1-\alpha(I^*))(1-D)^k\beta_1 I^*$, $a_{13} = -(1-\alpha(I^*))(1-D)^k\beta_1 S_1^* + \frac{abI^*}{(b+I^*)^2}(1-D)^k\beta_1 S_1^* + \theta\mu$, $a_{22} = -d - (1-\alpha(I^*))(1-D)^k\beta_2 I^*$, $a_{23} = -(1-\alpha(I^*))(1-D)^k\beta_2 S_2^* + \frac{abI^*}{(b+I^*)^2}(1-D)^k\beta_2 S_2^* + (1-\theta)\mu$, $a_{31} = (1-\alpha(I^*))(1-D)^k\beta_1 I^*$, $a_{32} = (1-\alpha(I^*)(1-D)^k\beta_2 I^*$, $a_{33} = \left[(1-\alpha(I^*)) - \frac{abI^*}{(b+I^*)^2}\right](1-D)^k(\beta_1 S_1^* + \beta_2 S_2^*) - p_1 + \epsilon R^* = -\frac{abI^*}{(b+I^*)^2}(\beta_1 S_1^* + \beta_2 S_2^*)$, $a_{34} = \epsilon I^*$, $a_{43} = \gamma - \epsilon R^*$, $a_{44} = -(\epsilon I^* + d)$.

Characteristic equation corresponding to $\overline{J}|_{E^*}$ is $\lambda^4 + A_1\lambda^3 + A_2\lambda^2 + A_3\lambda + A_4 = 0$, where

$$\begin{aligned} A_1 &= -(a_{11} + a_{22} + a_{33} + a_{44}) > 0 \\ A_2 &= (a_{11} + a_{22})(a_{33} + a_{44}) + a_{11}a_{22} + a_{33}a_{44} - a_{13}a_{31} - a_{23}a_{32} - a_{34}a_{43} \\ A_3 &= a_{23}a_{32}(a_{11} + a_{44}) + a_{13}a_{31}(a_{22} + a_{44}) - a_{11}a_{22}(a_{33} + a_{44}) - (a_{11} + a_{22})(a_{33}a_{44} - a_{34}a_{43}) \\ A_4 &= a_{11}a_{22}(a_{33}a_{44} - a_{34}a_{43}) - a_{44}(a_{11}a_{23}a_{32} + a_{22}a_{13}a_{31}). \end{aligned}$$

The equation have roots with negative real parts only when Routh–Hurwitz criterion is satisfied. Hence, the endemic state E^* is LAS if $A_1 > 0$, $A_4 > 0$, $A_1A_2 > A_3$ and $A_3(A_1A_2 - A_3) > A_1^2A_4$. □

7.2 Dynamics of model (2.2)

Next, we are going to focus on the dynamical characteristics of stochastic differential system (2.2) and establish certain findings relating the eradication of the ailment, stationary distribution as well as ergodicity, etc.

Infection-free dynamics of model (2.2): In the field of epidemiology, one of the foremost important issues to investigate whether or not it is possible to exert control over the evolution of a disease to eliminate it permanently over time. The condition $R_0 < 1$ does not indicate that infections have been eradicated from population in case of SDE system (2.2). Furthermore, the circumstances that result in the annihilation of disease for model (2.2) have been outlined here. First of all, let us introduce a term for the SDE model (2.2):

$$\hat{R}_s = \frac{1}{(\gamma+\mu+d+m)}\left[(1-D)^k(\beta_1+\beta_2)\frac{\Lambda}{d} + \frac{\epsilon\Lambda}{d} - \frac{\nu_3^2}{2}\right]. \tag{7.2}$$

Theorem 7.3 *The infectious population will die out in the long term if* $\hat{R}_s < 1$, *for any initial condition* $X_0 \in \mathbb{R}^4_+$.

Proof Assuming $\hat{U}_3(t) = \ln I(t)$ and employing Ito'*s* formula for 2nd equation of system (2.2):

$$\begin{aligned} d(\ln I(t)) &= \left\{\left(1-\frac{aI}{b+I}\right)(1-D)^k(\beta_1 S_1+\beta_2 S_2) - (\gamma+\mu+d+m) + \epsilon R - \frac{\nu_3^2}{2}\right\}\mathrm{d}t + \nu_3 \mathrm{d}W_3(t) \\ &\le \left\{(1-D)^k(\beta_1+\beta_2)\frac{\Lambda}{d} - (\gamma+\mu+d+m) + \frac{\epsilon\Lambda}{d} - \frac{\nu_3^2}{2}\right\}\mathrm{d}t + \nu_3 \mathrm{d}W_3(t). \end{aligned} \tag{7.3}$$

Hence

$$\begin{aligned} \ln I(t) &\le \ln I(0) + \int_0^t \left\{(1-D)^k(\beta_1+\beta_2)\frac{\Lambda}{d} - (\gamma+\mu+d+m) + \frac{\epsilon\Lambda}{d} - \frac{\nu_3^2}{2}\right\}\mathrm{d}s + \int_0^t \nu_3 \mathrm{d}W_3(s) \\ &= \ln I(0) + \left\{(1-D)^k(\beta_1+\beta_2)\frac{\Lambda}{d} - (\gamma+\mu+d+m) + \frac{\epsilon\Lambda}{d} - \frac{\nu_3^2}{2}\right\}t + M_1(t). \end{aligned} \tag{7.4}$$

It can be derived that $\limsup_{t\to\infty} \frac{M_1(t)}{t} = 0$ with probability one, by implementing a rigorous application of strong law of large numbers of martingales [24]. Consequently, it might be determined that

$$\frac{\ln I(t)}{t} \le \frac{\ln I(0)}{t} + \left\{(1-D)^k(\beta_1+\beta_2)\frac{\Lambda}{d} - (\gamma+\mu+d+m) + \frac{\epsilon\Lambda}{d} - \frac{\nu_3^2}{2}\right\} + \frac{M_1(t)}{t} \tag{7.5}$$

afterward making $t \to \infty$:

$$\limsup_{t\to\infty} \frac{\ln I(t)}{t} \le \left\{(1-D)^k(\beta_1+\beta_2)\frac{\Lambda}{d} - (\gamma+\mu+d+m) + \frac{\epsilon\Lambda}{d} - \frac{\nu_3^2}{2}\right\}. \tag{7.6}$$

Now, $\hat{R}_s < 1$ gives $\limsup_{t\to\infty} \frac{\ln I(t)}{t} < 0$ a.s. This implies $\lim_{t\to\infty} I(t) = 0$, a.s. As an outcome, the diseased population $I(t)$ eventually disappears over time. □

Remark 1 Theorem 7.3 states that the contagious species population will go extinct gradually with probability one if $\hat{R}_s < 1$ along with the notion that $R(t)$ becomes die out a.s. As a consequence of this, Theorem 7.3 generates a scenario in which the solutions of stochastic framework (2.2) are becoming progressively approach to disease-free situation. In this case, it can be noticed that the influence of social behavioral dynamics and public reaction, in addition to high level of noise, have a stronger effect on eradication of illness.

Existence of ergodic stationary distribution: Now, we will establish sufficient conditions for the existence of a unique ergodic stationary distribution. First of all, the following Lemma 7.4 and Assumption 1 will be needed.

Lemma 7.4 [30] *The Markov process X(t) has a unique ergodic stationary distribution* $\pi(\cdot)$ *if* $\exists$ *a bounded region* $\Gamma \subset \mathbb{R}^4_+$ *with boundary* $\partial\Gamma$ *and*

(i) there exists a number $\hat{M} > 0$ *s.t.* $\sum_{j,i=1}^4 a_{ji}(x)\theta_j\theta_i \ge \hat{M}|\theta|^2,\ x \in \Gamma,\ \theta \in \mathbb{R}^4_+$

(ii) $\exists$ *a non-negative* $\mathbb{C}^2$*-function V s.t. LV is negative for any* $x \in \mathbb{R}^4_+\backslash\Gamma$. *Then*

$$\mathbb{P}_x\left\{\lim_{\hat{T}\to\infty}\frac{1}{\hat{T}}\int_0^{\hat{T}} f(X(t))dt = \int_{\mathbb{R}^4_+} f(x)\pi(dx)\right\} = 1 \tag{7.7}$$

$\forall\, x \in \mathbb{R}^4_+$, *where* $f(\cdot)$ *is a function integrable w.r.t. the measure* π.

Assumption 1 *Let us define,* $\hat{b}_* := \left(d+\frac{\nu_1^2}{2}\right)^{1/2}\left\{2\left(\frac{\Lambda(1-a)(1-D)^k}{\gamma+\mu+d+m+\frac{\nu_3^2}{2}}\right)^{1/2}\left[(p\beta_1)^{1/2}+\left\{(1-p)\beta_2\frac{\left(d+\frac{\nu_1^2}{2}\right)}{\left(d+\frac{\nu_2^2}{2}\right)}\right\}^{1/2}\right]-3(d+\frac{\nu_1^2}{2})^{1/2}\right\}$, *assume that* $\hat{b}_* > 0$.

Theorem 7.5 *Suppose, Assumption 1 holds, then system (2.2) has a unique stationary distribution* $\pi(\cdot)$ *and it has the ergodic property.*

Proof To prove Theorem 7.5, we only need to validate the conditions (i) and (ii) in Lemma 7.4. We first verify the condition (i). Choose, $\hat{M} = \min\{\nu_1^2S_1^2,\ \nu_2^2S_2^2,\ \nu_3^2I^2,\ \nu_4^2R^2\} > 0$ such that

$$\sum_{j,i=1}^{4} a_{ji}(S_1, S_2, I, R)\theta_j\theta_i = \nu_1^2S_1^2\theta_1^2 + \nu_2^2S_2^2\theta_2^2 + \nu_3^2I^2\theta_3^2 + \nu_4^2R^2\theta_4^2 \geq \hat{M}|\theta|^2 \tag{7.8}$$

$(S_1,\ S_2,\ I,\ R) \in \Gamma \subset \mathbb{R}_+^4$, $\theta = (\theta_1,\ \theta_2,\ \theta_3,\ \theta_4) \in \mathbb{R}_+^4$. Then, the condition (i) in Lemma 7.4 is verified. Next, our aim is to establish condition (ii) of Lemma 7.4.

Assume a $\mathbb{C}^2$-function $\hat{U}_4 : \mathbb{R}_+^4 \to \mathbb{R}^4$ as follows:

$$\begin{aligned}\hat{U}_4(S_1,\ S_2,\ I,\ R) &= \hat{M}(-\ln S_1 - \hat{c}_2\ln S_2 - \hat{c}_3\ln I) + \frac{1}{\hat{\rho}+1}(S_1+S_2+I+R)^{\hat{\rho}+1} - \ln S_1 - \ln S_2 - \ln R\\ &:= \hat{M}\hat{U}_5 + \hat{U}_6 + \hat{U}_7 + \hat{U}_8 + \hat{U}_9\end{aligned}$$

where

$$\begin{aligned}&\hat{U}_5 = -\ln S_1 - \hat{c}_2\ln S_2 - \hat{c}_3\ln I, \quad \hat{U}_6 = \frac{1}{\hat{\rho}+1}(S_1+S_2+I+R)^{\hat{\rho}+1}\\ &\hat{U}_7 = -\ln S_1, \quad \hat{U}_8 = -\ln S_2, \quad \hat{U}_9 = -\ln R\\ &\hat{c}_2 = \frac{d+\frac{\nu_1^2}{2}}{d+\frac{\nu_2^2}{2}}, \quad \hat{c}_3 = \frac{d+\frac{\nu_1^2}{2}}{\gamma+\mu+d+m+\frac{\nu_3^2}{2}}.\end{aligned} \tag{7.9}$$

$\hat{M}$ and $\hat{\rho}$ are constants satisfying the following conditions:

$$-\hat{M}\hat{b}_1 + \hat{B} + 3d + \frac{\nu_1^2+\nu_2^2+\nu_4^2}{2} \leq -2, \ \text{ where } \hat{b}_1 = 2\left(d+\frac{\nu_1^2}{2}\right)^{1/2}\hat{b}_* \tag{7.10}$$

$$\hat{f} := d - \frac{\hat{\rho}}{2}(\nu_1^2 \vee \nu_2^2 \vee \nu_3^2 \vee \nu_4^2) > 0 \tag{7.11}$$

and

$$\hat{B} = \sup\left\{\Lambda(S_1+S_2+I+R)^{\hat{\rho}} - \frac{1}{2}\hat{f}(S_1+S_2+I+R)^{\hat{\rho}+1}\right\} < \infty. \tag{7.12}$$

It can be easily verified that

$$\liminf_{\hat{k}\to\infty,(S_1,S_2,I,R)\in\mathbb{R}_+^4\setminus U_{\hat{k}}} \hat{U}_4(S_1,\ S_2,\ I,\ R) = \infty,$$

where, $U_{\hat{k}} = \left(\frac{1}{\hat{k}}, \hat{k}\right)\times\left(\frac{1}{\hat{k}}, \hat{k}\right)\times\left(\frac{1}{\hat{k}}, \hat{k}\right)\times\left(\frac{1}{\hat{k}}, \hat{k}\right)$. Moreover, the function $\hat{U}_4(S_1,\ S_2,\ I,\ R)$ is continuous. Thus, $\hat{U}_4(S_1,\ S_2,\ I,\ R)$ must has a minimum point $(S_1(0),\ S_2(0),\ I(0),\ R(0))$ in the interior of $\mathbb{R}_+^4$. Then we define a non-negative $\mathbb{C}^2$-function $\hat{U}_{10} : \mathbb{R}_+^4 \to \mathbb{R}^4$ as follows:

$$\hat{U}_{10}(S_1,\ S_2,\ I,\ R) = \hat{U}_4(S_1,\ S_2,\ I,\ R) - \hat{U}_4(S_1(0),\ S_2(0),\ I(0),\ R(0)).$$

Using $It\hat{o}'s$ formula, we get

$$\begin{aligned}L\hat{U}_5 = &-\left[\frac{p\Lambda}{S_1} - (1-\alpha(I))(1-D)^k\beta_1I + \frac{\theta\mu I}{S_1} - d\right] - \left[\frac{\hat{c}_2(1-p)\Lambda}{S_2} - \hat{c}_2(1-\alpha(I))(1-D)^k\beta_2I\right.\\ &\left.+\frac{\hat{c}_2(1-\theta)\mu I}{S_2} - \hat{c}_2d\right] - \left[\hat{c}_3(1-\alpha(I))(1-D)^k(\beta_1S_1+\beta_2S_2) - \hat{c}_3(\gamma+\mu+d+m) + \hat{c}_3\epsilon R\right]\\ &+\frac{\nu_1^2}{2} + \frac{\hat{c}_2}{2}\nu_2^2 + \frac{\hat{c}_3}{2}\nu_3^2\end{aligned}$$

$$\leq -\left[\frac{p\Lambda}{S_1} - (1-\alpha(I))(1-D)^k\beta_1 I + \frac{\theta\mu I}{S_1} - d\right] - \left[\frac{\hat{c}_2(1-p)\Lambda}{S_2} - \hat{c}_2(1-\alpha(I))(1-D)^k\beta_2 I + \frac{\hat{c}_2(1-\theta)\mu I}{S_2} - \hat{c}_2 d\right] - \left[\hat{c}_3(1-a)(1-D)^k(\beta_1 S_1 + \beta_2 S_2) - \hat{c}_3(\gamma+\mu+d+m) + \hat{c}_3\epsilon R\right] + \frac{\nu_1^2}{2} + \frac{\hat{c}_2}{2}\nu_2^2 + \frac{\hat{c}_3}{2}\nu_3^2$$

$$= -\left[\frac{p\Lambda}{S_1} + \hat{c}_3(1-a)(1-D)^k\beta_1 S_1 + \frac{\hat{c}_2(1-p)\Lambda}{S_2} + \hat{c}_3(1-a)(1-D)^k\beta_2 S_2\right] + (1-\alpha(I))(1-D)^k\beta_1 I + \hat{c}_2(1-\alpha(I))(1-D)^k\beta_2 I - \frac{\theta\mu I}{S_1} - \frac{\hat{c}_2(1-\theta)\mu I}{S_2} - \hat{c}_3\epsilon R + \left(d + \frac{\nu_1^2}{2}\right) + \hat{c}_2\left(d + \frac{\nu_2^2}{2}\right) + \hat{c}_3\left(\gamma+\mu+d+m+\frac{\nu_3^2}{2}\right).$$

The inequality $AM \geq GM$, leads to

$$L\hat{U}_5 \leq -2\left\{\left[\hat{c}_3\Lambda(1-a)(1-D)^k\right]^{1/2}\left[(p\beta_1)^{1/2} + \{\hat{c}_2(1-p)\beta_2\}^{1/2}\right]\right\} + (1-D)^k\left[\beta_1 + \hat{c}_2\beta_2\right]I - \frac{\theta\mu I}{S_1} - \frac{\hat{c}_2(1-\theta)\mu I}{S_2} + \left(d + \frac{\nu_1^2}{2}\right) + \hat{c}_2\left(d + \frac{\nu_2^2}{2}\right) + \hat{c}_3\left(\gamma+\mu+d+m+\frac{\nu_3^2}{2}\right).$$

Using the expressions of $\hat{c}_2$ and $\hat{c}_3$ from (7.9), it is obtained that

$$L\hat{U}_5 \leq -\left(d + \frac{\nu_1^2}{2}\right)^{1/2}\left\{2\left(\frac{\Lambda(1-a)(1-D)^k}{\gamma+\mu+d+m+\frac{\nu_3^2}{2}}\right)^{1/2}\left[(p\beta_1)^{1/2} + \left\{(1-p)\beta_2\frac{(d+\frac{\nu_1^2}{2})}{(d+\frac{\nu_2^2}{2})}\right\}^{1/2}\right] - 3(d+\tfrac{\nu_1^2}{2})^{1/2}\right\} + (1-D)^k\left[\beta_1 + \hat{c}_2\beta_2\right]I - \frac{\theta\mu I}{S_1} - \frac{\hat{c}_2(1-\theta)\mu I}{S_2}$$

$$= -\hat{b}_1 + (1-D)^k\left[\beta_1 + \hat{c}_2\beta_2\right]I - \frac{\theta\mu I}{S_1} - \frac{\hat{c}_2(1-\theta)\mu I}{S_2}. \tag{7.13}$$

In addition, we have

$$L\hat{U}_6 = (S_1+S_2+I+R)^{\hat{\rho}}\left[\Lambda - \mathrm{d}S_1 - \mathrm{d}S_2 - (d+m)I - \mathrm{d}R\right] + \frac{1}{2}\rho(S_1+S_2+I+R)^{\hat{\rho}-1}(\nu_1^2S_1^2 + \nu_2^2S_2^2 + \nu_3^2I^2 + \nu_4^2R^2).$$

Using: $\nu_i^2 \leq (\nu_1^2 \vee \nu_2^2 \vee \nu_3^2 \vee \nu_4^2)$, for $i = 1, 2, 3, 4$, we get

$$L\hat{U}_6 \leq (S_1+S_2+I+R)^{\hat{\rho}}\left[\Lambda - d(S_1+S_2+I+R)\right] + \frac{1}{2}\rho(\nu_1^2 \vee \nu_2^2 \vee \nu_3^2 \vee \nu_4^2)(S_1+S_2+I+R)^{\hat{\rho}+1}$$

$$= \Lambda(S_1+S_2+I+R)^{\hat{\rho}} - (S_1+S_2+I+R)^{\hat{\rho}+1}\left[d - \frac{\hat{\rho}}{2}(\nu_1^2 \vee \nu_2^2 \vee \nu_3^2 \vee \nu_4^2)\right]$$

$$\leq \hat{B} - \frac{1}{2}\hat{f}(S_1+S_2+I+R)^{\hat{\rho}+1} \tag{7.14}$$

where $\hat{f}$ and $\hat{B}$ are mentioned in (7.11) and (7.12), respectively. Similarly

$$L\hat{U}_7 = -\frac{1}{S_1}\left[p\Lambda - (1-\alpha(I))(1-D)^k\beta_1 S_1 I + \theta\mu I - \mathrm{d}S_1\right] + \frac{\nu_1^2}{2}$$

$$\leq -\frac{p\Lambda}{S_1} + (1-D)^k\beta_1 I - \frac{\theta\mu I}{S_1} + d + \frac{\nu_1^2}{2} \tag{7.15}$$

$$L\hat{U}_8 \leq -\frac{(1-p)\Lambda}{S_2} + (1-D)^k\beta_2 I - \frac{(1-\theta)\mu I}{S_2} + d + \frac{\nu_2^2}{2} \tag{7.16}$$

$$L\hat{U}_9 \leq -\frac{\gamma I}{R} + \epsilon I + d + \frac{\nu_4^2}{2}. \tag{7.17}$$

Therefore, combining (7.13)–(7.17), we obtain

$$L\hat{U}_{10} \leq -\hat{M}\hat{b}_1 + \hat{B} + 3d + \frac{\nu_1^2+\nu_2^2+\nu_4^2}{2} + \left\{\hat{M}(1-D)^k\left[\beta_1 + \hat{c}_2\beta_2\right] + \epsilon\right\}I - \frac{1}{2}\hat{f}(S_1+S_2+I+R)^{\hat{\rho}+1}$$

$$
\begin{aligned}
&-(\hat{M}+1)\frac{\theta\mu I}{S_1}-(\hat{M}\hat{c}_2+1)\frac{(1-\theta)\mu I}{S_2}-\frac{p\Lambda}{S_1}-\frac{(1-p)\Lambda}{S_2}+(1-D)^k(\beta_1+\beta_2)I-\frac{\gamma I}{R}\\
&=-2\hat{M}\left(d+\frac{\nu_1^2}{2}\right)^{1/2}\left\{\left(\frac{\Lambda(1-\alpha)(1-D)^k}{\gamma+\mu+d+m+\frac{\nu_3^2}{2}}\right)^{1/2}\left[(p\beta_1)^{1/2}+\left\{(1-p)\beta_2\frac{(d+\frac{\nu_1^2}{2})}{(d+\frac{\nu_2^2}{2})}\right\}^{1/2}\right]-(d+\frac{\nu_1^2}{2})^{1/2}\right\}\\
&+\hat{B}+3d+\frac{\nu_1^2+\nu_2^2+\nu_4^2}{2}+\left[(1-D)^k\{(\hat{M}+1)\beta_1+(\hat{M}\hat{c}_2+1)\beta_2\}+\epsilon\right]I-\frac{1}{2}\hat{f}(S_1+S_2+I+R)^{\hat{\rho}+1}\\
&-(\hat{M}+1)\frac{\theta\mu I}{S_1}-(\hat{M}\hat{c}_2+1)\frac{(1-\theta)\mu I}{S_2}-\frac{p\Lambda}{S_1}-\frac{(1-p)\Lambda}{S_2}-\frac{\gamma I}{R}. \qquad (7.18)
\end{aligned}
$$

Now, we are in the position to construct a compact subset $\hat{D}$ such that the condition (ii) in Lemma 7.4 holds. Define the bounded closed set

$$\hat{D}=\left\{\varepsilon_1\le S_1\le\frac{1}{\varepsilon_1},\ \varepsilon_1\le S_2\le\frac{1}{\varepsilon_1},\ \varepsilon_1\le I\le\frac{1}{\varepsilon_1},\ \varepsilon_2\le R\le\frac{1}{\varepsilon_2}\right\}$$

where $0<\varepsilon_i<1$, for $i=1,2$, are sufficiently small. In the set $\mathbb{R}^4_+\backslash\hat{D}$ we can choose ε_1, ε_2 sufficiently small such that the following conditions hold:

$$2\hat{M}\left(d+\frac{\nu_1^2}{2}\right)+\hat{B}+3d+\frac{\nu_1^2+\nu_2^2+\nu_4^2}{2}+\left[(1-D)^k\{(\hat{M}+1)\beta_1+(\hat{M}\hat{c}_2+1)\beta_2\}+\epsilon\right]\frac{\Lambda}{d}-\frac{p\Lambda}{\varepsilon_1}\le-1 \qquad (7.19)$$

$$2\hat{M}\left(d+\frac{\nu_1^2}{2}\right)+\hat{B}+3d+\frac{\nu_1^2+\nu_2^2+\nu_4^2}{2}+\left[(1-D)^k\{(\hat{M}+1)\beta_1+(\hat{M}\hat{c}_2+1)\beta_2\}+\epsilon\right]\frac{\Lambda}{d}-\frac{(1-p)\Lambda}{\varepsilon_1}\le-1 \qquad (7.20)$$

$$-\hat{M}\hat{b}_1+\hat{B}+3d+\frac{\nu_1^2+\nu_2^2+\nu_4^2}{2}+\left[(1-D)^k\{(\hat{M}+1)\beta_1+(\hat{M}\hat{c}_2+1)\beta_2\}+\epsilon\right]\varepsilon_1\le-1 \qquad (7.21)$$

$$2\hat{M}\left(d+\frac{\nu_1^2}{2}\right)+\hat{B}+3d+\frac{\nu_1^2+\nu_2^2+\nu_4^2}{2}+\left[(1-D)^k\{(\hat{M}+1)\beta_1+(\hat{M}\hat{c}_2+1)\beta_2\}+\epsilon\right]\frac{\Lambda}{d}-\frac{\gamma}{\varepsilon_1}\le-1 \qquad (7.22)$$

$$2\hat{M}\left(d+\frac{\nu_1^2}{2}\right)+\hat{B}+3d+\frac{\nu_1^2+\nu_2^2+\nu_4^2}{2}+\left[(1-D)^k\{(\hat{M}+1)\beta_1+(\hat{M}\hat{c}_2+1)\beta_2\}+\epsilon\right]\frac{\Lambda}{d}-\frac{\hat{f}}{2\varepsilon_1^{\rho+1}}\le-1 \qquad (7.23)$$

$$2\hat{M}\left(d+\frac{\nu_1^2}{2}\right)+\hat{B}+3d+\frac{\nu_1^2+\nu_2^2+\nu_4^2}{2}+\left[(1-D)^k\{(\hat{M}+1)\beta_1+(\hat{M}\hat{c}_2+1)\beta_2\}+\epsilon\right]\frac{\Lambda}{d}-\frac{\hat{f}}{2\varepsilon_1^{2(\rho+1)}}\le-1. \qquad (7.24)$$

Note that for sufficiently small ε_1, the condition (7.21) holds due to (7.10). For convenience, we divide $\mathbb{R}^4_+\backslash\hat{D}$ into eight domains

$$\hat{D}_1=\left\{(S_1,\,S_2,\,I,\,R)\in\mathbb{R}^4_+:0<S_1<\varepsilon_1\right\},\quad \hat{D}_2=\left\{(S_1,\,S_2,\,I,\,R)\in\mathbb{R}^4_+:0<S_2<\varepsilon_1\right\}$$

$$\hat{D}_3=\left\{(S_1,\,S_2,\,I,\,R)\in\mathbb{R}^4_+:0<I<\varepsilon_1\right\},\quad \hat{D}_4=\left\{(S_1,\,S_2,\,I,\,R)\in\mathbb{R}^4_+:I\ge\varepsilon_1,\ 0<R<\varepsilon_2\right\}$$

$$\hat{D}_5=\left\{(S_1,\,S_2,\,I,\,R)\in\mathbb{R}^4_+:S_1>\frac{1}{\varepsilon_1}\right\},\quad \hat{D}_6=\left\{(S_1,\,S_2,\,I,\,R)\in\mathbb{R}^4_+:S_2>\frac{1}{\varepsilon_1}\right\}$$

$$\hat{D}_7=\left\{(S_1,\,S_2,\,I,\,R)\in\mathbb{R}^4_+:I>\frac{1}{\varepsilon_1}\right\},\quad \hat{D}_8=\left\{(S_1,\,S_2,\,I,\,R)\in\mathbb{R}^4_+:R>\frac{1}{\varepsilon_2}\right\}.$$

Now, we shall establish that $L\hat{U}_{10}(S_1,\,S_2,\,I,\,R)\le-1$ in $\mathbb{R}^4_+\backslash\hat{D}$, which is similar to verify in the aforementioned eight regions.

Case 1: If $(S_1,\,S_2,\,I,\,R)\in\hat{D}_1$, one can get that

$$
\begin{aligned}
L\hat{U}_{10}&\le 2\hat{M}\left(d+\frac{\nu_1^2}{2}\right)+\hat{B}+3d+\frac{\nu_1^2+\nu_2^2+\nu_4^2}{2}+\left[(1-D)^k\{(\hat{M}+1)\beta_1+(\hat{M}\hat{c}_2+1)\beta_2\}+\epsilon\right]I-\frac{p\Lambda}{S_1}\\
&\le 2\hat{M}\left(d+\frac{\nu_1^2}{2}\right)+\hat{B}+3d+\frac{\nu_1^2+\nu_2^2+\nu_4^2}{2}+\left[(1-D)^k\{(\hat{M}+1)\beta_1+(\hat{M}\hat{c}_2+1)\beta_2\}+\epsilon\right]\frac{\Lambda}{d}-\frac{p\Lambda}{\varepsilon_1}.
\end{aligned}
$$

Then it follows from (7.19) that

$$L\hat{U}_{10}\le-1,\ \text{ for any } (S_1,\,S_2,\,I,\,R)\in\hat{D}_1.$$

Case 2: If $(S_1,\,S_2,\,I,\,R)\in\hat{D}_2$, we have

$$L\hat{U}_{10}\le 2\hat{M}\left(d+\frac{\nu_1^2}{2}\right)+\hat{B}+3d+\frac{\nu_1^2+\nu_2^2+\nu_4^2}{2}+\left[(1-D)^k\{(\hat{M}+1)\beta_1+(\hat{M}\hat{c}_2+1)\beta_2\}+\epsilon\right]I-\frac{(1-p)\Lambda}{S_2}$$

$$\leq 2\hat{M}\left(d+\frac{\nu_1^2}{2}\right)+\hat{B}+3d+\frac{\nu_1^2+\nu_2^2+\nu_4^2}{2}+\left[(1-D)^k\{(\hat{M}+1)\beta_1+(\hat{M}\hat{c}_2+1)\beta_2\}+\epsilon\right]\frac{\Lambda}{d}-\frac{(1-p)\Lambda}{\varepsilon_1}.$$

In view of (7.20), it can be deducted for any sufficiently small ε_1:

$$L\hat{U}_{10}\leq -1,\ \text{ for any } (S_1,\ S_2,\ I,\ R)\in \hat{D}_2.$$

Case 3: If $(S_1,\ S_2,\ I,\ R)\in \hat{D}_3$, one may see

$$\begin{aligned}L\hat{U}_{10}&\leq -\hat{M}\hat{b}_1+\hat{B}+3d+\frac{\nu_1^2+\nu_2^2+\nu_4^2}{2}+\left[(1-D)^k\{(\hat{M}+1)\beta_1+(\hat{M}\hat{c}_2+1)\beta_2\}+\epsilon\right]I\\&\leq -\hat{M}\hat{b}_1+\hat{B}+3d+\frac{\nu_1^2+\nu_2^2+\nu_4^2}{2}+\left[(1-D)^k\{(\hat{M}+1)\beta_1+(\hat{M}\hat{c}_2+1)\beta_2\}+\epsilon\right]\varepsilon_1.\end{aligned}$$

According to the condition (7.21), one can get that

$$L\hat{U}_{10}\leq -1,\ \text{ for any } (S_1,\ S_2,\ I,\ R)\in \hat{D}_3.$$

Case 4: If $(S_1,\ S_2,\ I,\ R)\in \hat{D}_4$, we have

$$\begin{aligned}L\hat{U}_{10}&\leq 2\hat{M}\left(d+\frac{\nu_1^2}{2}\right)+\hat{B}+3d+\frac{\nu_1^2+\nu_2^2+\nu_4^2}{2}+\left[(1-D)^k\{(\hat{M}+1)\beta_1+(\hat{M}\hat{c}_2+1)\beta_2\}+\epsilon\right]I-\frac{\gamma I}{R}\\&\leq 2\hat{M}\left(d+\frac{\nu_1^2}{2}\right)+\hat{B}+3d+\frac{\nu_1^2+\nu_2^2+\nu_4^2}{2}+\left[(1-D)^k\{(\hat{M}+1)\beta_1+(\hat{M}\hat{c}_2+1)\beta_2\}+\epsilon\right]\frac{\Lambda}{d}-\frac{\gamma\varepsilon_1}{\varepsilon_2}\end{aligned}$$

Choosing

$$\varepsilon_2=\varepsilon_1^2 \tag{7.25}$$

that yields

$$\begin{aligned}L\hat{U}_{10}&\leq 2\hat{M}\left(d+\frac{\nu_1^2}{2}\right)+\hat{B}+3d+\frac{\nu_1^2+\nu_2^2+\nu_4^2}{2}+\left[(1-D)^k\{(\hat{M}+1)\beta_1+(\hat{M}\hat{c}_2+1)\beta_2\}+\epsilon\right]\frac{\Lambda}{d}-\frac{\gamma}{\varepsilon_1}\\&\leq -1.\end{aligned}$$

The last inequality holds according to (7.22).

Case 5: If $(S_1,\ S_2,\ I,\ R)\in \hat{D}_5$, one can derive that

$$\begin{aligned}L\hat{U}_{10}&\leq 2\hat{M}\left(d+\frac{\nu_1^2}{2}\right)+\hat{B}+3d+\frac{\nu_1^2+\nu_2^2+\nu_4^2}{2}+\left[(1-D)^k\{(\hat{M}+1)\beta_1+(\hat{M}\hat{c}_2+1)\beta_2\}+\epsilon\right]I\\&\quad-\frac{1}{2}\hat{f}(S_1^{\hat{\rho}+1}+S_2^{\hat{\rho}+1}+I^{\hat{\rho}+1}+R^{\hat{\rho}+1})\\&\leq 2\hat{M}\left(d+\frac{\nu_1^2}{2}\right)+\hat{B}+3d+\frac{\nu_1^2+\nu_2^2+\nu_4^2}{2}+\left[(1-D)^k\{(\hat{M}+1)\beta_1+(\hat{M}\hat{c}_2+1)\beta_2\}+\epsilon\right]\frac{\Lambda}{d}-\frac{1}{2}\hat{f}S_1^{\hat{\rho}+1}\\&\leq 2\hat{M}\left(d+\frac{\nu_1^2}{2}\right)+\hat{B}+3d+\frac{\nu_1^2+\nu_2^2+\nu_4^2}{2}+\left[(1-D)^k\{(\hat{M}+1)\beta_1+(\hat{M}\hat{c}_2+1)\beta_2\}+\epsilon\right]\frac{\Lambda}{d}-\frac{\hat{f}}{2\varepsilon_1^{\rho+1}}\end{aligned}$$

this together with (7.23), we conclude that

$$L\hat{U}_{10}\leq -1,\ \text{ for any } (S_1,\ S_2,\ I,\ R)\in \hat{D}_5.$$

Case 6: When $(S_1,\ S_2,\ I,\ R)\in \hat{D}_6$, it is obtained that

$$\begin{aligned}L\hat{U}_{10}&\leq 2\hat{M}\left(d+\frac{\nu_1^2}{2}\right)+\hat{B}+3d+\frac{\nu_1^2+\nu_2^2+\nu_4^2}{2}+\left[(1-D)^k\{(\hat{M}+1)\beta_1+(\hat{M}\hat{c}_2+1)\beta_2\}+\epsilon\right]I\\&\quad-\frac{1}{2}\hat{f}(S_1^{\hat{\rho}+1}+S_2^{\hat{\rho}+1}+I^{\hat{\rho}+1}+R^{\hat{\rho}+1})\\&\leq 2\hat{M}\left(d+\frac{\nu_1^2}{2}\right)+\hat{B}+3d+\frac{\nu_1^2+\nu_2^2+\nu_4^2}{2}+\left[(1-D)^k\{(\hat{M}+1)\beta_1+(\hat{M}\hat{c}_2+1)\beta_2\}+\epsilon\right]\frac{\Lambda}{d}-\frac{1}{2}\hat{f}S_2^{\hat{\rho}+1}\\&\leq 2\hat{M}\left(d+\frac{\nu_1^2}{2}\right)+\hat{B}+3d+\frac{\nu_1^2+\nu_2^2+\nu_4^2}{2}+\left[(1-D)^k\{(\hat{M}+1)\beta_1+(\hat{M}\hat{c}_2+1)\beta_2\}+\epsilon\right]\frac{\Lambda}{d}-\frac{\hat{f}}{2\varepsilon_1^{\rho+1}}.\end{aligned}$$

Combining (7.23), leads to

$$L\hat{U}_{10} \leq -1, \text{ for any } (S_1,\, S_2,\, I,\, R) \in \hat{D}_6.$$

Case 7: If $(S_1,\, S_2,\, I,\, R) \in \hat{D}_7$, it follows that

$$\begin{aligned} L\hat{U}_{10} \leq & 2\hat{M}\left(d+\frac{\nu_1^2}{2}\right)+\hat{B}+3d+\frac{\nu_1^2+\nu_2^2+\nu_4^2}{2}+\left[(1-D)^k\{(\hat{M}+1)\beta_1+(\hat{M}\hat{c}_2+1)\beta_2\}+\epsilon\right]I \\ & -\frac{1}{2}\hat{f}(S_1^{\hat{\rho}+1}+S_2^{\hat{\rho}+1}+I^{\hat{\rho}+1}+R^{\hat{\rho}+1}) \\ \leq & 2\hat{M}\left(d+\frac{\nu_1^2}{2}\right)+\hat{B}+3d+\frac{\nu_1^2+\nu_2^2+\nu_4^2}{2}+\left[(1-D)^k\{(\hat{M}+1)\beta_1+(\hat{M}\hat{c}_2+1)\beta_2\}+\epsilon\right]\frac{\Lambda}{d}-\frac{1}{2}\hat{f}I^{\hat{\rho}+1} \\ \leq & 2\hat{M}\left(d+\frac{\nu_1^2}{2}\right)+\hat{B}+3d+\frac{\nu_1^2+\nu_2^2+\nu_4^2}{2}+\left[(1-D)^k\{(\hat{M}+1)\beta_1+(\hat{M}\hat{c}_2+1)\beta_2\}+\epsilon\right]\frac{\Lambda}{d}-\frac{\hat{f}}{2\varepsilon_1^{\rho+1}} \end{aligned}$$

which together with (7.23) implies that

$$L\hat{U}_{10} \leq -1, \text{ for any } (S_1,\, S_2,\, I,\, R) \in \hat{D}_7.$$

Case 8: For $(S_1,\, S_2,\, I,\, R) \in \hat{D}_8$, it is derived that

$$\begin{aligned} L\hat{U}_{10} \leq & 2\hat{M}\left(d+\frac{\nu_1^2}{2}\right)+\hat{B}+3d+\frac{\nu_1^2+\nu_2^2+\nu_4^2}{2}+\left[(1-D)^k\{(\hat{M}+1)\beta_1+(\hat{M}\hat{c}_2+1)\beta_2\}+\epsilon\right]I \\ & -\frac{1}{2}\hat{f}(S_1^{\hat{\rho}+1}+S_2^{\hat{\rho}+1}+I^{\hat{\rho}+1}+R^{\hat{\rho}+1}) \\ \leq & 2\hat{M}\left(d+\frac{\nu_1^2}{2}\right)+\hat{B}+3d+\frac{\nu_1^2+\nu_2^2+\nu_4^2}{2}+\left[(1-D)^k\{(\hat{M}+1)\beta_1+(\hat{M}\hat{c}_2+1)\beta_2\}+\epsilon\right]\frac{\Lambda}{d}-\frac{1}{2}\hat{f}R^{\hat{\rho}+1} \\ \leq & 2\hat{M}\left(d+\frac{\nu_1^2}{2}\right)+\hat{B}+3d+\frac{\nu_1^2+\nu_2^2+\nu_4^2}{2}+\left[(1-D)^k\{(\hat{M}+1)\beta_1+(\hat{M}\hat{c}_2+1)\beta_2\}+\epsilon\right]\frac{\Lambda}{d}-\frac{\hat{f}}{2\varepsilon_2^{\rho+1}} \end{aligned}$$

then condition (7.25) combining with (7.24) leads to

$$\begin{aligned} L\hat{U}_{10} \leq & 2\hat{M}\left(d+\frac{\nu_1^2}{2}\right)+\hat{B}+3d+\frac{\nu_1^2+\nu_2^2+\nu_4^2}{2}+\left[(1-D)^k\{(\hat{M}+1)\beta_1+(\hat{M}\hat{c}_2+1)\beta_2\}+\epsilon\right]\frac{\Lambda}{d}-\frac{\hat{f}}{2\varepsilon_1^{2(\rho+1)}} \\ \leq & -1 \text{ in } \hat{D}_8. \end{aligned}$$

Based on the discussion of the above eight cases, one can see for any sufficiently small ε_1

$$L\hat{U}_{10} \leq -1, \ \forall\, (S_1,\, S_2,\, I,\, R) \in \mathbb{R}_+^4 \backslash \hat{D}.$$

Consequently, condition (*ii*) in Lemma 7.4 is satisfied. According to Lemma 7.4, we can conclude that system (2.2) is ergodic and admits a unique stationary distribution $\pi(\cdot)$. This completes the proof. □

8 Bifurcation analysis

The bifurcation analysis, in this section, is performed using the central manifold theory [31]. Let us consider $S_1 = x_1$, $S_2 = x_2$, $I = x_3$ and $R = x_4$, then system (2.1) is written as:

$$\begin{aligned} \frac{\mathrm{d}x_1}{\mathrm{d}t} =& p\Lambda-(1-\alpha(x_3))(1-D)^k\beta_1x_1x_3-\mathrm{d}x_1+\theta\mu x_3 \equiv f_1 \\ \frac{\mathrm{d}x_2}{\mathrm{d}t} =& (1-p)\Lambda-(1-\alpha(x_3))(1-D)^k\beta_2x_2x_3-\mathrm{d}x_2+(1-\theta)\mu x_3 \equiv f_2 \\ \frac{\mathrm{d}x_3}{\mathrm{d}t} =& (1-\alpha(x_3))(1-D)^k(\beta_1x_1+\beta_2x_2)x_3-p_1x_3+\epsilon x_3x_4 \equiv f_3 \\ \frac{\mathrm{d}x_4}{\mathrm{d}t} =& \gamma x_3-\epsilon x_3x_4-\mathrm{d}x_4 \equiv f_4. \end{aligned} \tag{8.1}$$

Theorem 8.1 *The system (2.1) exhibits a transcritical (forward) bifurcation around E_0 at $R_0 = 1$ considering β_1 as bifurcation parameter.*

Proof The bifurcation threshold at $R_0 = 1$ is $\beta_1 = \beta_{1[TC]} = \frac{1}{S_{10}}\left[\frac{p_1}{(1-D)^k} - \beta_2 S_{20}\right]$, where $S_{10} = \frac{p\Lambda}{d}$, $S_{20} = \frac{(1-p)\Lambda}{d}$, $p_1 = \gamma + \mu + d + m$. The linearized matrix corresponding to $E_0(S_{10}, S_{20}, 0, 0)$ is

$$\overline{J}|_{E_0} = \begin{pmatrix} -d & 0 & -(1-D)^k\beta_1 S_{10} + \theta\mu & 0 \\ 0 & -d & -(1-D)^k\beta_2 S_{20} + (1-\theta)\mu & 0 \\ 0 & 0 & (1-D)^k(\beta_1 S_{10} + \beta_2 S_{20}) - p_1 & 0 \\ 0 & 0 & \gamma & -d \end{pmatrix}.$$

The eigenvalues are $\lambda_1 = \lambda_2 = \lambda_3 = -d$ and $\lambda_4 = p_1(R_0 - 1)$. So at $R_0 = 1$, $\lambda_4 = 0$ implying $\overline{J}|_{E_0}(\beta_{1[TC]})$ has a zero eigenvalue. The right eigenvector associated with the zero eigenvalue is $w = (w_1, w_2, w_3, w_4)^T = (-(1-D)^k\beta_1 S_{10} + \theta\mu, -(1-D)^k\beta_2 S_{20} + (1-\theta)\mu, d, \gamma)^T$, whereas the left eigenvector is $v = (v_1, v_2, v_3, v_4) = (0, 0, 1, 0)$. Therefore,

$$\overline{a} = \sum_{k,i,j=1}^{n} v_k w_i w_j \frac{\partial^2 f_k}{\partial x_i \partial x_j}(E_0) = 2w_3[(1-D)^k(\beta_1 w_1 + \beta_2 w_2) + \epsilon w_4]$$

$$\overline{b} = \sum_{k,i=1}^{n} v_k w_i \frac{\partial^2 f_k}{\partial x_i \partial \beta_1}(E_0) = (1-D)^k S_{10} w_1 > 0.$$

The central manifold theory [31] states that the local dynamical behavior of a system around DFE can be obtained with the help of sign of $\overline{a}$ and $\overline{b}$, and from the theory there will an occurrence of forward bifurcation around DFE for $\overline{a} < 0$, $\overline{b} > 0$, and backward bifurcation for $\overline{a} > 0$, $\overline{b} > 0$. We have already got that $\overline{b} > 0$. So, from the result it can be stated that the DFE (E_0) changes its stability from stable to unstable through forward or backward bifurcation according to $\overline{a} < 0$ or $\overline{a} > 0$. And, there could be a chance of a negative unstable coexistence steady state turns into positive and locally asymptotic stable endemic state for $R_0 > 1$. □

There have been a few more model parameters such as β_2, D and k that have the potential to be regarded as regulatory parameters in order to govern the behavior of the proposed system.

Theorem 8.2 *System (2.1) exhibits a transcritical (forward) bifurcation around E_0 at $R_0 = 1$ for $\beta_2 = \beta_{2[TC]} = \frac{1}{S_{20}}\left[\frac{p_1}{(1-D)^k} - \beta_1 S_{10}\right]$ taking β_2 as a bifurcation parameter.*

Theorem 8.3 *System (2.1) undergoes transcritical bifurcation around E_0 at $R_0 = 1$ for $D = D_{[TC]} = 1 - \left(\frac{p_1}{\beta_1 S_{10} + \beta_2 S_{20}}\right)^{\frac{1}{k}}$ considering D as bifurcation parameter.*

Theorem 8.4 *System (2.1) undergoes transcritical bifurcation around E_0 at $R_0 = 1$ for $k = k_{[TC]} = \frac{[\ln(p_1) - \ln(\beta_1 S_{10} + \beta_2 S_{20})]}{\ln(1-D)}$ assuming k as bifurcation parameter.*

9 Assessment of partial rank correlation coefficient

Correlation is a statistical measure used to assess the strength of a linear relationship between two variables, typically an input and an output. The correlation coefficient, symbolized as $r_{u_j v}$ which quantifies the relationship between input variable u_j and output variable v. This coefficient is determined as follows:

$$r_{u_j v} = \frac{\mathrm{Cov}(u_j, v)}{\sqrt{\mathrm{Var}(u_j)}\sqrt{\mathrm{Var}(v)}} = \frac{\sum_{i=1}^{N}(u_{ij} - \bar{u})(v_i - \bar{v})}{\sqrt{\sum_{i=1}^{N}(u_{ij} - \bar{u})^2 \sum_{i=1}^{N}(v_i - \bar{v})^2}}, \quad j = 1, 2, ..., k \tag{9.1}$$

and varied between −1 and +1. The expression $\mathrm{Cov}(u_j, v)$ indicates the covariance between variables u_j and v. On the other hand, $\mathrm{Var}(u_j)$ and $\mathrm{Var}(v)$ specify the individual variances of the variables u_j and v, respectively; with $\bar{u}$ and $\bar{v}$ representing their respective sample means. When u_j and v are raw data, the derived coefficient r is referred to as the sample or Pearson correlation coefficient. If the data undergoes a process of rank transformation, the resulting correlation coefficient is referred to as the Spearman rank correlation coefficient. Partial correlation aims to clarify the precise linear association between an input variable, u_j, and an output variable, v, while considering the linear influences exerted on v by remaining input variables. To calculate the partial correlation coefficient (PCC) between u_j and v, we examine the correlation between the residuals of these two variables. The residuals, denoted as $(u_j - \hat{u_j})$ and $(v - \hat{v})$. These values are derived from their respective linear regression models:

$$\hat{u_j} = c_0 + \sum_{m=1, m\neq j}^{k} c_m u_m \quad \text{and} \quad \hat{v} = b_0 + \sum_{m=1, m\neq j}^{k} b_m u_m. \tag{9.2}$$

Table 1 Values of system parameters for numerical simulation

Parametric values						
p	Λ	d	a	b	D	k
0.4	15	0.5	0.03	1	0.4	2
β_1	β_2	m	γ	ϵ	μ	θ
0.2	0.08	0.2	0.2	0.03	0.01	0.26

In a manner akin to partial correlation coefficient (PCC), partial rank correlation (PRC) involves conducting a partial correlation analysis on data that has been transformed into ranks. Initially, both variables u_j and v are subjected to rank transformation, after which linear regression models are constructed as specified in Eq. (9.2). The resulting partial rank correlation coefficient (PRCC) is a robust sensitivity measure, well-suited for capturing nonlinear yet monotonic relationships between u_j and v. This approach allows for a more nuanced understanding of the relationship between variables.

The comprehensive LHS-PRCC method, detailed extensively in reference [32], involves several procedural steps:

1. Begin by establishing the parameter space in the Latin Hypercube Sampling (LHS) matrix.
2. Create a set of paired sample data using the results obtained from the model being analyzed.
3. Assign ranks to both the parameters and output values. Then, reorder the rank order of the parameters based on their correlation with the output values.
4. Calculate the Partial Rank Correlation Coefficient (PRCC) for each input parameter.

After conducting uncertainty analysis, we move on to sensitivity analysis to pinpoint the crucial parameters necessary for achieving our objectives.

Pearson's correlation coefficient quantifies the measure of a linear relationship between two variables. Conversely, both Kendall's tau and Spearman's rank correlation coefficient examine monotonic relationship, capturing the tendency for variables to change in the same direction without strictly adhering to a constant rate of change. Linear relationships suggest that variables move in a consistent rate, while monotonic relationships assess the probability of variables changing in same direction, accommodating fluctuations in their rates of change. Kendall's tau correlation coefficient is often preferred when data fails to meet the assumptions of Pearson's correlation. It is considered nonparametric, meaning it does not rely on assumptions about the distribution of the data. Additionally, Kendall's tau does not necessitate continuous data; it can be applied to both continuous and ordinal data. Ordinal data, which involve categories with a ranking but inconsistent intervals between ranks. Spearman's rank correlation coefficient is highly similar to Kendall's tau. Both are nonparametric measures that assess monotonic relationships using ranked data. Although they are often interchangeable, Kendall's tau is generally considered more robust and is often preferred over Spearman's. Additionally, Spearman's correlation coefficient tends to yield larger values compared to Kendall's.

10 Numerical investigation of deterministic and stochastic system

In this section, we have performed numerical illustration to observe the dynamical nature for chosen set of parametric values. Figure 3a depicts that trajectory starting from (30, 30, 15, 10) converges to disease-free equilibrium E_0(12, 18, 0, 0) if $\beta_2 = 0.001$ and remaining parameters are chosen from Table 1 along with reproduction number $0.9566(< 1)$. From this state, if we increase the value of β_2, then Fig. 3b shows the convergence of trajectory of system (2.1) toward endemic equilibrium with $R_0 = 1.5191$. For the model parameters listed in Table 1, the figure depicts that trajectory initiating from (30, 30, 15, 10) tends to E^*(6.7461, 13.7694, 5.5802, 1.6722). So, the infection is found to have invaded the system for $R_0 > 1$.

Hence, the rate of propagation of ailment from infected to susceptible individual with higher immunity (β_2) has the ability to control the stability of the proposed deterministic model. Figure 4b depicts that system (2.1) undergoes a transcritical bifurcation around the disease-free equilibrium point E_0 at $\beta_{2[TC]} = 0.0071$. The DFE loses its stability when β_2 exceeds the bifurcation threshold, and also a stable branch of endemic equilibrium point emerges from the critical point. Figure 4 reveals that not only the transmission among stronger people, but the disease transmission rate in weak susceptible (β_1), intensity of social interaction (D), and public reaction in susceptibles (k) also act as regulating parameters as change in value of any of these parameters can switch the stability in the system. Figure 4a, c and d shows that system (2.1) exhibits transcritical bifurcations around disease-free equilibrium at $\beta_{1[TC]} = 0.0906$, $D_{[TC]} = 0.5132$ and $k_{[TC]} = 2.8185$, respectively. In Fig. 4a, E_0 becomes unstable when β_1 crosses the transcritical threshold value ($\beta_{1[TC]}$) and we get a stable endemic equilibrium point. On the other hand, in Fig. 4c, d, it is observed that the DFE becomes stable when either of social interaction (D) and public reaction (k) exceeds their corresponding bifurcation threshold value, and stable branch of coexistence steady state exists only if the parameters lie below the corresponding critical points.

In Figs. 5 and 6, we have analyzed the sensitivity of some of the system parameters and corresponding sensitivity indices for the parametric values of Table 1. The fact that the spread of disease has an ascendancy for β_1 than β_2 is observed in Fig. 5 also. Moreover, higher disease transmission rates (β_1, β_2) actually proliferate the illness in a system as the chances of spreading the infection get

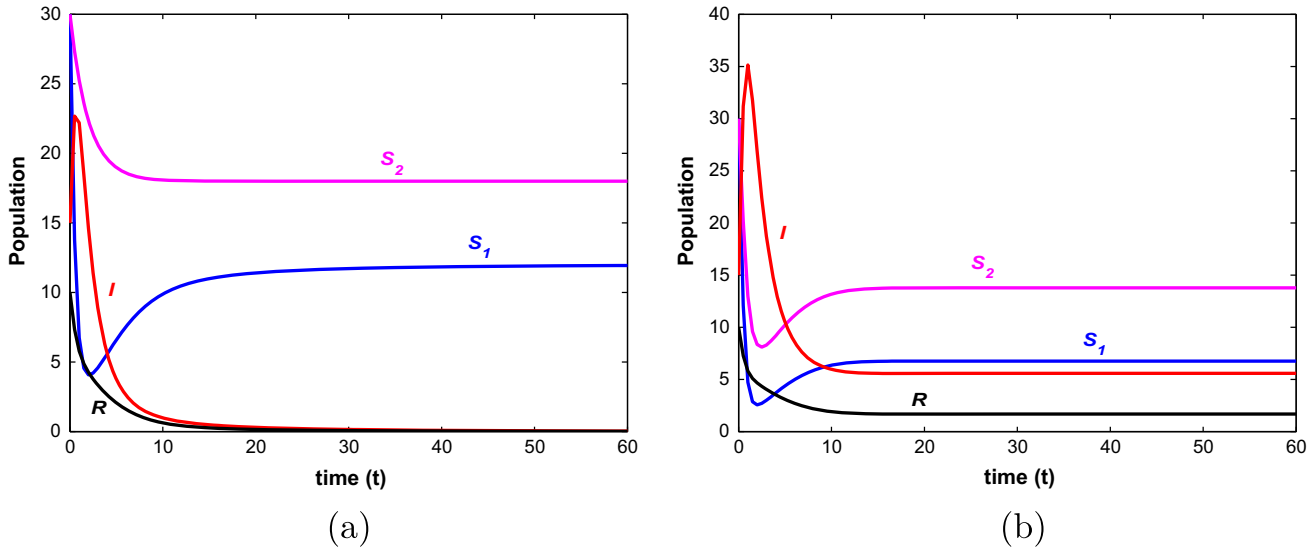

Fig. 3 Convergence of solution of system (2.1) around **a** E_0, and **b** E^*

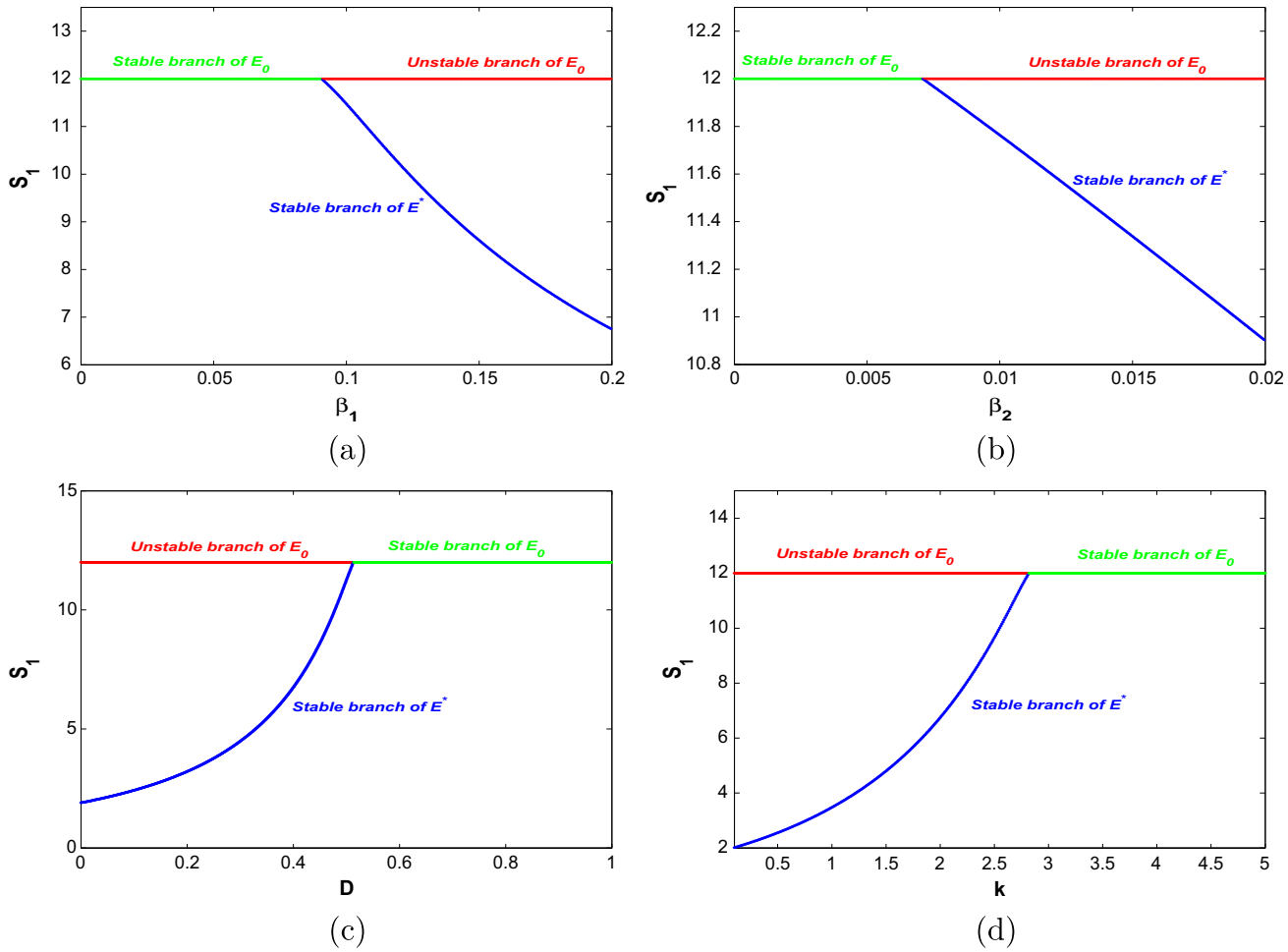

Fig. 4 Occurrence of transcritical bifurcations around DFE of model (2.1) considering **a** β_1, **b** β_2, **c** D and **d** k as bifurcation parameters

higher. On the other hand, increase in social interaction (D) and public reaction (k) lead to a declination in basic reproduction number. In addition, if more people recover from the sickness as a consequence of improved medical care, the prevalence of the illness may be somewhat controlled. The inversely proportional relationships of these parameters with R_0 indicates that an epidemic situation

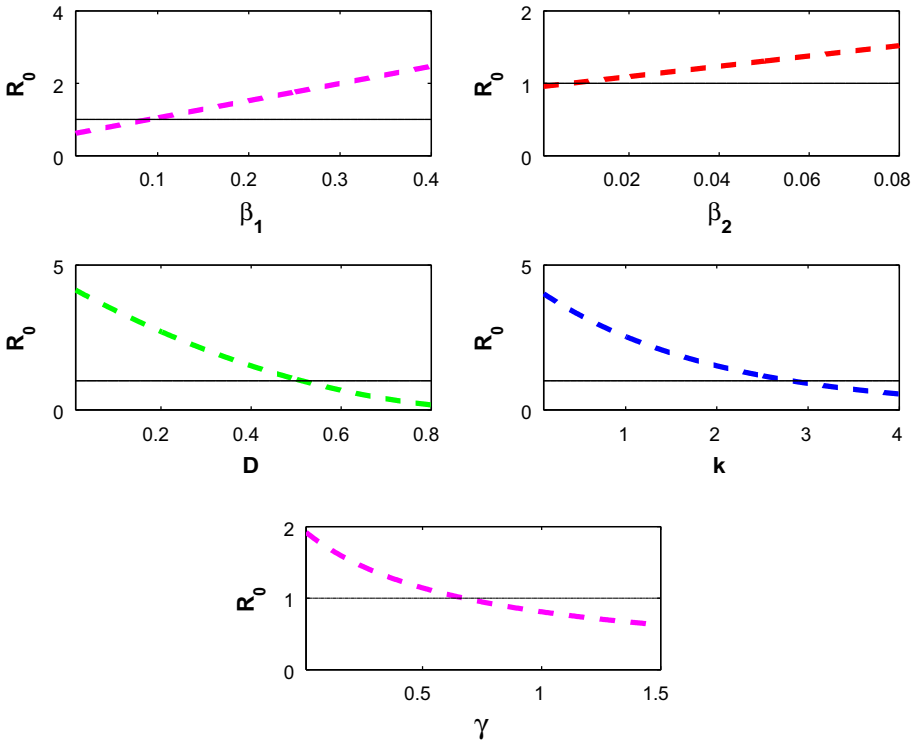

Fig. 5 Profile of basic reproduction number with the changes of β_1, β_2, D, k and γ in system (2.1)

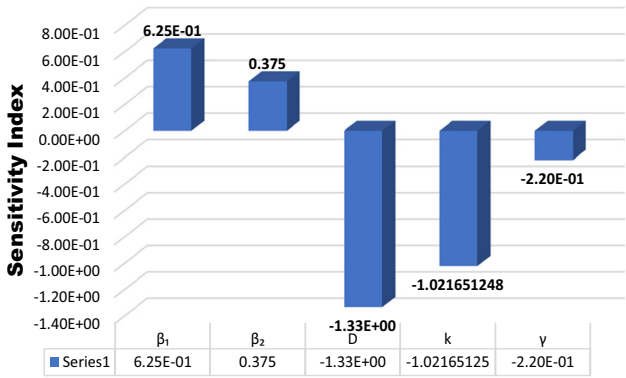

Fig. 6 Sensitivity index of β_1, β_2, D, k and γ on R_0 of model (2.1)

can be controlled by increasing people's effectiveness in social behavior, public response or by providing better treatment (γ) to infected people. The sensitivity indices for the parametric values of Table 1, are calculated as follows: $\Gamma_{\beta_1} = 0.625$, $\Gamma_{\beta_2} = 0.375$, $\Gamma_D = -1.333$, $\Gamma_k = -1.0217$ and $\Gamma_\gamma = -0.2198$, which are shown in Fig. 6.

The parameters a and b denote the rate at which governmental actions are imposed and the level of ineffectiveness of those actions due to people's negligence or due to lack of propagation of information. In Fig. 7, we have tried to show how these parameters make an impact on the count of infected population. Figure 7a shows a reduction in infected people for increasing governmental action. The graph though starts to decrease steeply, but tends to a saturation level ultimately. On the other hand, if the governmental actions fail to be effective within a community, then it will lead to an increase in infected population (see Fig. 7b).

Figure 8 explores the illustration of social interaction (D) and public reaction (k) of susceptible people on propagation of ailment. It is observed that increasing these sociological parameters reduce the count of infected people in a system.

Additionally, we have examined in Fig. 9 how the synchronized effect of governmental action and public reaction influences the system's capacity to control infection levels. Ministries use a variety of preventative measures during an epidemic outbreak to stop the spread of the illness, and the general public's reaction also varies depending on the prevalence of the ailment. Here, this graph illustrates that stringent government measures and effective public reaction lessen the likelihood of being contagious, ultimately leading to a drop in the number of affected people in the community. In fact, if the government acts quickly after an epidemic outbreak, a system becomes disease-free earlier.

By employing PRCC, we can identify and prioritize specific parameters that exert a significant influence on the reproduction number R_0. The parameters are considered as random variables, with some of them following a uniform probability distribution,

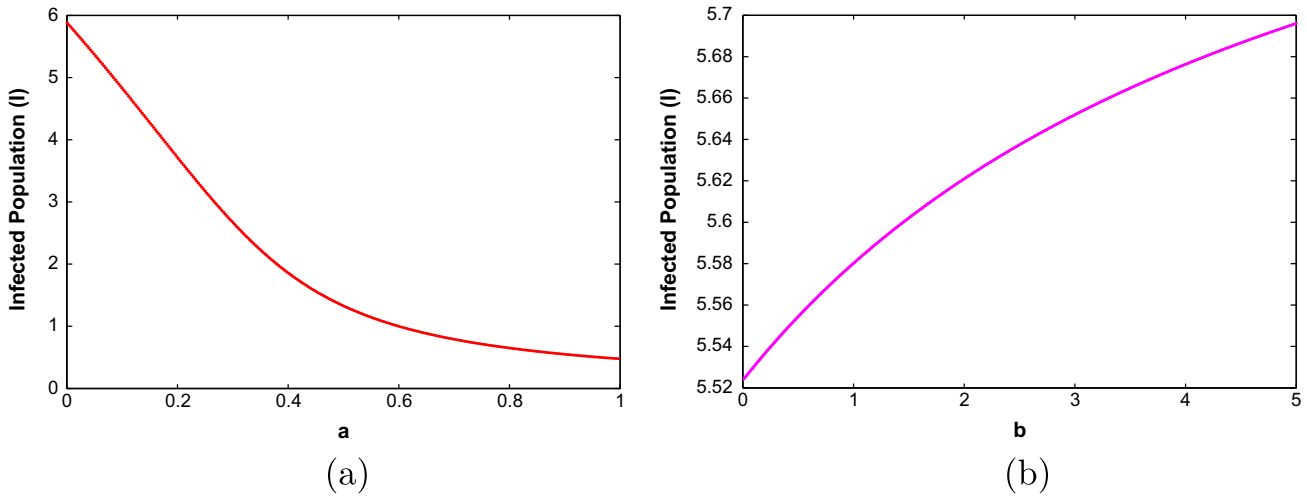

Fig. 7 The effects of **a** a and **b** b on the infected population (I) of system (2.1)

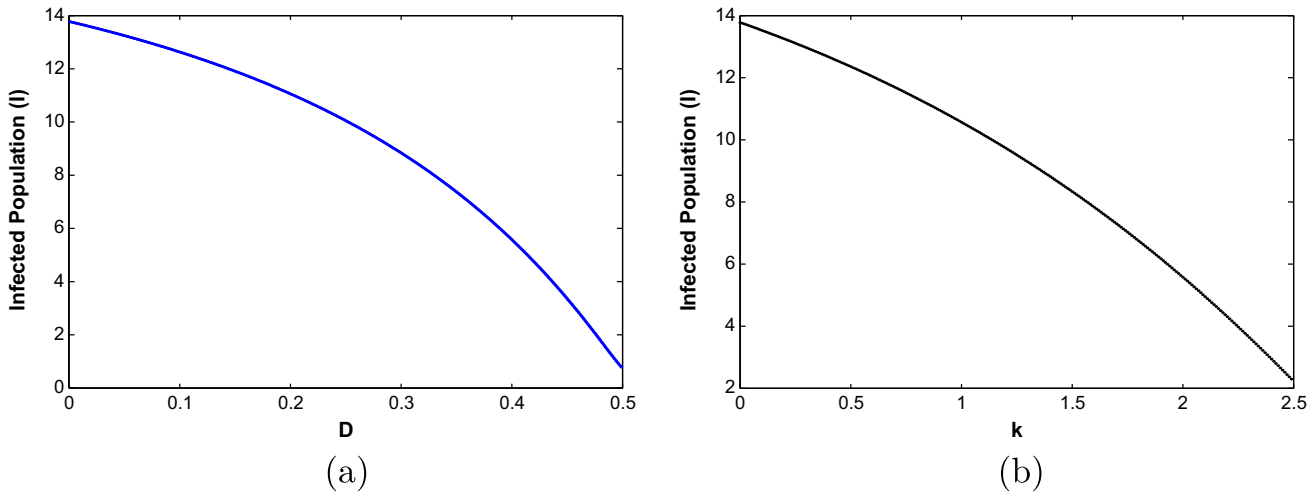

Fig. 8 The effects of **a** D and **b** k on infectious community (I) of model (2.1)

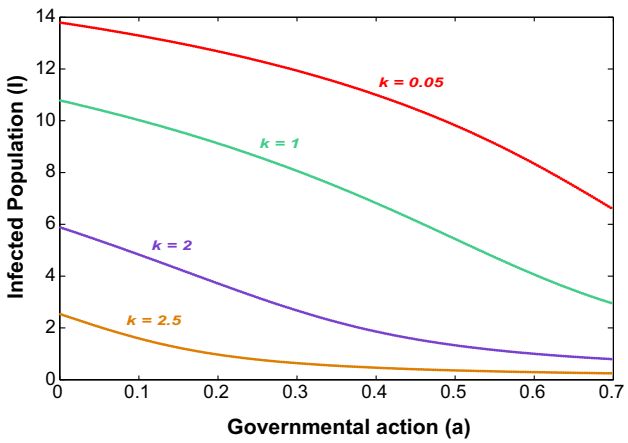

Fig. 9 Trajectory of infectious species (I) of system (2.1) for the increase of governmental restrictions (a) with different public response (k)

while the rest adhere to normal distribution. As a result, 6 parameters (specifically, D, k, β_1, β_2, p, Λ) are allocated uniform probability distributions, while 3 parameters (namely, d, γ, μ) are assigned normal probability distributions for PRCC analysis. These distributions are outlined in detail in Table 2.

Additionally, for each parameter, 1000 random values are sampled. Employing this methodology enables us to conduct an exhaustive sensitivity analysis, providing valuable insights into the relationship between the uncertain model parameters and reproduction

Table 2 Parameter space considered for PRCC analysis

Parameter	Distribution
D	Uniform (0.2, 0.3)
k	Uniform (1.5, 2.5)
β_1	Uniform (0.15, 0.25)
β_2	Uniform (0.06, 0.1)
p	Uniform (0.2, 0.3)
Λ	Uniform (11.25, 18.75)
d	Normal (0.5, 0.01)
γ	Normal (0.2, 0.01)
μ	Normal (0.01, 0.01)
m	Normal (0.2, 0.01)

Table 3 PRCC values and p values for R_0 in Spearman and Kendall methods

R_0				
	Spearman		Kendall	
Parameter	PRCC value	p value	PRCC value	p value
D	− 0.831091912860965	2.93560700814720e−254	− 0.307969731101412	9.48865816706979e−48
k	− 0.851136383912766	4.63776429579959e−279	− 0.322886818208989	2.60892643621793e−52
β_1	0.793120620959363	3.44106138315216e−215	0.271730104117886	1.46879028436692e−37
β_2	0.834661371177595	1.98170567169120e−258	0.312019772431695	5.75556193196410e−49
p	0.528848305452176	1.68255024254010e−72	0.131503511078680	5.69392855538548e−10
λ	0.946221786212192	0	0.546198934794901	3.55823033342646e−146
d	− 0.461599871365116	1.89475559469574e−53	− 0.113427852305786	8.95988507428859e−08
γ	− 0.212378407400233	1.43363780880028e−11	− 0.0465274071458920	0.0282957505836940
μ	− 0.212203369080426	1.49106532980324e−11	− 0.0452375241789802	0.0329772433206308

number. This comprehensive examination allows us to better understand how variations in these parameters impact on the key component R_0. Table 3 presents the PRCC values and their corresponding p values for model parameters for two methods (Spearman and Kendall).

The bar diagrams presented here, offer a visual representation of the parameters that significantly influence the reproduction number R_0. Through PRCC analysis, we assess the statistical impact of input parameters on R_0, identifying those parameters crucial to understand population dynamics. The sign of the PRCC provides insight into the qualitative relationship between parameters: a positive sign indicates an increasing trend in population classes, while a negative sign suggests a decreasing trend. A significance level of 0.05 is applied to the sensitivity test, ensuring robustness in our analysis. When PRCC values are low, it signifies that the associated parameter has a minimal or insignificant effect on reproduction number. As a result, we cannot consider such parameters as control variables in our analysis. Reproduction number (R_0) experiences adverse effects from parameters D, k, d, γ, μ. This implies that an increment in any of these parameters will result in a decrease in the level of R_0. Conversely, parameters such as β_1, β_2, p, Λ have a positive influence on R_0. Therefore, an increment in any of these parameters will lead to a rise in R_0 (see, Fig. 10). However, our analysis indicates that the reproduction number of model system (2.1) exhibits the highest sensitivity to parameters including D, k, β_1, β_2 and Λ. These parameters collectively exert significant influence on the dynamics of the entire epidemic system. We have also performed scatter plots of Partial Rank for reproduction number R_0. From Fig. 11, the scatter plots show the rank transformation from monotone to linear relations.

In order to obtain a more precise understanding of the effect of noise on SDE system (2.2), several numerical computations have been executed implementing the Euler Maruyama Method in MATLAB utilizing the information of Table 1. For the scenario of system (2.1), basic reproduction number $R_0 = 1.5191$, that is greater than 1, subsequently, it enables the occurrence of unique coexistence steady state $E^*(6.7461, 13.7694, 5.5802, 1.6722)$ which is locally asymptotically stable according to Theorem 7.2. Figure 3b depicts a graphical visualization of the result. Furthermore, with regard to corresponding stochastic model (2.2), the strength of noises have been considered as $\nu_1 = 0.06$, $\nu_2 = 0.05$, $\nu_3 = 0.08$ and $\nu_4 = 0.05$ while the levels of β_1, β_2 have been reduced as $\beta_1 = 0.04$, $\beta_2 = 0.001$. In this case, for $D = 0.7$, $k = 5$, the basic reproduction number for SDE system (2.2) becomes:

$$\hat{R}_s = \frac{1}{(\gamma + \mu + d + m)}\left[(1 - D)^k(\beta_1 + \beta_2)\frac{\Lambda}{d} + \frac{\epsilon\Lambda}{d} - \frac{\nu_3^2}{2}\right] = 0.988779 < 1.$$

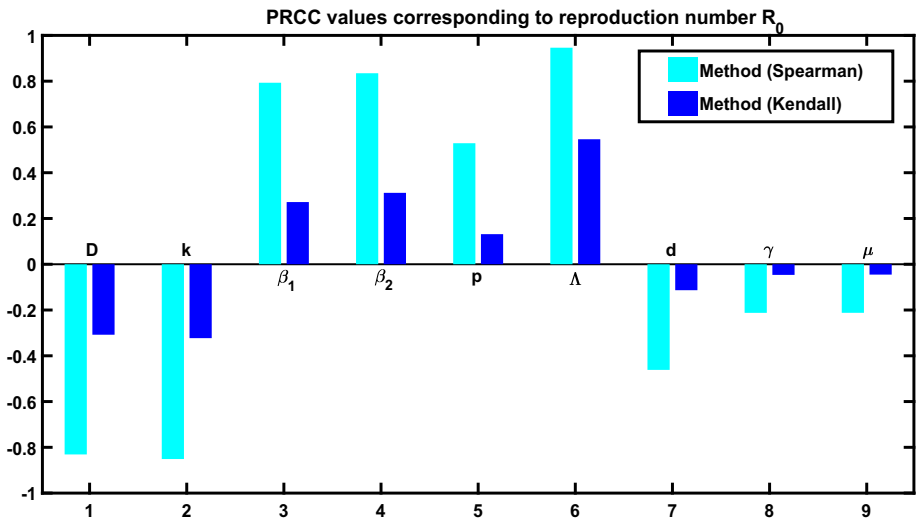

Fig. 10 Bar diagrams displaying PRCC values are employed to visualize the sensitivity analysis of reproduction number R_0. The analysis encompasses a sample size of 1000. A significance level of 0.05 is applied

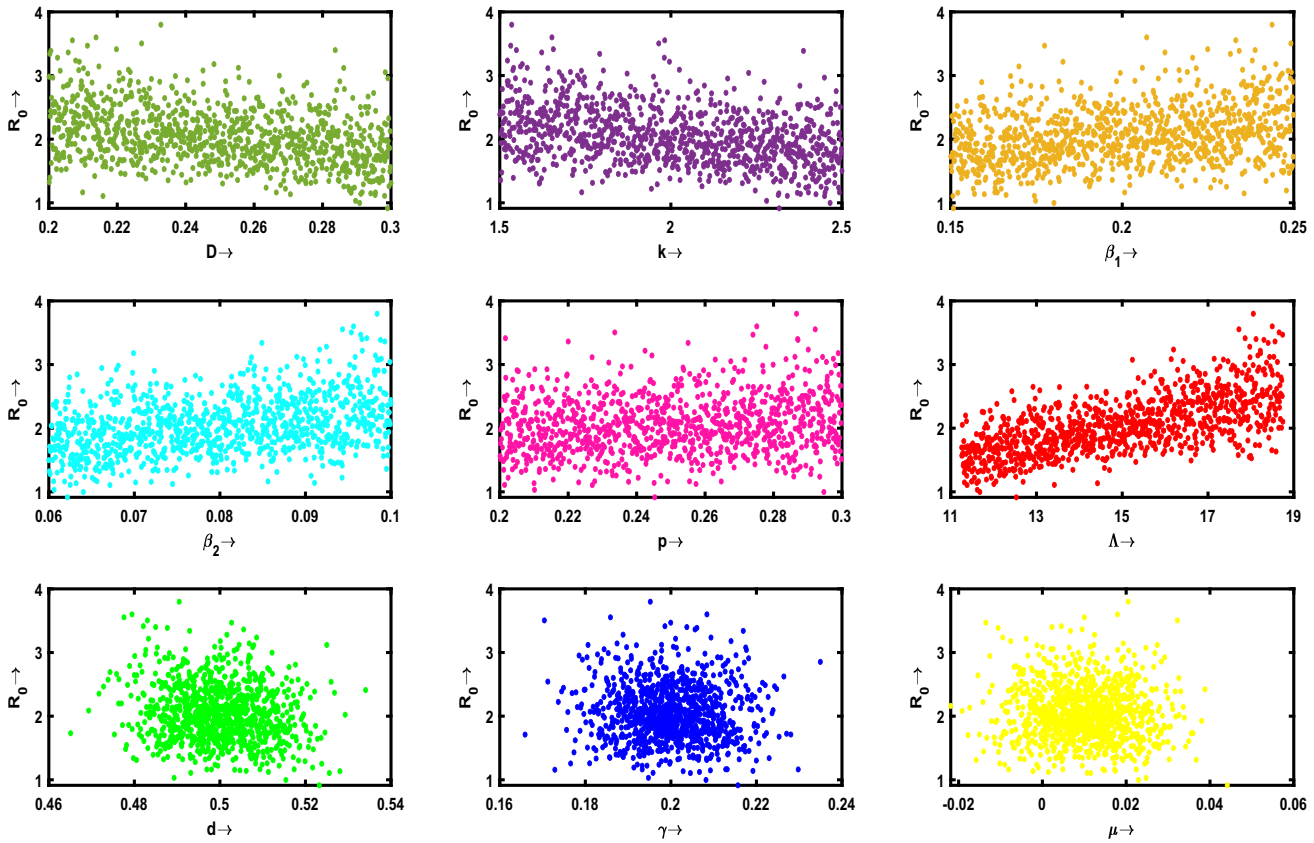

Fig. 11 Scatter plots of different parametric ranks correlated to R_0. Here, significance level is 0.05. Sample size = 1000 for each parameter is taken based on LHS approach with standard normal and uniform probability distribution

Hence, it can be realized that $\limsup_{t\to\infty} \frac{\ln I(t)}{t} < 0$ with probability one, as a consequence of Theorem 7.3. Thereafter, the contagious population size will eventually converge to zero exponentially a.s. as well as recovered species will also go extinct. These observations are graphically embellished through Fig. 12. Thus, it is conceivable to conclude that more robust actions taken by the government, more dynamic patterns of social activity, public response as well as disease transmission rate from susceptible to infectious population with lower and higher immunity could contribute to the reduction in disease transmission. The frequency histograms of susceptible classes, infected class, and recovered class are depicted at time $t = 100$ in Fig. 13. It is found that infected and recovered compartments disappear exponentially a.s., whereas density of susceptible species is almost symmetrical with regard to its mean.

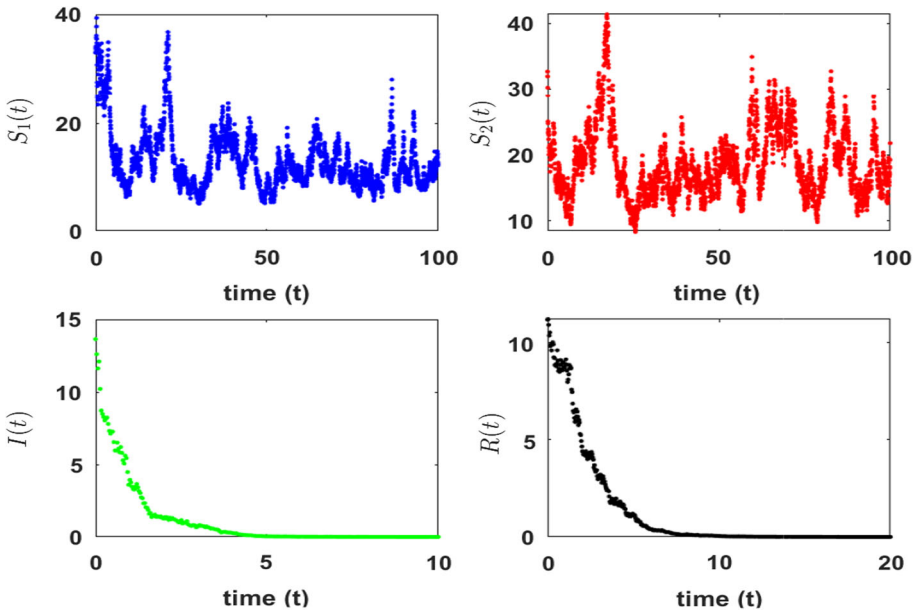

Fig. 12 After some time, both $I(t)$ as well as $R(t)$ become extinct as a result of intensified social interaction ($D = 0.7$), public response ($k = 5$) along with reduced rate of β_1, β_2 ($\beta_1 = 0.04$, $\beta_2 = 0.001$) and higher strength of noise. We choose, $\nu_1 = 0.06$, $\nu_2 = 0.05$, $\nu_3 = 0.07$ and $\nu_4 = 0.05$. All other remaining parameter values are provided in Table 1

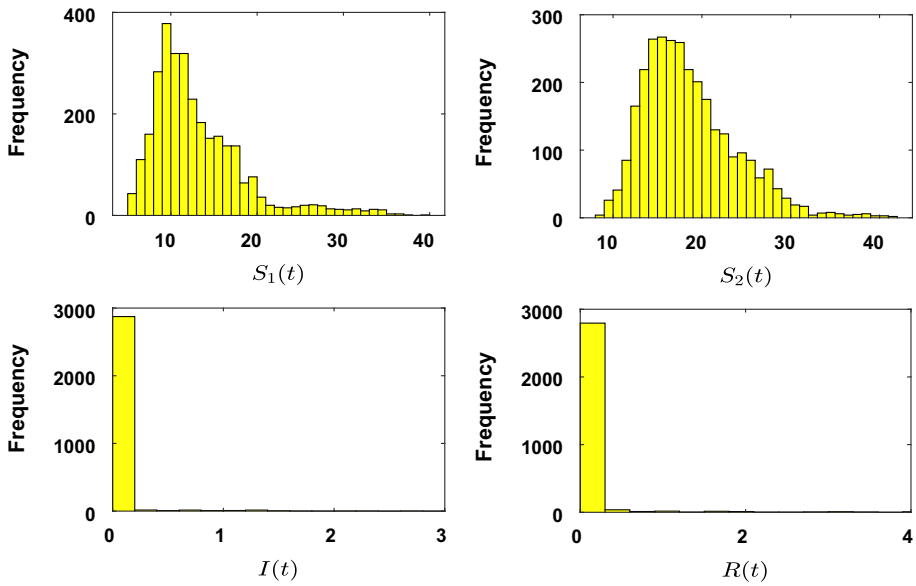

Fig. 13 Frequency histograms of susceptible compartment with lower immunity ($S_1(t)$), higher immunity ($S_2(t)$), infected compartment ($I(t)$) and recovered compartment ($R(t)$) at time $t = 100$. All parameters are being considered as in Fig. 12

When $\hat{R}_s > 1$, to observe the behavior of disease propagation of stochastic model (2.2), ν_3 is reduced to 0.07 and all other values of parameters have been chosen from Table 1. Afterward, basic reproduction number for SDE system (2.2) is determined as $\hat{R}_s = 4.3094 > 1$. In this situation, the condition outlined in Theorem 7.3 has not been satisfied. As a consequence, the simulations demonstrate that infected and recovered populations are stochastically persistent (for instance, see Fig. 14). In addition to this, the endemic stationary distribution develops while $\hat{R}_s$ is greater than 1. The stochastic version (2.2) has an unique stationary distribution of endemic steady state for $\hat{R}_s > 1$. In order to investigate the impact of intensity of noise, same parameter values, as mentioned in Table 1, have been implemented along with varying strength of noises. Now, let us take $\nu_1 = 0.06$, $\nu_2 = 0.05$, $\nu_3 = 0.07$ and $\nu_4 = 0.05$, that lead to $\hat{R}_s = 4.3094 > 1$ (which has previously been computed). If we leave each of the other parameters unchanged but decrease the level of intensities as $\nu_1 = 0.02$, $\nu_2 = 0.01$, $\nu_3 = 0.025$ and $\nu_4 = 0.01$, then $\hat{R}_s = 4.31174$. Subsequently, the solutions of stochastic model (2.2) are found to be oscillating about $E^*(6.7461, 13.7694, 5.5802, 1.6722)$ for (ν_1, ν_2, ν_3, ν_4) = (0.06, 0.05, 0.07, 0.05) (for convenience, see Fig. 14) and (ν_1, ν_2, ν_3, ν_4) = (0.02, 0.01, 0.025, 0.01) (for convenience, see Fig. 15). The frequency histograms of coexistence equilibrium point have been depicted in Fig. 16 at time $t = 100$, using the parametric values as mentioned in Table 1 with $\nu_1 = 0.02$, $\nu_2 = 0.01$, $\nu_3 = 0.025$, $\nu_4 = 0.01$. It has been noticed that population sizes of susceptible, infected and recovered compartments are all symmetric around their corresponding means.

Additionally, we must investigate how intensity of noise, for infectious compartment, influences the dynamical behavior and, in particular, the rate at which infected class is exterminated. An increasing value of ν_3 intends to decrease the average time required

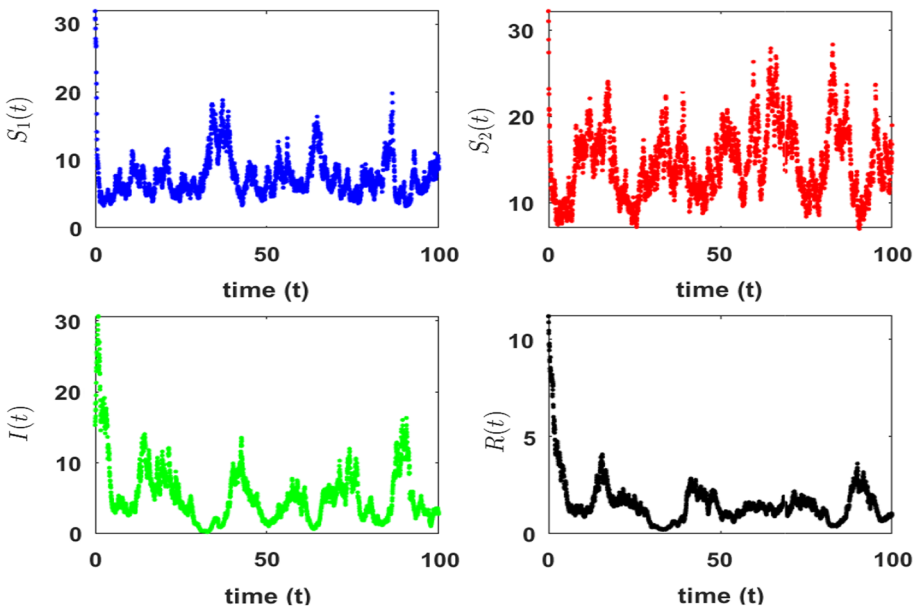

Fig. 14 Graphical representations of time-series evolution of the SDE model (2.2). The asymptotic nature of the solution of model (2.2) around endemic state $E^*(6.7461, 13.7694, 5.5802, 1.6722)$ of (2.1) has been depicted here, assuming initial point as (30, 30, 15, 10). We choose, $\nu_1 = 0.06$, $\nu_2 = 0.05$, $\nu_3 = 0.08$ and $\nu_4 = 0.05$. Moreover, blue-colored, red-colored, green-colored and black-colored curve displays the population sizes of $S_1(t)$, $S_2(t)$, $I(t)$ and $R(t)$, respectively

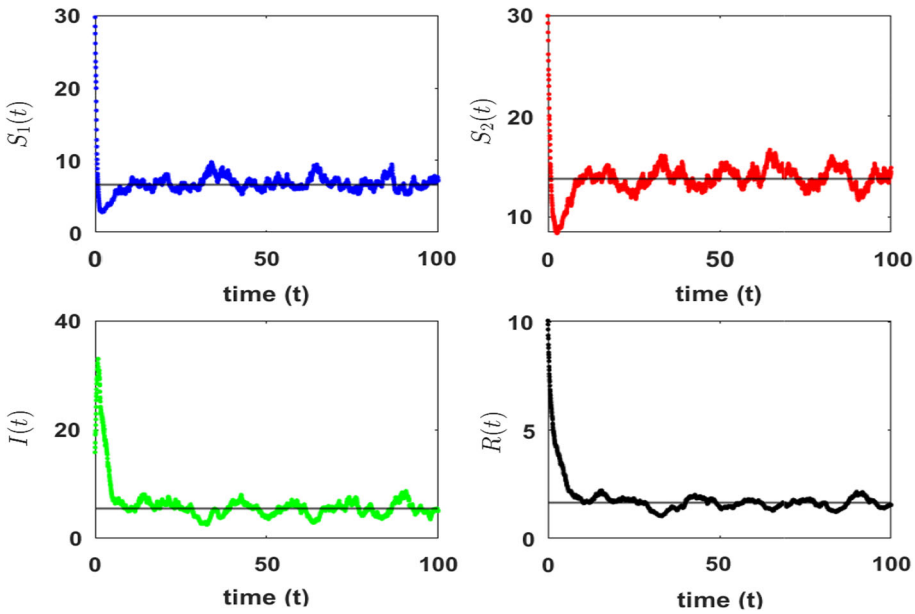

Fig. 15 Graphical representations of time-series evolution of the SDE model (2.2). The asymptotic nature of the solutions of system of equations (2.2) around endemic state $E^*(6.7461, 13.7694, 5.5802, 1.6722)$ of (2.1) have been depicted here, assuming initial point as (30, 30, 15, 10). We choose, $\nu_1 = 0.02$, $\nu_2 = 0.01$, $\nu_3 = 0.025$ and $\nu_4 = 0.01$

Table 4 Significance of noise (ν_3) for infectious class of the model system (2.2)

ν_3	$\hat{R}_s$	Time	Figure
0.10	0.9868	> 1.5	17a (black)
0.15	0.9799	> 1, < 1.5	17a (cyan)
0.20	0.9703	< 1	17a (magenta)

for removal of contagious species, whenever the model parameters satisfy the condition $\hat{R}_s < 1$. After that, the quantities 0.10, 0.15 and 0.20 are chosen to represent strength of noise (ν_3), and remaining parameter values have been considered as per Fig. 12. As a consequence, the time needed, to eradicate diseased population gradually, reduces as ν_3 increases. For $\nu_3 = 0.10$, the time to exterminate infected people reaches above 1.5 units as depicted in Fig. 17a (black-colored curve). When ν_3 is equal to 0.15, it requires close to around 1–1.5 unit of time (cyan-colored curve); moreover, if $\nu_3 \geq 0.20$, it will never exceed 1 unit of time (magenta-colored curve). The impact of noise on dynamical behavior of system (2.2) is mentioned in Table 4.

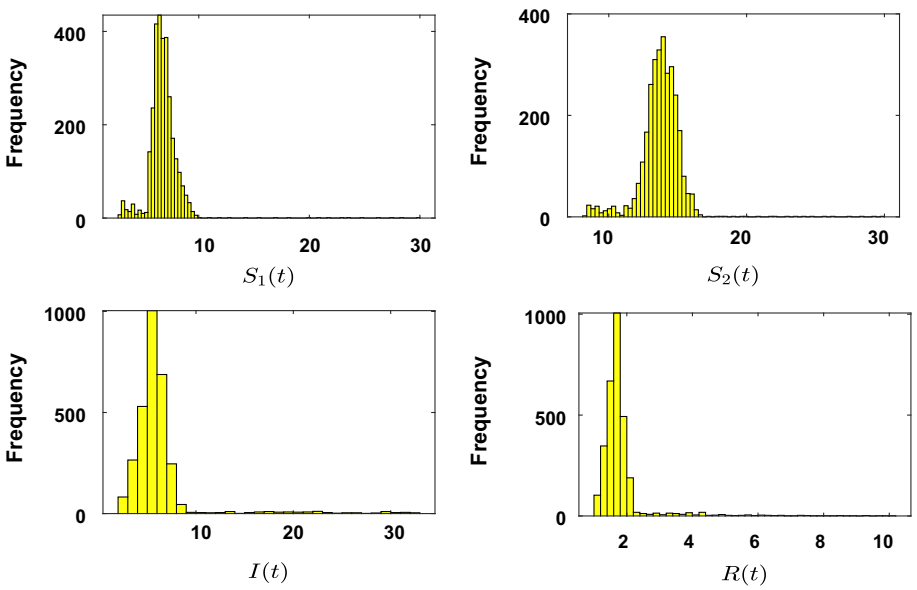

Fig. 16 Frequency histograms of susceptible compartment with lower immunity ($S_1(t)$), higher immunity ($S_2(t)$), infected compartment ($I(t)$) and recovered compartment ($R(t)$) at time $t = 100$. We choose, $\nu_1 = 0.02$, $\nu_2 = 0.01$, $\nu_3 = 0.025$ and $\nu_3 = 0.01$. All other remaining parameter values are provided in Table 1

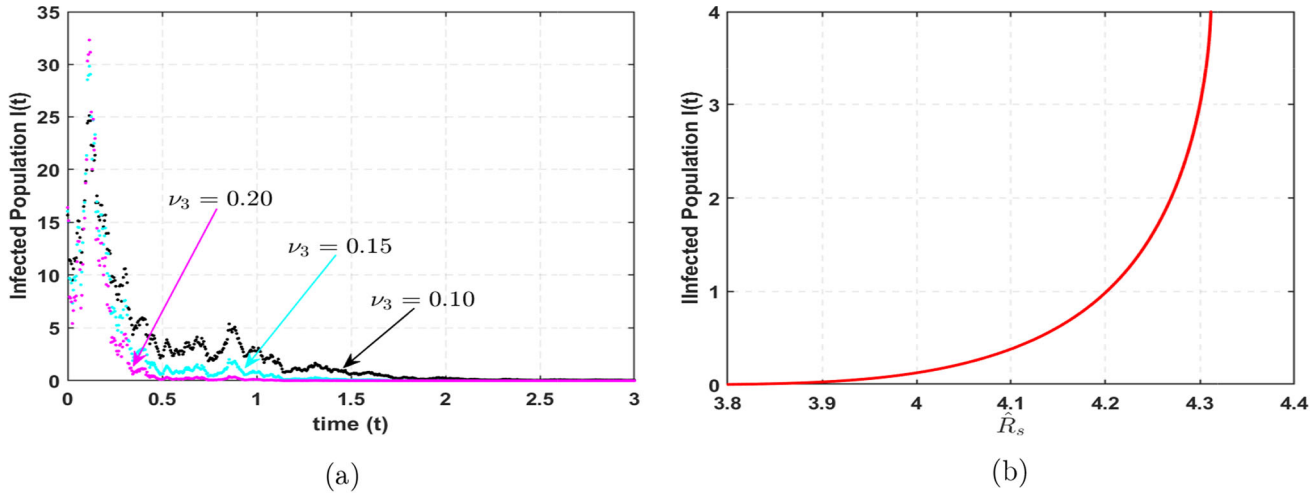

Fig. 17 **a** The influence of noise intensity for different levels of ν_3 over the stochastic system (2.2). **b** Change in the amount of infectious population $I(t)$ as a result of boost in basic reproduction number $\hat{R}_s$

The relation between the change in amount of infected individuals and the variation in basic reproduction number $\hat{R}_s$ is analyzed in Fig. 17b. Moreover, Fig. 18 has illustrated how the simultaneous interaction of social behavior (D), public reaction (k) and infection propagation rates from susceptible to infected class (β_1, β_2) as well as the level of noise has an influence to contribute to spread of the disease.

11 Optimal control problem associated with model (2.1)

In system (2.1) a SIRIS model is developed, where all of the model parameters have been set at their respective constant values. In order to prevent the propagation of a disease, we have come up with a relevant optimal control problem with certain significant approaches in this part. When a disease epidemic occurs, governmental action is one of those things that is dependent on the prevalence. In order to limit the increasing disease transmission, the restrictions imposed by governmental bodies may be regarded as an effective intervention. Furthermore, since improved medical care also lessens the burden of the condition, clinical care is seen as a pharmacological control intervention. Consequently, the effects of these time-dependent control policies over spread of virus have been examined as well as attempted for reducing the expenses associated with putting these policies to effect.

Effectiveness of governmental action: During the period of a pandemic, government of a country usually sets up some regulations, for all people, to mitigate the high propagation rate. In order to do so, they use some policies such as educational campaigns, media coverage to make aware the people regarding the symptoms, prevalence and precautions. The rules and regulations are mainly

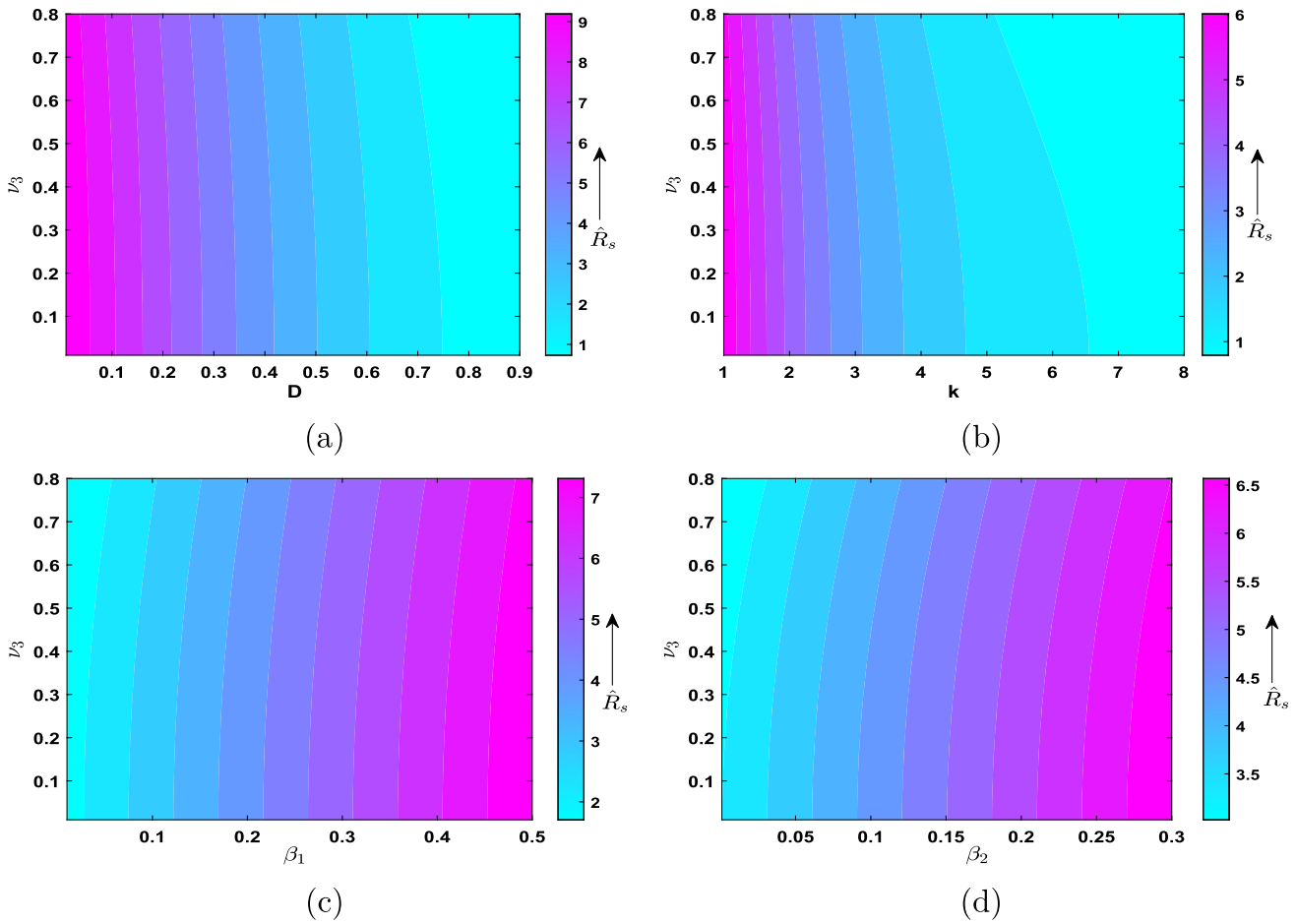

Fig. 18 Variations in the magnitude of basic reproduction number $\hat{R}_s$, in response to varying levels of D, k, β_1 and β_2 while the strength of noise ν_3 is raised

imposed on people by observing how severe the disease epidemic is. It is conceivable to utilize the restriction and relaxation of rules as a strategy to interrupt the relentless spread of a infection as it changes over time and in its prevalence. The parameter a denotes the rate at which the government has taken actions against a disease outbreak. As this is chosen as a time-dependent control intervention, it follows the condition $0 \leq a \leq 1$, where 0 represents no action is taken by government due to the heedless nature, and 1 denotes a complete limitation put in place by the government. Because a tight restriction and prompt broadcast will produce behavioral changes in the population and make them aware of the symptoms and preventative measures of an ailment, we regard $a(t)$ as control parameter. For lessening overall burden of a disease, we seek to determine the optimal rate at which the government should intervene.

Clinical treatment provided to infectious community: The prevalence of the disease is decreased when the infected are given pharmacological therapy, which also slows the disease's spread. After a diagnosis, it is believed that the infected individuals receive clinical medication. The process of therapy involves diagnosing symptoms medically, receiving clinical care, and other steps that vary and evolve through time. Given this information, the system considers the time-dependent treatment rate function $\gamma(t)$ to lessen the disease burden. In this instance, the expense of medicine, diagnostics, hospitalization, etc. is taken into account. With the limitation that $0 \leq \gamma(t) \leq 1$, where 0 and 1, respectively, signify the no response and complete response to the provided therapy, the treatment intensity $\gamma(t)$ is considered as another control variable.

While implementing the strategies, we need to decide the optimal level of socialized interaction as well as the optimal treatment approach with the least amount of expense. The feasible set, then, for control policies $a(t)$ along with $\gamma(t)$ is provided as:

$$\Delta = \left\{(a(t),\, \gamma(t))|(a(t),\, \gamma(t)) \in [0,\, 1] \times [0,\, 1],\, t \in [0,\, T_f]\right\}$$

where $a(t)$, $\gamma(t)$ are regarded as measurable and bounded functions, and T_f is the time during which the control strategies are applied.

11.1 Deduction of total cost

(i) Cost incurred in governmental action: The total cost incurred in governmental actions in order to increase the public response regarding disease prevalence and its precautions is denoted by $\int_0^{T_f}\left[w_2a^2(t)\right]\mathrm{d}t$. This expense covers the essential initiatives to educate individuals on the value of early preventative measures. Additionally, the price of upholding appropriate social interaction is covered here. The cost incurred for various mitigation solutions, such as educational campaigns, and news broadcasting is presented in some literature using the second-order nonlinearity term [33]. Here also, the same assumption is considered and the nonlinearity is taken up to order two.

(ii) Cost due to infectivity and clinical treatment: The overall expense as a result of disease load and treatment practises is: $\int_0^{T_f}\left[w_1I(t)+w_3\gamma^2(t)\right]\mathrm{d}t$, where $w_1I(t)$ represents the expense incurred for decreased manpower as a result of rapid spread. One may add the revenue loss caused by illness also. Additionally, the notation $w_3\gamma^2(t)$ denotes the expense incurred as a result of the treatment plan, including costs associated with hospitalization, medical costs, and diagnosis fees. Due to its applicability, the nonlinearity term of the control policy $\gamma(t)$ is regarded as being up to second order [3, 33].
The problem implementing the control policies is proposed in with the cost functional J:

$$J[a(t),\gamma(t)]=\int_0^{T_f}\left[w_1I(t)+w_2a^2(t)+w_3\gamma^2(t)\right]\mathrm{d}t \tag{11.1}$$

subject to the model system:

$$\begin{aligned}
\frac{\mathrm{d}S_1}{\mathrm{d}t}&=p\Lambda-\left(1-\frac{a(t)I}{b+I}\right)(1-D)^k\beta_1S_1I-\mathrm{d}S_1+\theta\mu I\\
\frac{\mathrm{d}S_2}{\mathrm{d}t}&=(1-p)\Lambda-\left(1-\frac{a(t)I}{b+I}\right)(1-D)^k\beta_2S_2I-\mathrm{d}S_2+(1-\theta)\mu I\\
\frac{\mathrm{d}I}{\mathrm{d}t}&=\left(1-\frac{a(t)I}{b+I}\right)(1-D)^k(\beta_1S_1+\beta_2S_2)I-(d+m)I-\gamma(t)I-\mu I+\epsilon IR\\
\frac{\mathrm{d}R}{\mathrm{d}t}&=\gamma(t)I-\epsilon IR-\mathrm{d}R
\end{aligned} \tag{11.2}$$

with initial conditions $S_1(0)>0,\ S_2(0)>0,\ I(0)\geq 0$ and $R(0)\geq 0$. The total incurred cost which needs to be minimized is represented by the functional J where the integrand is:

$$L(S_1,\,S_2,\,I,\,R,\,a(t),\,\gamma(t))=w_1I(t)+w_2a^2(t)+w_3\gamma^2(t)$$

which denotes the cost at time t. Here w_1, w_2 and w_3 denote the positive weight constants which balance the unit of the integrand [3, 33]. The main aim is to optimize the control interventions a^* and γ^* as these will minimize the cost functional (J) too.

Theorem 11.1 *The control system (11.1)–(11.2) possesses a pair of optimal control strategies* $(a^*,\ \gamma^*)$ *in* Δ *with* $J(a^*,\,\gamma^*)=\min[J(a,\,\gamma)]$.

Proof See Appendix A. □

Theorem 11.2 *For the optimal states* $(S_1^*,\,S_2^*,\,I^*,\,R^*)$ *with the optimal control interventions* $(a^*,\ \gamma^*)$ *there exist adjoint variables* $\lambda=(\lambda_1,\,\lambda_2,\,\lambda_3,\,\lambda_4)\in\mathbb{R}^4$ *satisfying the canonical equations:*

$$\begin{aligned}
\frac{d\lambda_1}{dt}&=\lambda_1\left[\left(1-\frac{aI}{b+I}\right)(1-D)^k\beta_1I+d\right]-\lambda_3\left[\left(1-\frac{aI}{b+I}\right)(1-D)^k\beta_1I\right]\\
\frac{d\lambda_2}{dt}&=\lambda_2\left[\left(1-\frac{aI}{b+I}\right)(1-D)^k\beta_2I+d\right]-\lambda_3\left[\left(1-\frac{aI}{b+I}\right)(1-D)^k\beta_2I\right]\\
\frac{d\lambda_3}{dt}&=-w_1-\lambda_1\left[\left\{-\left(1-\frac{aI}{b+I}\right)+\frac{abI}{(b+I)^2}\right\}(1-D)^k\beta_1S_1+\theta\mu\right]\\
&\quad-\lambda_2\left[\left\{-\left(1-\frac{aI}{b+I}\right)+\frac{abI}{(b+I)^2}\right\}(1-D)^k\beta_2S_2+(1-\theta)\mu\right]\\
&\quad-\lambda_3\left[\left(1-\frac{aI}{b+I}-\frac{abI}{(b+I)^2}\right)(1-D)^k(\beta_1S_1+\beta_2S_2)-\gamma-(\mu+d+m)+\epsilon R\right]-\lambda_4[\gamma-\epsilon R]\\
\frac{d\lambda_4}{dt}&=-\lambda_3[\epsilon I]+\lambda_4[d+\epsilon I]
\end{aligned} \tag{11.3}$$

Table 5 Values of system parameters for numerical simulation for model (11.2)

Parametric values								
p	Λ	d	a	b	D	k	β_1	β_2
0.65	30	0.004	0.3	0.1	0.4	6	0.0002	0.00005
m	γ	ϵ	μ	θ	w_1	w_2	w_3	–
0.005	0.005	0.0001	0.001	0.008	1.5	500	100	–

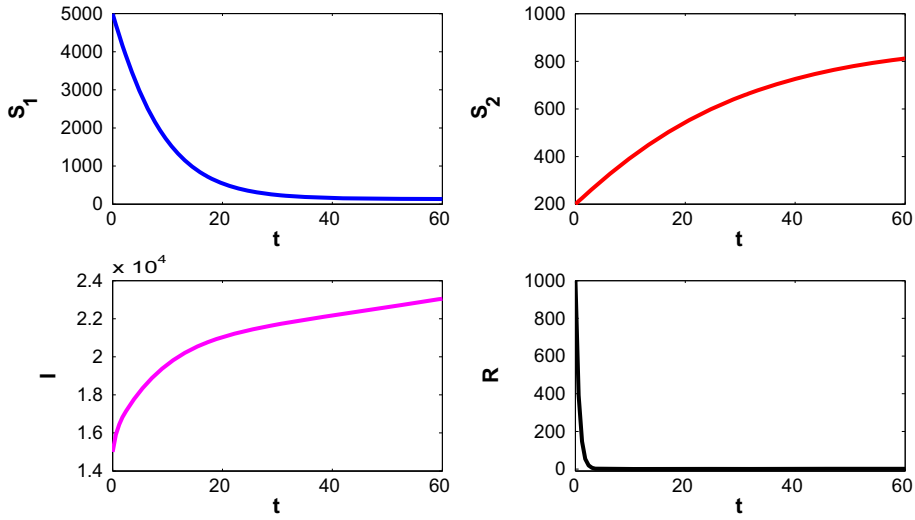

Fig. 19 Profiles of population in absence of time-dependent control strategies

with the transversality conditions $\lambda_i(T_f) = 0$ *for* $i = 1, 2, 3$. *The relevant pair of optimal control interventions* (a^*, γ^*) *in* Δ *that minimize J(a,* γ*) are provided as:*

$$a^* = \min\left\{\max\left\{0, \left(\frac{(1-D)^k I^{*2}}{2w_2(b+I^*)}[(\lambda_3-\lambda_1)\beta_1 S_1^* + (\lambda_3-\lambda_2)\beta_2 S_2^*]\right)\right\}, 1\right\}$$
$$\gamma^* = \min\left\{\max\left\{0, \left(\frac{I^*}{2w_3}(\lambda_3-\lambda_4)\right)\right\}, 1\right\}. \tag{11.4}$$

Proof See Appendix A. □

12 Numerical investigation of optimal control problem

In the proposed system (11.2), we have implemented two control strategies, named as, governmental action (a) and pharmaceutical treatment (γ) to analyze their impact on reduction of infection level. The control interventions are assumed to be time-independent as these change according to the disease prevalence and fatality. Through employing forward-backward sweep approach, numerical simulation has been carried out to demonstrate the affect of control strategies over the behavior of system [34]. To determine the minimum cost, we take into account several scenarios for implementing either one or both control strategies. The parametric values along with the positive weight constants w_1, w_2 and w_3 are listed down in Table 5. Additionally, it is presumed that the control techniques will be used consistently for a period of two months, or $T_f = 60$ days.

The dynamics of the model (11.2) are shown in Fig. 19 when time-dependent control strategies are not taken into account. In this scenario, the population is (133.6602, 811.6747, 23050.5583, 1.3595) at $T_f = 60$.

We now consider the scenario where governmental intervention in susceptible phases varies over time but consistent treatment rates are offered to those who are afflicted. The population profiles are shown in Fig. 20 under the conditions of $a = a^*$ and $\gamma = 0.005$. When $T_f = 60$, the population is (5852.3015, 1747.5213, 15933.8067, 5.1634). As more people become cautious of the infection, because of governmental measures that minimize the disease transmission, the number of susceptible individuals is increasing in this situation. Additionally, although there are fewer infected people in this instance, the number of recovered cases is larger than it would be if no control measures were taken. Figure 21 depicts the equivalent graph of the optimal control intervention, which demonstrates that the control variable operates with the highest intensity right away after being implemented and then wane over suddenly in the last 2 to 3 days.

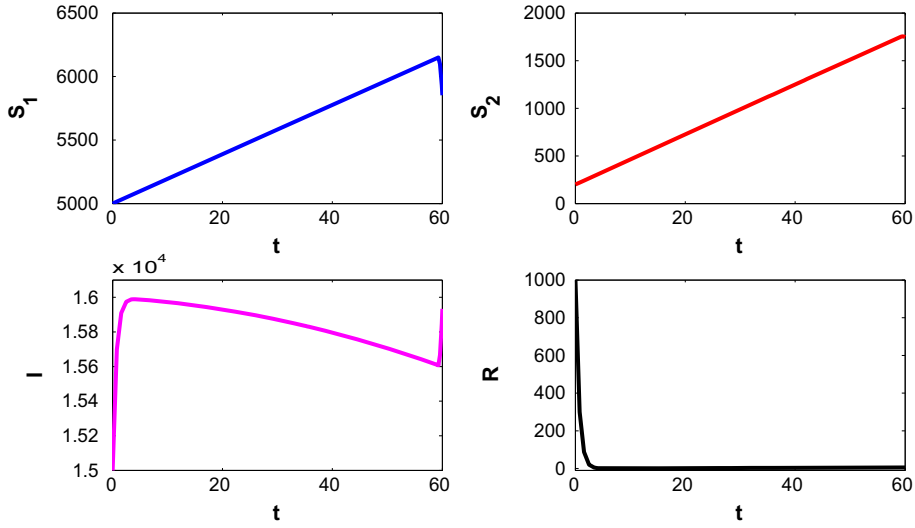

Fig. 20 Diagrams of the population in presence of optimal control a^* only

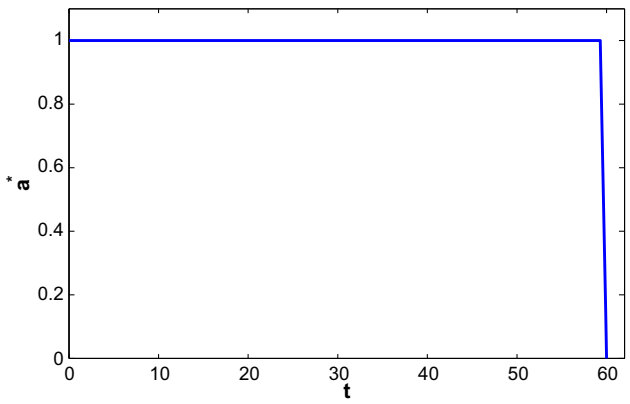

Fig. 21 Profile of optimal control a^*

The next scenario that we analyze is one in which the severity of the infection alone determines the therapy given to afflicted individuals. The population profiles for $a = 0.3$ and $\gamma = \gamma*$ are shown in Fig. 22. When $T_f = 60$, the population changes to (135.9998, 813.09, 22675, 7488, 355.5558). The number of recovered people goes up compared to the situation when no control measures are put in place, since the optimal treatment is more successful at reducing the infected population. Additionally, because of a partial recovery, the susceptible population count increase in both stages in this instance. Figure 23 shows the optimal path of the control strategy (a^*). It is noted that the control variable's efficacy remains at its highest level during the whole implementation period.

If the control strategies are properly implemented simultaneously, the disease load may be managed more effectively. Therefore, we have taken into account that in order to lower the increased disease transmission, government's involvement at susceptible stages and treatment of affected individuals perform according to the severity. The population trajectories are shown in Fig. 24 in presence of both control strategies, and at $T_f = 60$, the population is represented as (5784.6124, 1705.6461, 14855.4058, 1161.7971). In this instance, the count of infected population declines the most. Here, we get the highest number of recovery cases also. Moreover, higher recovery in this case results in a slightly lower susceptible population count than the scenario when only governmental intervention is used as a control approach. Figure 25 reveals the optimal graphs of both control interventions, where it is shown that the intensity of both controls remains at their highest level for almost full implementation period, but the intensity of a^* begins to diminish in the last few days.

The acceptability of implemented control measures is determined by how cost-effective they are. Figure 26 illustrates the impact of time-dependent control measures ($a(t)$, $\gamma(t)$) on the cost design analysis (J) (Fig. 26a) and infected population count (I) (Fig. 26b). Without any control measures, the cost is caused by the diseased population's contribution to the production loss. When control measures are not implemented, the infected population is at its maximum count, which results in higher opportunity loss and increased economic burden. Since we have the fewest affected people in presence of both control policies, the optimal cost is much lower in the case. The findings also indicate that implementing a single control strategy always results in higher cost profiles than implementing both measures. Therefore, it may be said that it is financially viable to approach both control policies at once.

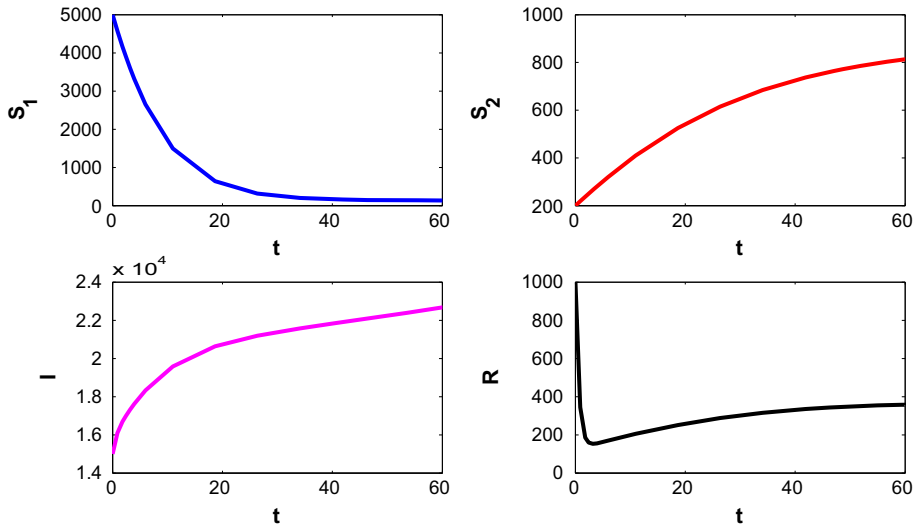

Fig. 22 Diagrams of the population in presence of optimal control γ^* only

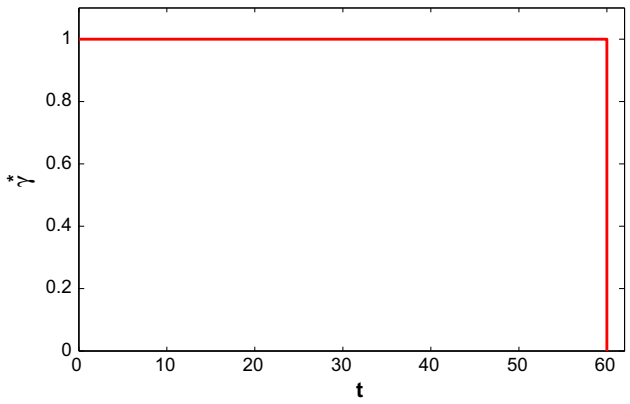

Fig. 23 Profile of optimal control γ^*

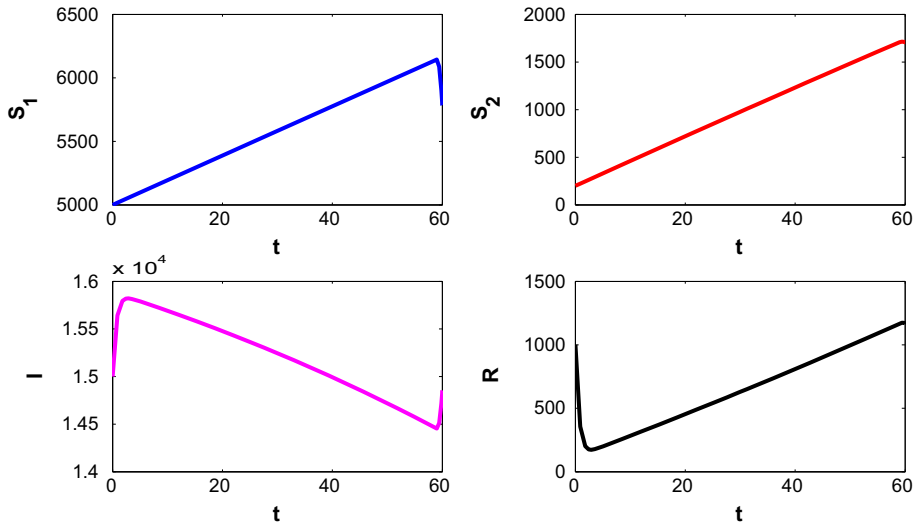

Fig. 24 Diagrams of the population in presence of both optimal control interventions a^* and γ^*

In Fig. 27, it is noted how the effectiveness of governmental action makes an impact to reduce the disease load when both time-dependent control strategies are already implemented in the system. It is shown that efficient enforcement of governmental norms and regulations (lower value of b) among those who are more vulnerable to infection actually reduces the load of illness by lowering the number of affected individuals.

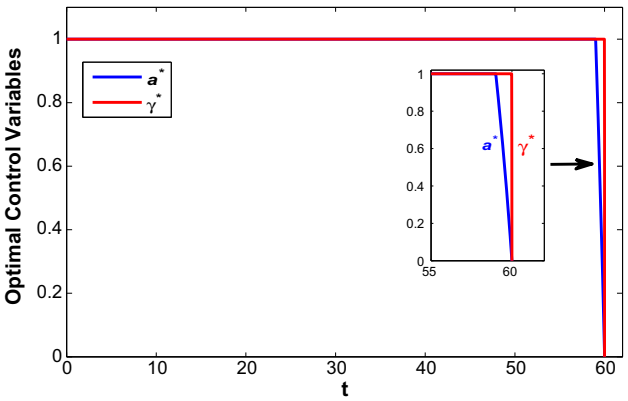

Fig. 25 Profile of optimal controls a^* and γ^*

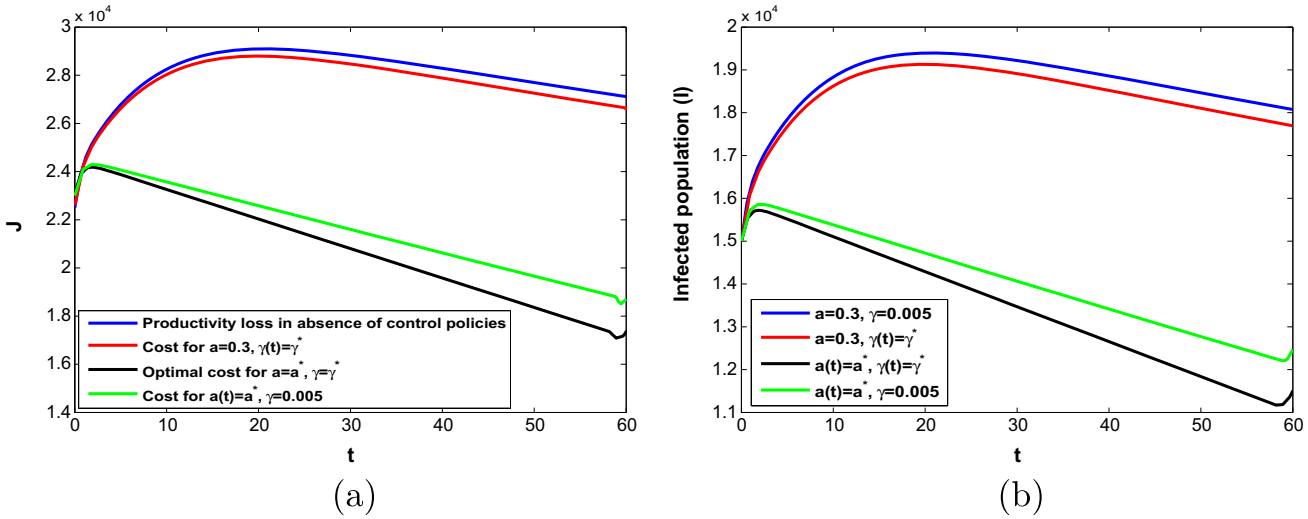

Fig. 26 **a** Cost distribution (J) and **b** Infected population (I) for different time-dependent control strategies

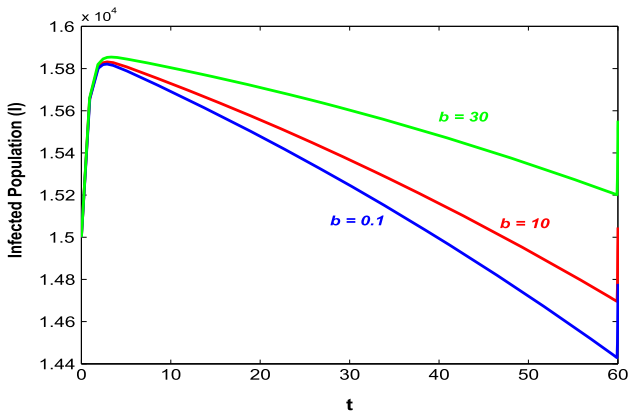

Fig. 27 Profile of infectious community (I) in presence of both implemented control strategies for different effectiveness of governmental action (b)

13 Conclusion

The potential to recognize the dynamical intricacy of an epidemiological system and identification of epidemic components that affect this structure are the most prominent aspects of epidemiological study. For a substantial amount of time, a number of researchers have studied significantly epidemic modeling of SIRS frameworks. However, in recent times, the main strength of research in this field has switched to examine the possible control techniques. Throughout this study, a nonlinear SIRIS compartmental framework has been suggested to investigate the dynamics of contagious diseases, taking into consideration the influence of governmental intervention, social behavioral response and public reaction, involving two separate susceptible stages, depending on immunity strength. This work is based on the possibility that some formerly infected individuals become immune to the illness after infection,

some formerly infectious population becomes susceptible to the disease again after recovery, and some formerly infected people are re-infected after recovering from disease. There are various illnesses from which people, if they survive the infection, only make a partial recovery. After a certain amount of time, there is always a possibility that one may become infected again, either with a new or similar variant of virus. Some of the ailments that provide evidence in favor of SIRS epidemiological model include the following: malaria, Influenza, Hepatitis Delta, Hepatitis B, dengue, encephalitis, meningitis, tuberculosis, etc. COVID-19 is the latest virus to be added to this list; similar to other diseases, it is found incidences of reinfection in previously healthy population. The governmental policies of a nation exert an important impact to maintain the panic scenario among people during an epidemic or pandemic breakout by establishing certain stringent laws and guidelines. There are different National Health Programs that have been running for many years with the purpose of preventing and controlling various diseases [35]. For instance, between the years 2000 and 2018, India was able to accomplish a decrease of 59% in morbidity rate along with a reduction of 90% in fatality rate associated with malaria; there is no denying that governmental actions seemed to have a contribution in this achievement. Furthermore, the Government of India has established a goal of eliminating Kala Azar (KA), which entails reducing the yearly case occurrence to < 1 per 10,000 inhabitants at block level. It is observed that there has been a 24% reduction in the amount of cases of KA in 2018 as compared with 2017. In recent times, when the virus hit the nation during 2020, the Government of India enforced a nationwide lockdown and made people informed by taking appropriate preventive steps to regulate the heightened viral propagation. This was really beneficial in maintaining things under control. Alterations in individuals' behaviors, in addition to those made by the government, make a significant contribution to decrease the possibility of spreading disease. As a means of drawing attention to the positive effects that governmental activities and increased public knowledge may have on spread of sickness, the disease transmission rate has been modified as $(1-\alpha(I))(1-D)^k(\beta_1 S_1(t)+\beta_2 S_2(t))I(t)$. Moreover, numerical computations illustrate that the rate of restrictions (a), effectiveness of imposed limitations (b^{-1}) by government, social behavior (D) as well as public response (k) are efficient in reducing the contamination level in a pandemic scenario. The deterministic model can eventually be extended to an SDE version by incorporating multiplicative noise components.

The use of sociological parameters reduces the incidence of the virus transmission here. The populace in each compartment is non-negative and bounded as time increases, making the system (2.1) biologically acceptable. The basic reproduction number (R_0) determines the disease's transmissibility: $R_0 > 1$ indicates the invasion of a disease in a community. The effectiveness of the parameters reflecting people's social behavior (D), public reaction (k), and virus propagation rates (β_1, β_2) in controlling the system dynamics is demonstrated in the numerical figures in Sect. 10. The local sensitivity study also indicates that the system's ability to manage infection level is most sensitive to the rate at which the disease spreads from the people with lower immunity power. Figure 7a reveals that the government imposed restrictions decrease the infected population with a higher rate when first implemented, but the level of infection tends to saturation state for increasing rate of restrictions. On the other hand, Fig. 7b depicts that if the implemented restrictions do not provide as much effective (larger value of b), then it ultimately leads to an inclination on the count of infected people. Moreover, Fig. 8 demonstrates that infection level might be controlled more if people response to the recommended regulations without expressing any uncertainty and begins to adjust their social behavioral pattern in accordance with these restrictions. Also, it is observed from Fig. 9 that higher response of a population (increasing value of k) toward a strict restriction (increasing value of a) significantly reduces the infectivity in a system which signifies that the public response is equally important as the governmental restrictions. Only the government imposed regulations are not sufficient to reduce the infection if the people do not follow them. Now, the amount of governmental limitations and medical care provided to afflicted people depends on the disease's severity and evolves with time. Therefore, in Sect. 11 an optimal control problem is put forth by considering governmental actions and treatment policies as the time-dependent control strategies to examine their effects on the system. The simulation outcomes, discussed in Sect. 12, provide evidences that when both control strategies are implemented, the size of affected persons reduces to a great extent. It implies that the implementation of control programs lessens both the economic burden and the severity of disease. The contagiousness during a pandemic outbreak is therefore observed to be reduced by these time-dependent control efforts. A thorough sensitivity analysis has been undertaken to precisely examine and point out the factors influencing this epidemiological modeling. This involves analyzing PRCC values and corresponding p values of model parameters at two distinct methods (Spearman and Kendall). Our sensitivity test is conducted with a significance level, set at 0.05. This analysis reveals that reproduction number (R_0) of model system (2.1) is most sensitive to parameters such as D, k, β_1, β_2 and Λ. Specifically, an increase in D, k, d, γ, μ significantly decrease the level of R_0. Furthermore, increase in parameters like β_1, β_2, p, Λ lead to substantial reduction in R_0.

Researchers may able to develop epidemic systems in a more sensible manner by including stochastic impacts in the model. This is possible owing to the fact that many circumstances that occur in reality are not deterministic. As a consequence of variations in environment, the biological parameters may be perturbed by random fluctuations. Changes in environment could play a crucial role in the development of infections. In this study, it is assumed that each compartment in the system has been affected by stochastic environmental factor. In addition, we presume that the stochastic fluctuations manifest themselves mainly as fluctuations in the natural mortality rate d and it is of white-noise type. Moreover, the basic reproduction number R_0 governs the behavior of deterministic model (2.1), however dynamical complexities of stochastic version (2.2) can in fact be controlled by basic reproduction number of stochastic system ($\hat{R}_s$). According to Theorem 4.4, the solutions of model (2.2) will lie in $\mathbb{R}^4_+$ a.s. Furthermore, the analytical results on the existence of positive solution, stochastically ultimate boundedness, and permanence of solution to the SDE model (2.2) have been studied in Sect. 4. Theorem 4.6 indicates that the norm of $(S_1(t),\ S_2(t),\ I(t),\ R(t))$ for stochastic counterpart (2.2) is bounded

away from extinction with probability one. It is shown in Theorem 7.3 that environmental fluctuations have the potential to stop the spread of ailment and this phenomenon is numerically depicted in Fig. 12. Whenever $R_0 > 1$, the deterministic system (2.1) ensures the occurrence of a stable endemic steady state $E^*(S_1^*, S_2^*, I^*, R^*)$, while the SDE model (2.2) might eradicate the infection in case of a high intensity of noise in infectious individuals. It is essential to emphasize that the stochastic reproduction number $\hat{R}_s$ is responsible for transmission of disease across the population:

- for $\hat{R}_s < 1$, the contagious species population goes extinct with probability 1 (for convenience, see Fig. 12)
- for $\hat{R}_s > 1$, the contagious species population persists (for convenience, see Figs. 14, 15).

Next, in Theorem 7.5, the existence of ergodic property subject to Assumption 1 is proved, where it is shown that the positive solution converges to unique stationary distribution. Moreover, Fig. 16 graphically displays that endemic stationary distribution of susceptible compartments with lower and higher immunity as well as infected and recovered class persists and is unique. Numerous numerical studies have been carried out in attempt to acquire a better understanding of the role of strength of noise on disease dynamics. It is concluded from Fig. 14, that strong level of noises may cause the solutions of stochastic system (2.2) to fluctuate substantially about the endemic equilibrium point, whereas the oscillation decreases for reduced noise intensities (see Fig. 15). Figure 17a reveals that the strength of noise (ν_3) has a significant impact on the rate of decline in size of infected compartment. Table 4 provides the explanation of this situation. The influence of noise (ν_3) on the reproduction number is illustrated numerically (see Fig. 18) with varying social behavioral dynamics (D), public reaction (k) and infection propagation rate from susceptible to infectious class with lower and higher immunity (β_1, β_2), respectively.

14 Study limitation and future direction

Despite considering various realistic issues and obtaining reasonable results, our investigation has identified several intriguing areas that require further exploration in the future. The approaches discussed in this study can be applied to investigate various models, such as SIQR model, SEIR model and many others. Additionally, in future, this study may also be conducted involving colored noises (or, Ornstein Uhlenbeck processes) which are more realistic noises than white noises. For a better understanding of more complex systems with more realistic behaviors, like those that consider a diversity of response functions and those that involve time delays in separate compartments, further research is required.

Acknowledgements The authors are grateful to the anonymous referees and Prof. Panagiotis Theodorakis (Editor) for their careful reading, valuable comments and helpful suggestions, which have helped them to improve the presentation of this work significantly.

Data Availability Statement The data used to support the findings of the study are available within the article.

Declarations

Conflict of interest With reference to the study, the authors claim that they do not have any Conflict of interest.

Appendix A

A.1 Existence of optimal control functions

Here, the existence of optimal control interventions which minimized the cost functional, within a finite time interval, have been provided.

Proof of Theorem 11.1 *In model (11.2), the overall population N is assumed as,* $N = S_1 + S_2 + I + R$.

$$\text{Thus we have, } \frac{dN}{dt} = \Lambda - d(S_1 + S_2 + I + R) - mI \leq \Lambda - dN$$
$$\Rightarrow 0 < N(t) \leq \frac{\Lambda}{d} + \left(N(0) - \frac{\Lambda}{d}\right)e^{-dt}$$

where $N(0) = S_1(0) + S_2(0) + I(0) + R(0)$. *As* $t \to \infty$, $0 < N(t) \leq \frac{\Lambda}{d} + \varepsilon$, *for any* $\varepsilon > 0$.

Here, system (11.2) has a bounded solution when control interventions are present in the system. Also, the right side functions of the system are Lipschitzian in Δ. *So, control system (11.2) has a non-trivial solution in* Δ *by Picard-Lindelöf theorem [36].*

Also, Δ *is a closed, convex set within which the control variables lie. And, system (11.2) can be written as linear in control variables a and* γ *with coefficients depending on state variables. Moreover, the integrand* $L(S_1, S_2, I, R, a, \gamma)$ *is convex because of the quadratic nature of control variables a and* γ.

$$\text{Now, } L(S_1, S_2, I, R, a, \gamma) = w_1 I + w_2 a^2 + w_3 \gamma^2 \geq w_2 a^2 + w_3 \gamma^2$$

Let us choose, $\widetilde{w} = \min(w_2, w_3) > 0$ *and* $h(a, \gamma) = \widetilde{w}(a^2 + \gamma^2)$*. Then we have,* $h(a, \gamma)$ *as a continuous function, and* $L(S_1, S_2, I, R, a, \gamma) \geq h(a, \gamma)$*. Also,* $||(a, \gamma)||^{-1}h(a, \gamma) \to \infty$ *when* $||(a, \gamma)|| \to \infty$*. So, the results of [3, 37] help to conclude that there exists a control pair* a^* *and* γ^* *such that* $J(a^*, \gamma^*) = \min[J(a, \gamma)]$. □

A.2 Characterization of control interventions

Pontryagin's Maximum Principle helps to find the control interventions of an optimal system [37, 38]. Assume that, the Hamiltonian function as:

$$\begin{aligned} H(S_1, S_2, I, R, a, \gamma, \lambda) &= L(S_1, S_2, I, R, a, \gamma) + \lambda_1 \frac{\mathrm{d}S_1}{\mathrm{d}t} + \lambda_2 \frac{\mathrm{d}S_2}{\mathrm{d}t} + \lambda_3 \frac{\mathrm{d}I}{\mathrm{d}t} + \lambda_4 \frac{\mathrm{d}R}{\mathrm{d}t} \\ \text{So, } H &= w_1 I + w_2 a^2 + w_3 \gamma^2 + \lambda_1 \left[p\Lambda - \left(1 - \frac{a(t)I}{b+I}\right)(1-D)^k \beta_1 S_1 I - \mathrm{d}S_1 + \theta \mu I \right] + \lambda_2 [(1-p)\Lambda \\ &\quad - \left(1 - \frac{a(t)I}{b+I}\right)(1-D)^k \beta_2 S_2 I - \mathrm{d}S_2 + (1-\theta)\mu I \Big] + \lambda_3 \Big[\left(1 - \frac{a(t)I}{b+I}\right)(1-D)^k (\beta_1 S_1 + \beta_2 S_2) I \\ &\quad - (d+m)I - \gamma(t)I - \mu I + \epsilon I R \Big] + \lambda_4 [\gamma(t)I - \epsilon I R - \mathrm{d}R] \end{aligned} \tag{A.1}$$

where $\lambda = (\lambda_1, \lambda_2, \lambda_3, \lambda_4)$ denote the adjoint variables. We mainly intend to minimize the cost functional by minimizing the Hamiltonian function by Pontryagin's Maximum Principle.

Proof of Theorem 11.2 *For system (11.2),* (a^*, γ^*) *and* (S_1^*, S_2^*, I^*, R^*) *be the applied optimal control interventions and corresponding optimal state variables, respectively, which minimize the cost functional J mentioned in (11.1). So, there will be adjoint variables* $(\lambda_1, \lambda_2, \lambda_3, \lambda_4)$ *which satisfy the following canonical equations:*

$$\frac{d\lambda_1}{dt} = -\frac{\partial H}{\partial S_1}, \quad \frac{d\lambda_2}{dt} = -\frac{\partial H}{\partial S_2}, \quad \frac{d\lambda_3}{dt} = -\frac{\partial H}{\partial I}, \quad \frac{d\lambda_4}{dt} = -\frac{\partial H}{\partial R}.$$

So, we have

$$\begin{aligned} \frac{d\lambda_1}{dt} &= \lambda_1 \left[\left(1 - \frac{aI}{b+I}\right)(1-D)^k \beta_1 I + d \right] - \lambda_3 \left[\left(1 - \frac{aI}{b+I}\right)(1-D)^k \beta_1 I \right] \\ \frac{d\lambda_2}{dt} &= \lambda_2 \left[\left(1 - \frac{aI}{b+I}\right)(1-D)^k \beta_2 I + d \right] - \lambda_3 \left[\left(1 - \frac{aI}{b+I}\right)(1-D)^k \beta_2 I \right] \\ \frac{d\lambda_3}{dt} &= -w_1 - \lambda_1 \left[\left\{ -\left(1 - \frac{aI}{b+I}\right) + \frac{abI}{(b+I)^2} \right\}(1-D)^k \beta_1 S_1 + \theta\mu \right] \\ &\quad - \lambda_2 \left[\left\{ -\left(1 - \frac{aI}{b+I}\right) + \frac{abI}{(b+I)^2} \right\}(1-D)^k \beta_2 S_2 + (1-\theta)\mu \right] \\ &\quad - \lambda_3 \left[\left(1 - \frac{aI}{b+I} - \frac{abI}{(b+I)^2}\right)(1-D)^k (\beta_1 S_1 + \beta_2 S_2) - \gamma - (\mu + d + m) + \epsilon R \right] - \lambda_4 [\gamma - \epsilon R] \\ \frac{d\lambda_4}{dt} &= -\lambda_3 [\epsilon I] + \lambda_4 [d + \epsilon I] \end{aligned} \tag{A.2}$$

with the transversality conditions $\lambda_i(T_f) = 0$*, for* $i = 1, 2, 3, 4$.

$$\textit{From optimality conditions : } \left.\frac{\partial H}{\partial a}\right|_{a=a^*} = 0, \textit{ and } \left.\frac{\partial H}{\partial \gamma}\right|_{\gamma=\gamma^*} = 0, \textit{ which gives}$$

$a^* = \dfrac{(1-D)^k I^{*2}}{2w_2(b+I^*)}[(\lambda_3 - \lambda_1)\beta_1 S_1^* + (\lambda_3 - \lambda_2)\beta_2 S_2^*]$, *and* $\gamma^* = \dfrac{I^*}{2w_3}(\lambda_3 - \lambda_4)$*. Hence, in* Δ *we have*

$$a^* = \begin{cases} 0, & \text{if } \frac{(1-D)^k I^{*2}}{2w_2(b+I^*)}[(\lambda_3 - \lambda_1)\beta_1 S_1^* + (\lambda_3 - \lambda_2)\beta_2 S_2^*] < 0 \\ \frac{(1-D)^k I^{*2}}{2w_2(b+I^*)}[(\lambda_3 - \lambda_1)\beta_1 S_1^* + (\lambda_3 - \lambda_2)\beta_2 S_2^*], & \text{if } 0 \leq \frac{(1-D)^k I^{*2}}{2w_2(b+I^*)}[(\lambda_3 - \lambda_1)\beta_1 S_1^* + (\lambda_3 - \lambda_2)\beta_2 S_2^*] \leq 1 \\ 1, & \text{if } \frac{(1-D)^k I^{*2}}{2w_2(b+I^*)}[(\lambda_3 - \lambda_1)\beta_1 S_1^* + (\lambda_3 - \lambda_2)\beta_2 S_2^*] > 1 \end{cases}$$

$$\gamma^* = \begin{cases} 0, & \text{if } \frac{I^*}{2w_3}(\lambda_3 - \lambda_4) < 0 \\ \frac{I^*}{2w_3}(\lambda_3 - \lambda_4), & \text{if } 0 \leq \frac{I^*}{2w_3}(\lambda_3 - \lambda_4) \leq 1 \\ 1, & \text{if } \frac{I^*}{2w_3}(\lambda_3 - \lambda_4) > 1 \end{cases}$$

and it is same as (11.4). □

A.3 Optimal system

The optimal system is stated below along with the optimal control policies a^* and γ^*. The optimal system at (S_1^*, S_2^*, I^*, R^*, λ_1, λ_2, λ_3, λ_4) along with the minimized Hamiltonian H^* is as follows:

$$\begin{aligned}
\frac{dS_1}{dt} &= p\Lambda - \left(1 - \frac{a^*I^*}{b+I^*}\right)(1-D)^k\beta_1 S_1^* I^* - dS_1^* + \theta\mu I^* \\
\frac{dS_2}{dt} &= (1-p)\Lambda - \left(1 - \frac{a^*I^*}{b+I^*}\right)(1-D)^k\beta_2 S_2^* I^* - dS_2^* + (1-\theta)\mu I^* \\
\frac{dI}{dt} &= \left(1 - \frac{a^*I^*}{b+I^*}\right)(1-D)^k(\beta_1 S_1^* + \beta_2 S_2^*)I^* - (d+m)I^* - \gamma^* I^* - \mu I^* + \epsilon I^* R^* \\
\frac{dR}{dt} &= \gamma^* I^* - \epsilon I^* R^* - dR^*
\end{aligned}$$

with non-negative initial conditions $S_1^*(0) > 0$, $S_2^*(0) > 0$, $I^*(0) \geq 0$, $R^*(0) \geq 0$, and associated adjoint model system have been given as:

$$\begin{aligned}
\frac{d\lambda_1}{dt} &= \lambda_1\left[\left(1 - \frac{a^*I^*}{b+I^*}\right)(1-D)^k\beta_1 I^* + d\right] - \lambda_3\left[\left(1 - \frac{a^*I^*}{b+I^*}\right)(1-D)^k\beta_1 I^*\right] \\
\frac{d\lambda_2}{dt} &= \lambda_2\left[\left(1 - \frac{a^*I^*}{b+I^*}\right)(1-D)^k\beta_2 I^* + d\right] - \lambda_3\left[\left(1 - \frac{a^*I^*}{b+I^*}\right)(1-D)^k\beta_2 I^*\right] \\
\frac{d\lambda_3}{dt} &= -w_1 - \lambda_1\left[\left\{-\left(1 - \frac{a^*I^*}{b+I^*}\right) + \frac{a^*bI^*}{(b+I^*)^2}\right\}(1-D)^k\beta_1 S_1^* + \theta\mu\right] \\
&\quad - \lambda_2\left[\left\{-\left(1 - \frac{a^*I^*}{b+I^*}\right) + \frac{a^*bI^*}{(b+I^*)^2}\right\}(1-D)^k\beta_2 S_2^* + (1-\theta)\mu\right] \\
&\quad - \lambda_3\left[\left(1 - \frac{a^*I^*}{b+I^*} - \frac{a^*bI^*}{(b+I^*)^2}\right)(1-D)^k(\beta_1 S_1^* + \beta_2 S_2^*) - \gamma^* - (\mu + d + m) + \epsilon R^*\right] - \lambda_4[\gamma^* - \epsilon R^*] \\
\frac{d\lambda_4}{dt} &= -\lambda_3[\epsilon I^*] + \lambda_4[d + \epsilon I^*]
\end{aligned} \tag{A.3}$$

with transversality conditions $\lambda_i(T_f) = 0$, for $i = 1, 2, 3, 4$ and the control interventions a^*, γ^* are similar as provided in (11.4).

References

1. D. Bernoulli, Essai d'une nouvelle analyse de la mortalité causée par la petite vérole, et des avantages de l'inoculation pour la prévenir, Histoire de l'Acad. Roy. Sci. (Paris) avec Mem (1766), pp. 1–45
2. W.O. Kermack, A.G. McKendrick, A contribution to the mathematical theory of epidemics. Proc. Roy. Soc. Lond. Ser. A Contain. Pap. Math. Phys. Charact. **115**(772), 700–721 (1927). https://doi.org/10.1098/rspa.1927.0118
3. H. Gaff, E. Schaefer, Optimal control applied to vaccination and treatment strategies for various epidemiological models. Math. Biosci. Eng. **6**(3), 469–492 (2009). https://doi.org/10.3934/mbe.2009.6.469
4. S. Lee, G. Chowell, C. Castillo-Chávez, Optimal control for pandemic influenza: the role of limited antiviral treatment and isolation. J. Theor. Biol. **265**(2), 136–150 (2010). https://doi.org/10.1016/j.jtbi.2010.04.003
5. M. De la Sen, S. Alonso-Quesada, A. Ibeas, On the stability of an SEIR epidemic model with distributed time-delay and a general class of feedback vaccination rules. Appl. Math. Comput. **270**, 953–976 (2015). https://doi.org/10.1016/j.amc.2015.08.099
6. M. Turkyilmazoglu, Explicit formulae for the peak time of an epidemic from the SIR model. Physica D **422**, 132902 (2021). https://doi.org/10.1016/j.physd.2021.132902
7. S. Saha, G. Samanta, Analysis of a host-vector dynamics of a dengue disease model with optimal vector control strategy. Math. Comput. Simul. **195**, 31–55 (2022). https://doi.org/10.1016/j.matcom.2021.12.021
8. S. Spencer, Stochastic Epidemic Models for Emerging Diseases (P.hD. thesis), University of Nottingham, Nottinghamshire, CRC Press (2008)
9. X. Mao, G. Marion, E. Renshaw, Environmental Brownian noise suppresses explosions in population dynamics. Stochast. Process. Appl. **97**(1), 95–110 (2002). https://doi.org/10.1016/S0304-4149(01)00126-0
10. A. Saltelli, K. Chan, E. Scott, Sensitivity Analysis. Wiley Series in Probability and Statistics, vol. 830 (2000)
11. J.C. Helton, J.D. Johnson, C.J. Sallaberry, C.B. Storlie, Survey of sampling-based methods for uncertainty and sensitivity analysis. Reliab. Eng. Syst. Saf. **91**(10–11), 1175–1209 (2006). https://doi.org/10.1016/j.ress.2005.11.017
12. V. Savatorova, Exploring parameter sensitivity analysis in mathematical modeling with ordinary differential equations. CODEE J. **16**(1), 4 (2023). https://doi.org/10.5642/codee.CZKZ5996
13. F. Brauer, C. Castillo-Chavez, Z. Feng, *Mathematical Models in Epidemiology*, vol. 32 (Springer, Berlin, 2019)
14. H. Heesterbeek, R.M. Anderson, V. Andreasen, S. Bansal, D. De Angelis, C. Dye, K.T. Eames, W.J. Edmunds, S.D. Frost, S. Funk et al., Modeling infectious disease dynamics in the complex landscape of global health. Science **347**(6227), aaa4339 (2015). https://doi.org/10.1126/science.aaa4339

15. A. Bonifacius, S. Tischer-Zimmermann, A.C. Dragon, D. Gussarow, A. Vogel, U. Krettek, N. Gödecke, M. Yilmaz, A.R. Kraft, M.M. Hoeper et al., COVID-19 immune signatures reveal stable antiviral T cell function despite declining humoral responses. Immunity **54**(2), 340–354 (2021). https://doi.org/10.1016/j.immuni.2021.01.008
16. M. Clements, R. Betts, E. Tierney, B. Murphy, Serum and nasal wash antibodies associated with resistance to experimental challenge with influenza A wild-type virus. J. Clin. Microbiol. **24**(1), 157–160 (1986). https://doi.org/10.1128/jcm.24.1.157-160.1986
17. R. Pagliara, B. Dey, N.E. Leonard, Bistability and resurgent epidemics in reinfection models. IEEE Control Syst. Lett. **2**(2), 290–295 (2018). https://doi.org/10.1109/LCSYS.2018.2832063
18. R. Pagliara, N.E. Leonard, Adaptive susceptibility and heterogeneity in contagion models on networks. IEEE Trans. Autom. Control **66**(2), 581–594 (2020). https://doi.org/10.1109/TAC.2020.2985300
19. G. Katriel, The size of epidemics in populations with heterogeneous susceptibility. J. Math. Biol. **65**(2), 237–262 (2012). https://doi.org/10.1007/s00285-011-0460-2
20. Y. Nakata, R. Omori, Epidemic dynamics with a time-varying susceptibility due to repeated infections. J. Biol. Dyn. **13**(1), 567–585 (2019). https://doi.org/10.1080/17513758.2019.1643043
21. Y. Svirezhev, D.O. Logofet, *The Stability of Biological Communities* (Mir Publishers, Moscow, 1978)
22. G.P. Samanta, Influence of environmental noises on the Gomatam model of interacting species. Ecol. Model. **91**(1–3), 283–291 (1996). https://doi.org/10.1016/0304-3800(95)00195-6
23. J.K. Hale, *Theory of Functional Differential Equations* (Springer, New York, 1977)
24. X. Mao, *Stochastic Differential Equations and Applications* (Horwood, New York, 1997)
25. S. Saha, P. Dutta, G. Samanta, Dynamical behavior of SIRS model incorporating government action and public response in presence of deterministic and fluctuating environments. Chaos Solitons Fractals **164**, 112643 (2022). https://doi.org/10.1016/j.chaos.2022.112643
26. A. Athreya, T. Kolba, J. Mattingly, Propagating Lyapunov functions to prove noise-induced stabilization. Electron. J. Probab. **17**(96), 1–38 (2012). https://doi.org/10.1214/EJP.v17-2410
27. X. Li, X. Mao, Population dynamical behavior of non-autonomous Lotka–Volterra competitive system with random perturbation. Discrete Contin. Dyn. Syst. **24**(2), 523–545 (2009). https://doi.org/10.3934/dcds.2009.24.523
28. P. van den Driessche, J. Watmough, Reproduction numbers and sub-threshold endemic equilibria for compartmental models of disease transmission. Math. Biosci. **180**(1), 29–48 (2002). https://doi.org/10.1016/S0025-5564(02)00108-6
29. L. Arriola, J. Hyman, Lecture Notes, Forward and Adjoint Sensitivity Analysis: With Applications in Dynamical Systems, Linear Algebra and Optimisation (Mathematical and Theoretical Biology Institute, Summer, 2005)
30. R. Z. Has'minskii, Stochastic stability of differential equations, in *Monogram Textbook Mechanics Solids Fluids*, vol. 7 (Sijthoff & Noordhoff, Alphen aan den Rijn, Netherlands, 1980)
31. C. Castillo-Chavez, B. Song, Dynamical models of tuberculosis and their applications. Math. Biosci. Eng. **1**(2), 361–404 (2004). https://doi.org/10.3934/mbe.2004.1.361
32. S. Marino, I.B. Hogue, C.J. Ray, D.E. Kirschner, A methodology for performing global uncertainty and sensitivity analysis in systems biology. J. Theor. Biol. **254**(1), 178–196 (2008). https://doi.org/10.1016/j.jtbi.2008.04.011
33. S.M. Kassa, A. Ouhinou, The impact of self-protective measures in the optimal interventions for controlling infectious diseases of human population. J. Math. Biol. **70**(1–2), 213–236 (2015). https://doi.org/10.1007/s00285-014-0761-3
34. D.E. Kirk, *Optimal Control Theory: An Introduction, Dover Books on Electrical Engineering* (Dover Publications, New York, 2012) https://books.google.co.in/books?id=onuH0PnZwV4C
35. Disease Control Programmes (NHM). https://main.mohfw.gov.in/sites/default/files/05%20ChapterAN2018-19.pdf
36. A. Coddington, N. Levinson, *Theory of Ordinary Differential Equations International Series in Pure and Applied Mathematics* (Tata McGraw-Hill Companies, New York, 1955)
37. W. Fleming, R. Rishel, *Deterministic and Stochastic Optimal Control*, vol. 1 (Springer, New York, 1975)
38. L.S. Pontryagin, *Mathematical Theory of Optimal Processes* (CRC Press, Boca Raton, 1987)